

**College of
Engineering**

**UNIVERSITY OF
BAHRAIN**

**Department of Civil
Engineering**



Design Optimization of Composite Steel Plate Girder Bridges

A Thesis Submitted in Partial Fulfillment of
the Requirements for the MSc. Degree in Civil Engineering

**Submitted by
Muhammed Fouad Muhammed Al Malazi**

Student's ID: 20126173

A handwritten signature in black ink, appearing to read 'M Al Malazi'.

**Supervised by
Dr. Semih Erhan**
Assistant Professor
University of Bahrain

Dr. Mona Abdullatif Ismail
Assistant Professor
University of Bahrain

Kingdom of Bahrain

December 2022

بسم الله الرحمن الرحيم

Thesis Discussion Committee Decision

Abstract

This thesis investigated the optimization process of composite plate girder bridges to AASHTO LRFD provisions using the evolutionary optimization model within Excel Solver. Evolutionary [also known as genetic] algorithms implement principles of natural selection and survival of the fittest in a mathematical model that seeks to find the best solution to a problem. Commercially-available software tools such as Solver, have streamlined the process of optimization to a degree where individuals can directly implement a form of optimization to a problem or product in order to gain market leverage and reduce costs, without any programming prerequisites. The design process of composite plate girder bridges is a highly iterative procedure that can be swayed in many unpredictable directions, given the site conditions. As a result, generalizing a set of [golden]-rules, doesn't always yield a commercially optimum design. Moreover, at the heart of AASHTO LRFD provisions, you will find yourself confined in a discrete, highly nonlinear problem, where conventional methods do not scale well. This is where the use of metaheuristic algorithms shines.

The implemented genetic algorithm facilitated the search for optimum design configurations for a single-span composite plate girder bridge, having 9 variables. While also adhering to 57 constraints. The design constraints covered a wide spectrum of the code provisions, ranging from Strength, Fatigue, Service limit states to constructability and wind checks. 3 different models have been established and results were validated with existing literature. 20.5% weight reduction in the steel component was achieved, presenting a 2.1% improvement on referenced literature while also reducing the computation time to 5% of the referenced example.

The model confirmed site conditions permitting the use of deeper webs will yield the highest return on investment in terms of capturing the maximum potential of the girders for the least amount of material, as opposed to adding additional girders.

Finally, the viability of Solver as a readily-available tool for addressing the design of highly complex and nonlinear structures was confirmed

Acknowledgments

Words cannot express my gratitude to my professors, Prof. Dr. Mehmet Polat Saka, Dr. Semih Erhan and Dr. Mona Abdullatif Ismail.

To say that writing and finalizing this thesis was smooth sailing, is a far cry from the truth. Only through their unprecedented patience and support I was able to pull through.

This also serves as an admission of guilt, an apology to whom it may concern. [As much as I wanted to, and as much as my professors wanted to] The things we planned and had in mind and the things I was able to fit in time...These two rarely overlapped.

I am grateful to my parents for their exceptional support and prayers. I owe it them for having gone this path. And I hope to have done up to their expectations.

Special thanks also go to my boss, Eng. Nasri Majzoub. For his constant support. It is through his introductions of me as a Master's student, I felt the most pressured to persevere.

Finally, my sincere appreciation and thanks go to my friend, Abdullah Sultan. Much of the writing is owed to his constant cheering and encouragement.



Table of Contents

Thesis Discussion Committee Decision	A
Abstract	B
Acknowledgments.....	D
Table of Contents	E
List of Tables	H
List of Figures	J
Chapter 1 Introduction.....	14
1.1 General	14
1.2 Research Problem.....	18
1.3 Research Questions	18
1.4 Research Objectives	19
1.5 Research Significance	20
1.6 Research Outline	22
Chapter 2 Optimization	24
2.1 Introduction	24
2.2 Evolutionary Algorithm	27
2.3 Evolutionary Algorithm Drawbacks	32
2.4 Excel Solver	34
2.5 Excel Solver Example	36
2.6 Making the case for Excel Solver	39
Chapter 3 Bridge Engineering	43
3.1 Introduction	43
3.2 Bridge Types	45
3.3 Honorable Mention – Bailey Bridge.....	50
3.4 Composite Bridge.....	53
3.5 Design Code	58

3.6	Design Philosophy	59
3.7	Literature Review.....	62
Chapter 4 Design Example		66
4.1	Problem Parameters	66
4.2	Proportional Limits	68
4.3	Section Properties.....	70
4.4	Unfactored Dead Loads	75
4.5	Unfactored Live Loads.....	79
4.6	Live load summary.....	93
4.7	Dynamic Load Allowance	95
4.8	Live Load Distribution Factors	97
4.8.1	Approximate Method.....	99
4.9	Complete Load Effect Summary.....	103
4.10	Permanent Deformations.....	106
4.11	Plastic Moment of Composite Section.....	109
4.12	Flexural Resistance of Composite Section	112
4.13	Shear Design	115
4.14	Fatigue Design	121
4.15	Miscellaneous checks.....	126
4.16	Summary	129
Chapter 5 Methods & Procedures.....		132
5.1	Introduction	132
5.2	The Mapping Process	133
5.3	Excel Setup.....	134
5.4	Variables	137
5.5	Constraints.....	142
5.6	Objective Function	146
Chapter 6 Results and Discussions.....		149

6.1	Introduction	149
6.2	Model 1	151
6.2.1	Variables	151
6.2.2	Expectations.....	151
6.2.3	Results.....	152
6.2.4	Observations	153
6.3	Model 2	155
6.3.1	Variables	155
6.3.2	Expectations.....	155
6.3.3	Results.....	156
6.3.4	Observations	157
6.4	Model 3	158
6.4.1	Variables	158
6.4.2	Expectations.....	159
6.4.3	Results.....	160
6.4.4	Observations	162
Chapter 7	Conclusions	171
7.1	Research Findings	171
7.2	Use Cases	175
7.3	Recommendations for Future Work.....	177
References	178

List of Tables

Table 3-1 Algorithm & computation time. (Mona & Saka, 2019).....	63
Table 4-1 Assigned design parameters. (Kim, Kim, & Eberle, 2013)	67
Table 4-2 Short/long-term composite section properties	74
Table 4-3 Moment due to DC1, DC2 & DW.....	77
Table 4-4 Table 4-5 Shear due to DC1, DC2 & DW	77
Table 4-6 Moment summary due to live load.....	94
Table 4-7 Shear summary due to live load	94
Table 4-8 AASHTO LRFD specifications, table 3.6.2.1-1	95
Table 4-9 Moment summary due to live load including impact factor	96
Table 4-10 Shear summary due to live load including impact fact.....	96
Table 4-11 Excerpt from AASHTO Table 4.6.2.2.1-1	99
Table 4-12 Live load distribution factor summary (interior). AASHTO Tables 4.6.2.2.2b-1 & 4.6.2.2.3a-1	100
Table 4-13 Table 4.10 Live load distribution factor summary (exterior). AASHTO Tables 4.6.2.2.2d-1 & 4.6.2.2.3b-1.....	100
Table 4-14 Multiple presence factor - AASHTO Table 3.6.1.1.2-1.....	102
Table 4-15 Moment summary due to live load.....	103
Table 4-16 Shear summary due to live load	104
Table 4-17 Permanent deformations calculation summary	108
Table 4-18 Calculation summary for flexural resistance of composite section	114
Table 4-19 Calculation summary for nominal shear resistance. Part-1.....	119
Table 4-20 Calculation summary for nominal shear resistance. Part-2.....	120
Table 4-21 Excerpt from AAHTO Table 6.6.1.2.3-1. Detail Categories for Load-Induced Fatigue	124
Table 4-22 Calculation summary for Fatigue I limit state.....	125
Table 4-23 Calculation summary for live load deflection.....	127
Table 5-1 Girder parameters	134
Table 5-2 General Parameters Setup	135
Table 5-3 Constraints table 1 / 6.....	142
Table 5-4 Constraints table 2 / 6.....	143
Table 5-5 Constraints table 3 / 6.....	143
Table 5-6 Constraints table 4 / 6.....	144
Table 5-7 Constraints table 5 / 6.....	144
Table 5-8 Constraints table 6 / 6.....	145

Table 6-1 Optimization output for model 1	152
Table 6-2 Optimization output for model 2.....	156
Table 6-3 Results of model-3, part 1 of 2.....	160
Table 6-4 Results of model-3, part 2 of 2.....	161
Table 6-5 Optimization summary for I-beam bridge, (Mona & Saka, 2019)	169

List of Figures

Figure 1-1 Hypothetical scenario for the fence problem.....	16
Figure 1-2 Search results for documents with mention to "optimization". ScienceDirect	17
Figure 1-3 Performing Topology Optimization with the Density Method - Kristian Jensen	20
Figure 2-1 Desire path example. by Duncan Rawlinson.	24
Figure 2-2 1977 Chrysler Lebaron VS 1993 Dodge Neon. VOX news.....	25
Figure 2-3 Fuel economy by model year – PEW environment group.....	26
Figure 2-4 Example of one iteration through an evolutionary algorithm. Ragsdale, Cliff. Spreadsheet Modeling & Decision Analysis.....	29
Figure 2-5 Excel Solver main dialog window. www.solver.com.....	36
Figure 2-6 Excel Solver, addition of constraints. www.solver.com.....	37
Figure 2-7 Excel solver, results dialog box. www.solver.com.....	38
Figure 2-8 Excel Solver, options for evolutionary method	41
Figure 3-1 King Fahad Causeway Bridge. www.commercialinteriordesign.com.....	43
Figure 3-2 Golden Gate Bridge - California, USA. www.cnn.com	44
Figure 3-3 Beam Bridge example, location: unknown. www.nbmcw.com .	45
Figure 3-4 Concrete box girder bridge, location: unknown. www.shanghaimetal.com.....	46
Figure 3-5 Ting Kau Bridge in Hong Kong. www.alamy.com	47
Figure 3-6 Oregon City Bridge. www. bridgehunter.com.....	48
Figure 3-7 Truss bridge, location: unknown. www.usbridge.com	49
Figure 3-8 Churchill tank. www.britannica.com	50
Figure 3-9 Inglis bridge. www.thinkdefence.co.uk	50
Figure 3-10 Heavily camouflaged Sherman tank crosses a Bailey bridge over the River Santerno near Imola, 12 April 1945. www.thinkdefence.co.uk ...	51
Figure 3-11 Assembly reference. www.vox.com	52
Figure 3-12 Assembly reference. www.vox.com	52
Figure 3-13 Typical cross-section for a composite bridge	54
Figure 3-14 Composite overpass in Al Madinah, Saudi Arabia. www.Constructionweekonline.com.....	56
Figure 4-1 Bridge cross-section. (Kim, Kim, & Eberle, 2013)	66
Figure 4-2 I-beams with extreme proportions	68
Figure 4-3 W24x76 steel profile. (Kim, Kim, & Eberle, 2013)	68

Figure 4-4 Three-dimensional view of the composite bridge. (Mona & Saka, 2019)	70
Figure 4-5 Composite section for interior girder. (Kim, Kim, & Eberle, 2013)	71
Figure 4-6 Non-composite section.....	72
Figure 4-7 Stress profile for a typical simply supported beam	72
Figure 4-8 DC1 dead load components for interior girder	75
Figure 4-9 Side barrier	76
Figure 4-10 Moment diagram due to DC1, DC2 & DW	78
Figure 4-11 Shear diagram due to DC1, DC2 & DW	78
Figure 4-12 HL-93 design truck, longitudinal position. (AASHTO, 2017). 81	
Figure 4-13 HL-93 design truck, transverse position. (AASHTO, 2017)....	81
Figure 4-14 Moment (kN.m) values due to design truck	83
Figure 4-15 Shear (kN) values due to design truck.....	84
Figure 4-16 Moment (kN.m) values due to fatigue design truck	85
Figure 4-17 Shear (kN) values due to fatigue design truck.....	86
Figure 4-18 Tandem load configuration.....	87
Figure 4-19 Real-life tandem trailer	87
Figure 4-20 Moment (kN.m) values due tandem load.....	88
Figure 4-21 Shear (kN) values due to tandem load	89
Figure 4-22 Incremental introduction of lane load.....	90
Figure 4-23 Moment (kN.m) values due design lane	91
Figure 4-24 Shear (kN) values due to design lane.....	92
Figure 4-25 Section geometry showing <i>eg</i>	99
Figure 4-26 Lever rule configuration	101
Figure 4-27 Cross section showing location of PNA	110
Figure 4-28 Flowchart for AASHTO LRFD Art.6.10.7.....	112
Figure 4-29 Flowchart for Shear Design of I-Sections. AASHTO C6.10.9.1-1	115
Figure 4-30 Longitudinal & transverse stiffeners.....	117
Figure 4-31 Maximum spacing of transverse stiffeners	117
Figure 4-32 Effect of Grade of Steel on Fatigue Life. (Fisher, Kulak, & Smith, 1998).....	121
Figure 4-33 Endurance (or S–N) curve. (Fisher, Kulak, & Smith, 1998)..	122
Figure 4-34 Slopes and deflection of beams. (Hibbeler, 2014).....	128
Figure 5-1 Flowchart for Shear Design of I-Sections. AASHTO C6.10.9.1-1	133

Figure 5-2 X-Y scatter graph of selected girder profile	136
Figure 5-3 X-Y scatter graph of bridge cross section.....	136
Figure 5-4 I-Girder geometry	137
Figure 5-5 Populated Solver dialogue box	138
Figure 5-6 Deck overhang & cross frames	140
Figure 6-1 Selected Solver settings	150
Figure 6-2 X-Y scatter graph of original bridge.....	154
Figure 6-3 X-Y scatter graph of model 1.....	154
Figure 6-4 Solution range of model 1 & 2.....	155
Figure 6-5 Span length (m) VS objective function (mm ²)	162
Figure 6-6 Span length (m) VS web height (mm)	164
Figure 6-7 Span length (m) VS web thickness (mm)	165
Figure 6-8 Span length (m) vs cross-sectional area of the different girder components (mm ²)	166
Figure 6-9 Span length (m) vs overhang width (m)	168

Chapter 1

Introduction

Chapter 1 Introduction

1.1 General

One of the earliest instances of dealing with optimization in a student's career dates to high school-level math courses. Students are tasked with solving a shepherd's fencing problem. The problem presents the need to fence the largest possible plot of land. However, to achieve this goal, one is subjected to a number of constraints:

- Limited amount of wire.
- The land needs to maintain a rectangular shape.

Other variants of this problem included a river side as an additional constraint. While the term "optimization" was nowhere to be mentioned, the problem still entailed the three elements that make out and define an optimization problem (Ragsdale, 2007), regardless of the narrative.

- Decision variables: Given the fencing problem, the variables include, but are not limited to, width and height of the land. These can be represented as $X_1, X_2, X_3, \dots, X_n$. In this narrative, these variables can take the form of integer numbers with a (m) or (ft) as a measure of distance. Other narratives may call for decimal numbers.
- Constraints: These are what keeps the problem within the realm of realism, maintaining its integrity and feasibility. Constraints Provide us with rules & boundaries, on which we may act. Given the fencing problem, this could include a fixed amount of wire or a stipulation preventing one dimension from exceeding a certain value. Mathematically represented as:

$$f(X_1, X_2, \dots, X_n) \geq b_2$$

$$f(X_1, X_2, \dots, X_n) = b_3$$

The number of constraints in a problem is not limited to the above constraints. However, as the number of variables and constraints increase, so does the complexity of the problem. All constraints need to be satisfied for a trial to be considered a viable solution.

- **Objective:** This is the end-goal which we aim to achieve. Given the fencing problem, this refers to maximizing the fenced area. The objective function is not always limited to maximization. Other narratives could see benefit in minimizing a value, or even reaching certain values. Mathematically represented as: maximize or minimize $f(X_1, X_2, \dots, X_n)$.

The most primitive way of approaching the fence problem would be to do trial runs until you end with input variables that result in the largest possible output while still maintaining the total wire length constraint.

On the otherhand, take the hypothetical scenario, where a state-wide dispute was concluded with new state borders that traverse a parabolic line on a single property, Figure 1-1.

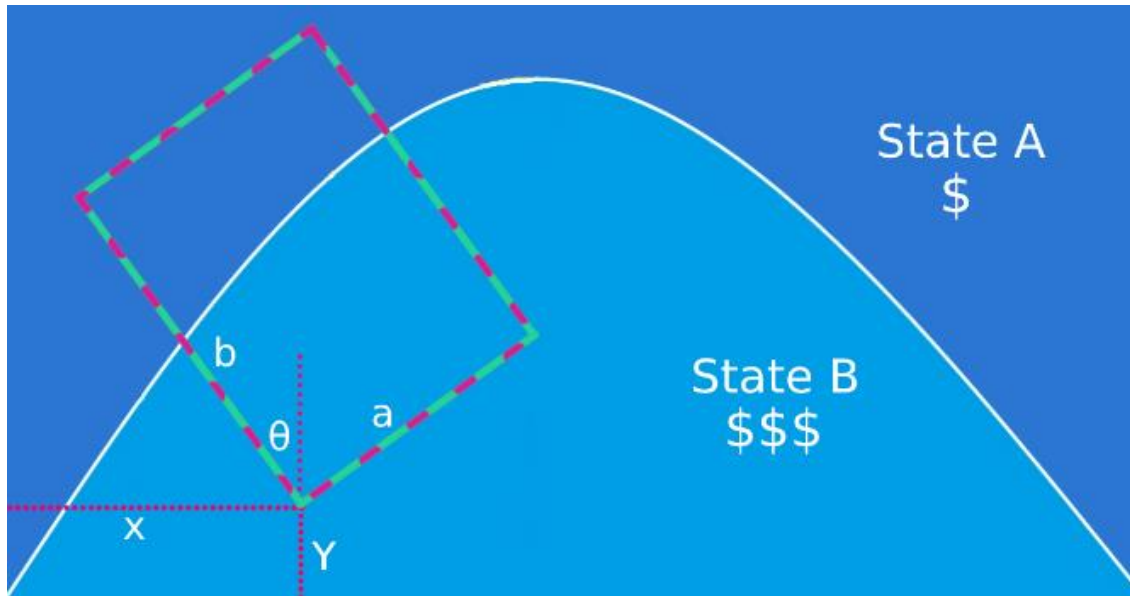
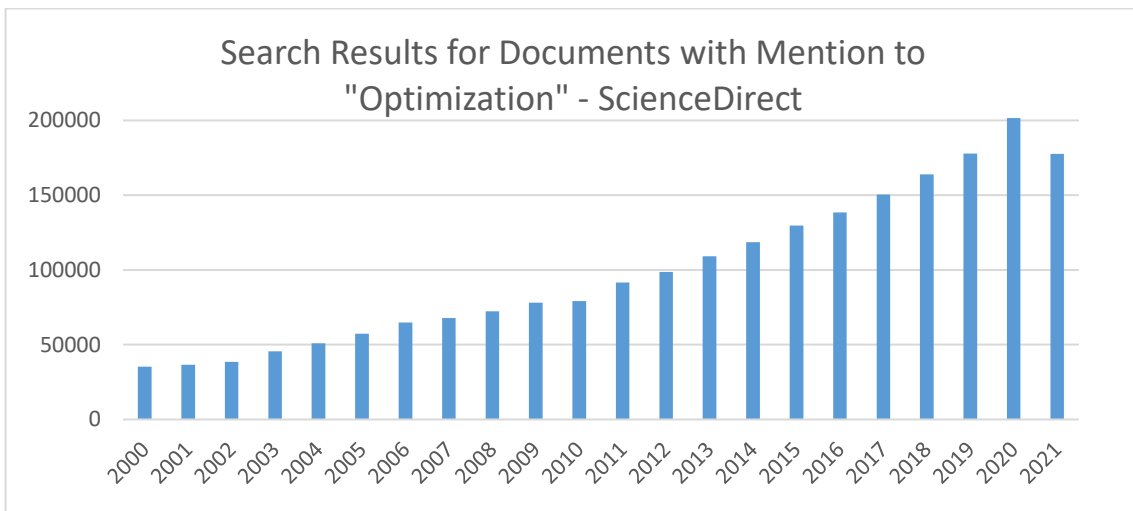


Figure 1-1 Hypothetical scenario for the fence problem

The property owner has the potential to maximize the fenced area on one side of the property with the lowest tax brackets while still maintaining the total wire length constraint. In this case, the width (a), height (b), orientation (θ) & starting point (X, Y), should all be considered as problem variables.

Quickly you come to realize that guessing and checking stops being a viable method, although we are still maintaining the simple scope of maximizing the total area of the fenced land. The constraint entailing a parabolic border will lead to the need to re-approach this problem methodically utilizing calculus and derivatives. Trial-and-error would not scale and could not keep up with the additional constraints.

This field of science is often referred to as optimization (Ragsdale, 2007). And the application of this field is not only limited to logistics and operations research. In fact, the ever-rising number of published scientific papers and articles with mentions to “optimization” should send a clear message that resource allocation and the conscience and mentality of doing as much as possible with (X) while using as little as possible of (Y), has never been so crucial the way it is today, Figure 1-2.



**Figure 1-2 Search results for documents with mention to "optimization".
ScienceDirect**

Limited resourced and increased competitiveness in today’s market can be attributed to the higher demand for optimum solutions. Moreover, the rise in the performance of today’s computers made it seem like an embargo on optimization has been lifted, which explains the onslaught to optimize everything surrounding us. Bridges are no exception.

1.2 Research Problem

Modeling the design procedure of composite plate girder bridges in a spreadsheet format and incorporating the use of commercially available Solver tool to optimize the design for different bridge configurations. While also conforming to the AASHTO provisions, with the objective of reducing the weight of the steel components.

1.3 Research Questions

- Can commercially available tools such as Excel Solver be integrated in the design of highly regulated structures?
- How does this approach compare with existing literature on the topic of bridge optimization.
- How to streamline the optimization process of composite plate girder bridges?
- Does the design improvement justify the metaheuristic nature of this approach?
- How high is the risk of getting stuck in a local optimum solution rather than global optimum?
- Can this method be applied to other engineered products?
- Does the bridge overhang width provide any benefits to the overall design or is it purely aesthetic?
- Is there any relationship between the bridge length and the number of girders?

1.4 Research Objectives

- To establish an optimization model for composite plate girder bridges that utilizes the maximum number of design variables that is yet to be undertaken in the literature.
- To present a bridge model that conforms to the highest number of provisions in AASHTO LRFD Bridge Design Specifications.
- To study the capability of Excel Solver as a readily-available tool for tackling non-linear problems using the genetic algorithm.
- To compare the efficiency of this approach with existing literature.
- To confirm the fidelity and repeatability of the genetic optimization algorithm.
- To quantify any behavior that may arise between the different bridge components.
- To achieve a level of optimization that matches or exceeds that of existing literature.

1.5 Research Significance

Many researchers have the impression that the field of optimization is a perilous path with such high requirements and a steep learning curve that it is almost impossible for an outsider to even get started. There seem to be an unspoken agreement that the term optimization is only analogous to the beautiful 3-D stress diagrams made using finite element analysis, Figure 1-3. This paper aims to refute this consensus.

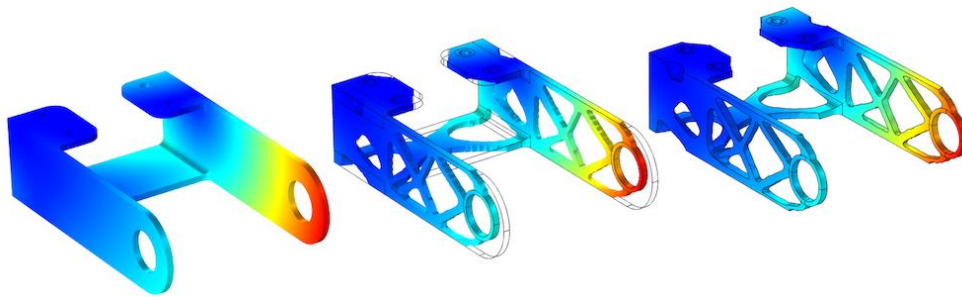


Figure 1-3 Performing Topology Optimization with the Density Method - Kristian Jensen

The significance of this paper far exceeds the field of bridge engineering. First and foremost, it is a showcase of how simple and streamlined the field has become. And also, to highlight that almost any product whose design relies on an iterative process, can be made into a parametric model that implements some sort of genetic optimization, regardless of how intricate and convoluted the design procedure might be.

Moreover, this paper touches on a very fine line, which is the direct and natural interaction between this paper and the AASHTO LRFD provisions. Existing structural design software have blurred the line between the user and the design procedure to an extent. This is by no means a call to abolish the use of structural design software. It is merely a reminder that these packages shouldn't be the only way of proceeding forward.

Finally, with time, the reader will come to notice that the poster child of this document is not the composite plate girder bridge but rather it is the mythology.

1.6 Research Outline

This document comprises 7 chapters.

- Chapter 1 establishes the goals and motives behind writing this paper.
- Chapter 2 presents the topic of optimization as well as the tools to be used.
- Chapter 3 is an introduction to the field of bridge engineering.
- Chapter 4 lays down design aspects procedures unique to the design of bridges.
- Chapter 5 combines the previous chapters into a single procedure.
- Chapter 6 illustrates the results
- Chapter 7 concludes this paper with the conclusion.

Chapter 2

Optimization

Chapter 2 Optimization

2.1 Introduction

Having the title “Design Optimization of Composite Steel Plate Girder Bridges”, it is only right that the initial chapters of this paper begin with a more in-depth introduction on design optimization. Moreover, it is of essence that we lay down some background in order to answer one of the many “Why” questions that may arise.



Figure 2-1 Desire path example. by Duncan Rawlinson.

Why do we optimize? As broad as this question might be, the term “Desire paths” from urban planning can help us shed light on the human nature to optimize for the least resistance. The phenomenon, “Desire paths”, is characterized by flattened, worn out pathways, originally not intended to be where they are, Figure 2-1. These paths slowly cement themselves in cities, campuses and parks. Attracting other commuters, until traversing them becomes the norm.

This behavior highlights our consensus and the human desire to obtain as much as possible by spending as little resources as possible. In this case, it would be traversing the shortest distance in order to reach the target location, even when the reward is as imperceptible as saving 2 seconds of the daily commute.



Figure 2-2 1977 Chrysler Lebaron VS 1993 Dodge Neon. VOX news

In other cases, laws & regulations can be the initiative behind other optimization examples. Take the two vehicles in Figure 2-2. There is no mistaking, the vehicle on the right belongs to a time period that precedes that of the one to the left. This observation is supported by the vehicle's blocky design, comprising a series of three blocks, hood, cabin & trunk. A design trait known for vehicles from the 70's and early 80's. Whereas the sleek body of the vehicle on the left is the result of years of wind tunnel optimization and modern computing techniques. This design is attributed to vehicles from the late 80's onwards.

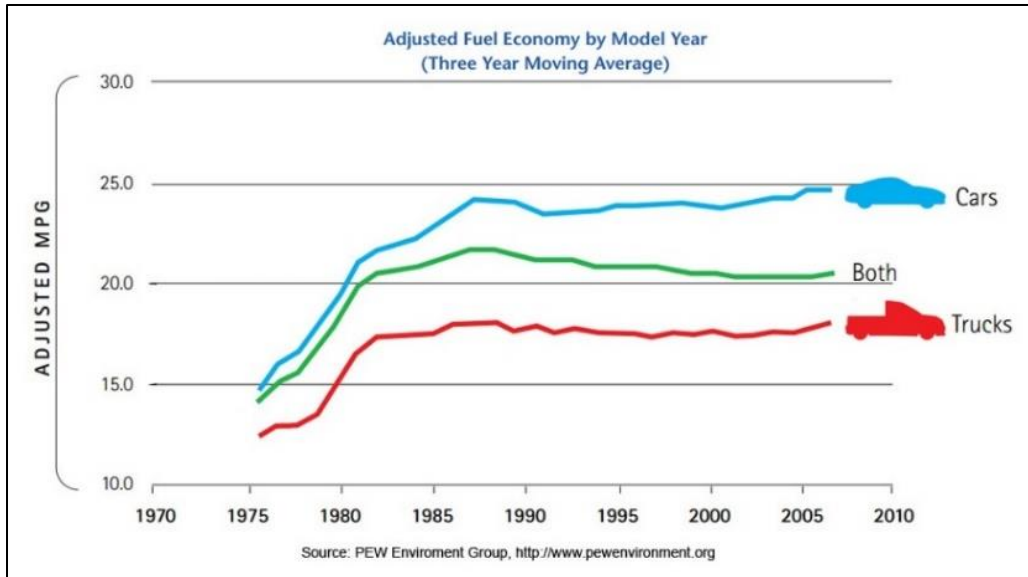


Figure 2-3 Fuel economy by model year – PEW environment group

The shift between the two design models can be attributed, in part, to fuel economy regulations in the late 70's, see Figure 2-3. The increased fuel economy has left automakers with no choice but to find ways to optimize the vehicle design, be it by optimizing the engine block or by exploiting curved edges. As it turned out, adding curves significantly outperformed engine modifications at that time (A Century of Car Design, 2002).

Many other aspects of our lives have been heavily optimized. For instance, take the use of GPS applications with the goal of navigating between two points. The application does not solely rely on the pre-defined routes. Instead, it takes current traffic data and solves its parameters in order to come up with the best route.

Upcoming subsections explore design optimization using nature-inspired search methods. More specifically, the evolutionary algorithm, which falls under the broader umbrella of optimization techniques with the name of genetic algorithms.

2.2 Evolutionary Algorithm

Evolutionary algorithms rely on mimicking the principle of “survival of the fittest” in nature, in order to find the best solution. The underlying procedure intends to simulate the problem as a biological system, where living beings evolve, mutate and reproduce with each iteration (generation) (Arora, 2016). Hence the use of the term evolution or evolutionary.

As futuristic as this algorithm might seem, you would be surprised to know that several studies on this topic have been released over 30 years ago (Goldberg & Holland , 1988). Many researchers took interest in this field. Not only that but some went as far as developing their own techniques that carry resemblance to other biological phenomena such as ant colonies (Dorigo, 1992). Others saw bird swarms as the source of inspiration for their algorithm (Kennedy & Eberhart, 1995).

The appeal of using evolutionary algorithms can be attributed to the following points (Ragsdale, 2007):

The use of genetic algorithms is not contingent on the problem variables being discrete or continuous. Discrete variables are characterized by gaps and discontinuities in the values that they can carry. They present themselves in problems where a variable can only be in increments of (2 cm) as an example. Material availability and municipal design codes heavily influence the variable type, being continuous or discrete.

Instances where the design procedure splits into two or more different branches depending on a condition. Such cases result in problems that cannot be modeled accurately using linear functions. Non-linearity disqualifies many of the conventional optimization techniques. However, evolutionary algorithms have been shown to tackle non-linearity successfully.

The working mechanism of evolutionary algorithms is summarized in Figure 2-4. The problem context is irrelevant to the procedure. Suffice to say, this problem involves 4 decision variables with the objective of maximizing a function value.

INITIAL POPULATION					
Chromosome	X ₁	X ₂	X ₃	X ₄	Fitness
1	7.84	24.39	28.95	6.62	282.08
2	10.26	16.36	31.26	3.55	293.38
3	3.88	23.03	25.92	6.76	223.31
4	9.51	19.51	26.23	2.64	331.28
5	5.96	19.52	33.83	6.89	453.57
6	4.77	18.31	26.21	5.59	229.49
7	8.72	22.12	29.85	2.30	409.68

CROSSOVER & MUTATION					
Chromosome	X ₁	X ₂	X ₃	X ₄	Fitness
1	7.84	24.39	31.26	3.55	334.28
2	10.26	16.36	28.95	6.62	227.04
3	3.88	19.75	25.92	6.76	301.44
4	9.51	19.51	32.23	2.64	495.52
5	4.77	18.31	33.83	6.89	332.38
6	5.96	19.52	26.21	5.59	444.21
7	8.72	22.12	29.85	4.60	478.93

NEW POPULATION					
Chromosome	X ₁	X ₂	X ₃	X ₄	Fitness
1	7.84	24.39	31.26	3.55	334.28
2	10.26	16.36	31.26	3.55	293.38
3	3.88	19.75	25.92	6.76	301.44
4	9.51	19.51	32.23	2.64	495.52
5	5.96	19.52	33.83	6.89	453.57
6	5.96	19.52	26.21	5.59	444.21
7	8.72	22.12	29.85	4.60	478.93

Diagram annotations: Arrows labeled 'Crossover' point from the X₃ and X₄ cells of Chromosome 2 in the 'CROSSOVER & MUTATION' table to the X₃ and X₄ cells of Chromosome 1. Arrows labeled 'Mutation' point from the X₃ and X₄ cells of Chromosome 4 to the X₃ and X₄ cells of Chromosome 7.

Figure 2-4 Example of one iteration through an evolutionary algorithm. Ragsdale, Cliff. Spreadsheet Modeling & Decision Analysis

- Multiple sets are generated, where each set is the same problem solved with different random input variables. Each of the generated sets is referred to as a “chromosome”.
- All generated sets are referred to as “population”. This problem has a population size of 7.

- Decision variables within each chromosome are referred to as “genes”. The 4 variables are (X1, X2, X3, X4).
- Each of the generated sets “chromosome” can either be a feasible solution or not, depending on the objective function. The result of the objective function is referred to as “fitness”. This example aims to maximize the fitness value.
- The best fitness for the first generation has a value of 453.57.
- In order to improve the first generation, a series of operations are performed. These include crossover, mutation and reproduction:
 1. Crossover: the process of exchanging genes between the different chromosomes. Given Figure 2-4, the variables X3 and X4 from the sets #1 and #2 are exchanged respectively. Thereby creating new sets with different fitness results.
 2. Mutation: the term implies the probability of a variable “gene” being altered. As the case with set #3, the value of X3 has mutated from being 23.03 to 19.75. The result of this mutation can be observed in the increased fitness function, shifting from 223.31 to 301.44. The premise & purpose of mutation is to randomly explore design aspects that otherwise would not be used.
 3. Reproduction: It is important to note that both, crossover and mutation can result in cases where the new set is inferior to the one that proceeds it. Taking that into consideration, reproduction is performed in order to safeguard the population quality from degrading. This is done by maintaining the best performing sets and copying them into the next generation. The crossover that occurred on set 5# resulted in a reduced

fitness value. However, since set #5 had the best fitness initially, it is copied into the next generation and the resulting crossover is disregarded. Best performing sets are referred to as “population leader/s”.

The probability with which crossover and mutation occur is up to the researcher to finetune, depending on the nature of the problem, number of variables, population size and many other factors.

The procedure is repeated. Each time resulting in a new population that evolve over time until the number of generations exceeds a predefined value or until the improvement in the fitness function is less than a predefined tolerance value.

2.3 Evolutionary Algorithm Drawbacks

It should be made clear that using evolutionary algorithms or any of the nature-inspired search methods does come at a cost. The tradeoff involved is the result of this approach being stochastic - also known as heuristic or metaheuristic –. That is, it relies on probability. The opposite of stochastic is deterministic approaches, which have been shown to fall short with discrete variables and non-linear problems. You will come to note that stochastic search methods circumvent the use of calculus by relying on probability and statistics.

Firstly, the word stochastic entails the notion that the resulting solution is a local optimal solution. Meaning that a better solution may exist, and there is no direct way of locating it. This uncertainty is inescapable. However, running the problem multiple times with different initial arguments may help in ensuring that the final solution is within an acceptable tolerance of the global optimum solution.

Secondly, solution re-productibility or rather the lack thereof is a point that further highlights the stochastic behavior. There is no guarantee that after running the optimization procedure on different devices or even at different times, both will have the same result. Nevertheless, modern optimization techniques make use of a “seed” variable that aims to eliminate total randomness and assist with re-productibility.

Additionally, there is no rule of thumb when it comes to specifying the stopping criteria for stochastic search methods. It is up to the researcher's judgement to finetune the environment in order to strike a balance, where the problem does not stop too early or run for an arbitrarily long period of time.

Finally, stochastic approaches can be deemed as biased randomness, where the bias is tailored and tweaked to fit the problem. This fact does carry a negative connotation. However, in cases where the optimization landscape is as broad as we will soon come to see with bridges, then there is no alternative but biased randomness.

2.4 Excel Solver

Technological advancements in the field of computer science meant that many of the proposed optimization theories and techniques could finally be tested and pushed to their limits. It took no time for the evolutionary algorithm to be commercialized and made available to the market.

The company “Frontline Systems” succeeded in 1999 by publishing a tool with the name of “Premium Solver V3.5”. The tool was bundled with Microsoft’s flagship application, Excel. And it included a state-of-the-art implementation of the genetic algorithm, outperforming competitive solutions at the time. The fact that the tool came pre-installed with Excel resulted in a wider range of users and applications. Nowadays, this tool is referred to as “Excel Solver” and it provides the user with a total of 3 methods to pick from for solving any system of equations. Moving onwards, this paper focuses exclusively on the evolutionary algorithm. For the sake of listing, the methods available are:

- GRG Nonlinear (Generalized Reduced Gradient).
- Simplex LP.
- Evolutionary.

The use of Excel solver spans a wide spectrum of applications & operation research problems. Some include:

- Capital budgeting: used to maximize the NPV (Net Present Value) by determining the optimum combination of projects to undertake under a limited budget.
- Inventory management: used to optimize the EOQ (Economic Order Quantity), which results in a more efficient stock levels and an overall better cash-flow.
- Portfolio optimization: used to construct stock portfolios with maximum return on investment while minimizing risk based on historical data.
- Crew scheduling: used in assigning airline flights while ensuring trips begin and end in the same city for the respective staff member.

2.5 Excel Solver Example

The aim of this subsection is to present a simplified summary, showcasing the basic setup and formulation of a problem using Excel Solver. For a more comprehensive series of steps & extensive examples, the reader is encouraged to follow up with Frontline Solver's official website, www.solver.com (Step by step guide for Excel's Solver, n.d.)

The goal of the provided spreadsheet example is to determine the most profitable combination of 4 panel types to be manufactured (Tahoe, Pacific, Savannah, Aspen). Each panel has its own profit margin as well as the required raw material quantities. The total raw material available in stock is provided as a constraint that should not be exceeded.

	Panel Type				
	Tahoe	Pacific	Savannah	Aspen	
4 Pallets	0	0	0	0	Total Profit
5 Profit	\$450	\$1,150	\$800	\$400	\$0
	Resources Required per Pallet Type				Used Available
8 Glue	50	50	100	50	0 5,800
9 Pressing	5	15	10	5	0 730
10 Pine chips	500	400	300	200	0 29,200
11 Oak chips	500	750	250	500	0 60,500

Figure 2-5 Excel Solver main dialog window. www.solver.com

- The problem is formulated and is laid out the way it would normally be done in Excel spreadsheet. That is, no special structure is dictated, and cells are free to reference other cells or maintain equations.

- Once enabled in the toolbar, Excel Solver window is launched, prompting the user for the basic Solver parameters, Figure 2-5.
- The input field titled “Set Objective” references the objective function, which we aim to maximize. Cell “F5” (highlighted in blue) is selected.
- The radio button titled “Max” is selected since the goal is to maximize total profit.
- The input field titled “By Changing Variable Cells” references the decision variables which are set to be modified until an optimum solution is found. Cells “B4 to E4” (highlighted in green) are selected.
- By clicking the button “Add”, a new dialog box prompting the user for problem constraints, is shown. Cells “F8 to F11” (highlighted in red) are selected as the reference cells while cells “G8 to G11” are selected as the constraints. In this case, the logical operator “<=” is selected to ensure that the cells highlighted in red should never exceed its counterpart constraints, Figure 2-6.



Figure 2-6 Excel Solver, addition of constraints. www.solver.com

- The input field titled “Select a Solving Method” is used to method of choice. As previously noted, the evolutionary method is the primary scope of this paper. However, the provided example uses the “Simplex LP”.

- By clicking the button “Solve”, the Solver process is initiated. Depending on the problem complexity, it may take several seconds or several minutes or even more until one of the stopping criteria is met. In cases where the problem has been incorrectly formulated, a message box conveying the error type would be returned to the user.
- The resulting output of this problem indicates that one of the most profitable combinations, is one that completely omits the sale of the 4th panel type, Aspen. See Figure 2-7 for complete results breakdown.

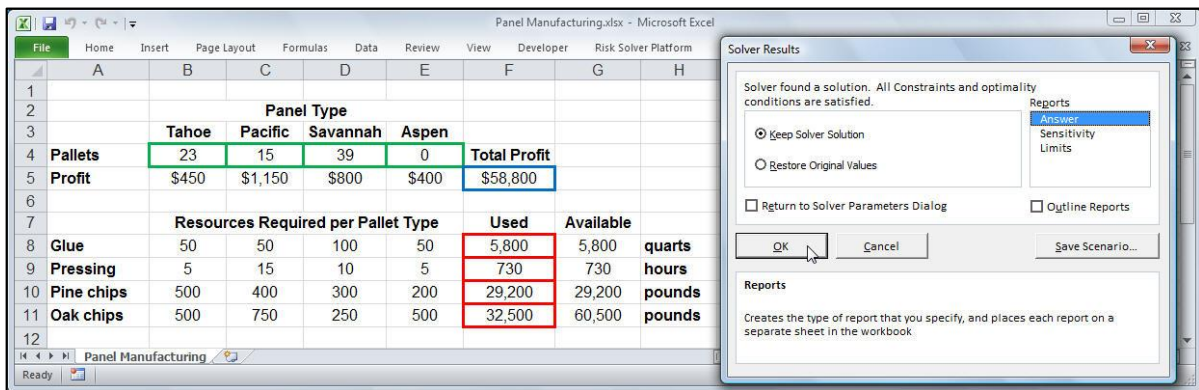


Figure 2-7 Excel solver, results dialog box. www.solver.com

To sum up, the procedure is best applied to problems that originally rely on iterative solution processes. This can be said of operation research problems or even the design of structural elements such as the superstructure of a bridge, as we will soon come to see. Moreover, the nature of the mutation operator incentivizes the problem to explore unconventional situations such the one explored in the example above.

2.6 Making the case for Excel Solver

The ability to solve both, linear and non-linear system of equations is not exclusive to Excel Solver. Other tools with similar functionality do exist. Among these are Mathematica and MATLAB. Nevertheless, this subsection is provided to make a case for using Excel Solver by listing some of the major benefits and advantages:

- The likelihood of an individual with an engineering or science degree, having dealt with Excel spreadsheets is much higher than that for any other optimization tool. Not only that but also the exposure to Excel is likely to have taken place at the undergrad level, if not prior. This exposure here implies the user is well-equipped to tackle most of what is required of him using Excel. Moreover, it has become the industry standard when it comes to basic planning, project management and overall bookkeeping. This is further substantiated by the widespread use of macros and VBA (Visual Basic for Applications) functions that serve to further automate most of the tedious work on daily basis.
- Solver is a part of a much bigger set of tools developed by Frontline Systems. The free of charge version that comes bundled with Excel provides the user a total of 200 decision variables and up to 100 design constraints. These numbers are sufficient to tackle many engineering problems. Problems with higher number of decision variables or design constraints can still be solved using the default Solver version. However, additional steps should be taken to divide the problem into multiple sub-problems.

- Many of the parameters that govern the optimization methods are made available to the user to be modified and finetuned through a user-friendly GUI (graphical user interface), Figure 2-8.
- Problems with complex flow charts, comprising multiple “if-condition” branches can easily be formulated in an understandable fashion. This way, relations between the different design variables can be better understood.
- Optimization remains a well-frequented topic of research. However, the design of composite steel plate girder bridges remains by large unexplored territory.

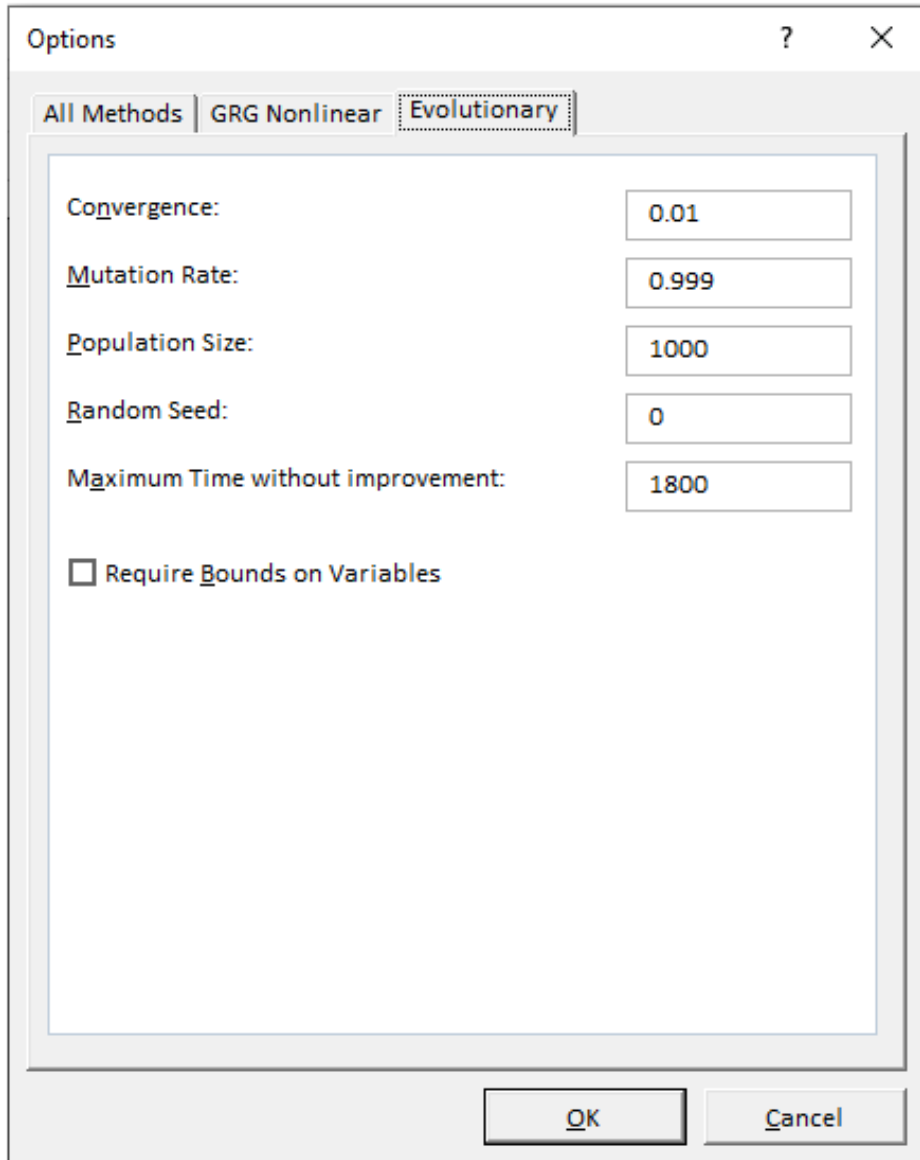


Figure 2-8 Excel Solver, options for evolutionary method

Chapter 3

Bridge Engineering

Chapter 3 Bridge Engineering

3.1 Introduction

The transportation network, more specifically bridges, are one of the key structures that govern our daily commute. We've become used and desensitized to these structures so much that crossing one stopped being an opportunity to marvel at this engineering feat. Instead, it became a chance to express our inconvenience as our vehicles hit an in-need-for-repair expansion joint. Whenever the word "bridge" is brought up, the first image to come to mind is that of the King Fahad causeway, at least for residence of Bahrain and the Eastern Province of Saudi Arabia, Figure 3-1. While the image would be to that of the Golden Gate bridge for residence of California in the United States, Figure 3-2.



Figure 3-1 King Fahad Causeway Bridge. www.commercialinteriordesign.com



Figure 3-2 Golden Gate Bridge - California, USA. www.cnn.com

This consensus takes place across all lands and countries. The economical, historical and geopolitical impact of these bridges is undeniable. However, the general mindset seems to disregard the common highway bridge. Moreover, this structure has been stripped of the name “bridge” and replaced with the word “overpass”. Further diminishing their significance, further contributing to them being underappreciated.

Lifetimes of research and countless tragedies that befell bridges in the modern human history still linger in the design of your average highway overpass. Even after commissioning new overpasses had stopped being a ceremony worthy of ribbon-cutting, they do remain by large an engineering feat worthy of admiration.

This chapter concerns itself with bridges as a general overview, without delving into the design parameters and constraints behind the design process.

3.2 Bridge Types

Bridges come in many shapes and forms based on their structural systems. The list below provides a brief overview for each bridge category:

1. Beam bridge or Slab-on-Girder bridge: The backbone of any transportation network. These bridges comprise a deck, usually made of concrete that rests on top of longitudinal beams. This configuration is not exclusive to steel beams as the same design could benefit from a precast prestressed concrete beam where needed. See Figure 3-3.



Figure 3-3 Beam Bridge example, location: unknown. www.nbmchw.com

2. Steel and Concrete Box Girder bridge: These bridges take advantage of their high torsional rigidity and are deployed especially for curved roads. These structures make use of a reinforced concrete box that is integrated with the slab or a steel box. See Figure 3-4. This bridge configuration is capable of meeting longer spans than that of the slab-on-girder bridges (Zhao & Tonias, 2017).



Figure 3-4 Concrete box girder bridge, location: unknown. www.shanghaimetal.com

3. Cable-Stayed bridge: Considered to be the bridge of choice for medium- and long-span bridges spanning as much as 1000 m, particularly due to the ease of construction and low cost. This might contradict initial assumptions about these structures, this is due to the fact that construction does not require falsework or shoring for the bridge spans. Instead, construction sequence propagates from the bridge pylons (towers) in both directions. See Figure 3-5.



Figure 3-5 Ting Kau Bridge in Hong Kong. www.alamy.com

4. Arch bridge: The highlight of urban cities. preferred mainly where bridge aesthetics are of major concern. Arch bridges with span length of 300 m have been constructed before, which makes them a suitable choice for medium-span bridges.

The term arch bridge in this case could encompass multiple bridge arrangements. In cases where the bridge deck is partially or fully suspended from the arch, the design is referred to as through arch bridge. In case the bridge deck rests on top of the arch, design is referred to as deck arch bridge (Zhao & Tonias, 2017). See Figure 3-6.



Figure 3-6 Oregon City Bridge. [www. bridgehunter.com](http://www.bridgehunter.com)

5. Truss bridge: A historical marvel, considered to be the bridge of choice one century ago. However, the use of this design has since fallen by the wayside. It is highly unlikely that such a design would be constructed nowadays. This is in part due to these structures' constant need for maintenance, and mostly since truss structures are typically fracture-critical. This term indicates that the failure of one member would lead to compromising the integrity of the entire structure (Zhao & Tonia, 2017). See Figure 3-7.



Figure 3-7 Truss bridge, location: unknown. www.usbridge.com

The list above by no means cover all bridge types. However, it serves to provide a glimpse on the possible directions that a bridge may take. Evidently, the main purpose of this structure is to lay safe ground for us to cross from one point to another.

3.3 Honorable Mention – Bailey Bridge



Figure 3-8 Churchill tank.
www.britannica.com

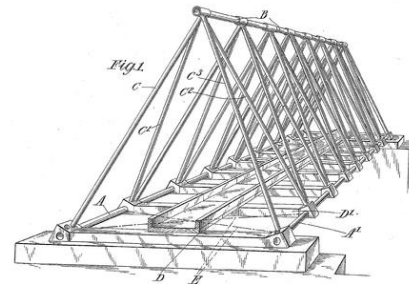


Figure 3-9 Inglis bridge.
www.thinkdefence.co.uk

The Churchill tank, a British infantry unit used in the second World War, Figure 3-8. At 40-45 Tons, the Tank has fallen victim to its own strength, its weight and heavy armor. Designed and deployed to be a counter offensive, yet it stood still as its weight was too much to handle for the heavily bombarded bridges. Even military-grade portable bridges such as the Inglis bridge could not help but buckle under the tank's weight, Figure 3-9.

Upon presenting a design concept by Donald Bailey, further investigation has been immediately authorized and work began the following day. Subsequently leading to the development and deployment of the Bailey bridge. A prefabricated portable bridge design, Figure 3-10.



Figure 3-10 Heavily camouflaged Sherman tank crosses a Bailey bridge over the River Santerno near Imola, 12 April 1945. www.thinkdefence.co.uk

Irrespective of the mythology, with which the design was brought to light. The bridge had to adhere to very specific design constraints, namely:

- Bridge construction should allow for a modular and adjustable design to accommodate different spans and terrains.
- Refrain from using Aluminum alloys, given that construction of airplanes had been a priority at the time.
- Single panels should not exceed the carrying capacity of a six-man load. See Figure 3-11, Figure 3-12.
- Parts should fit in a standard 3-ton lorry.

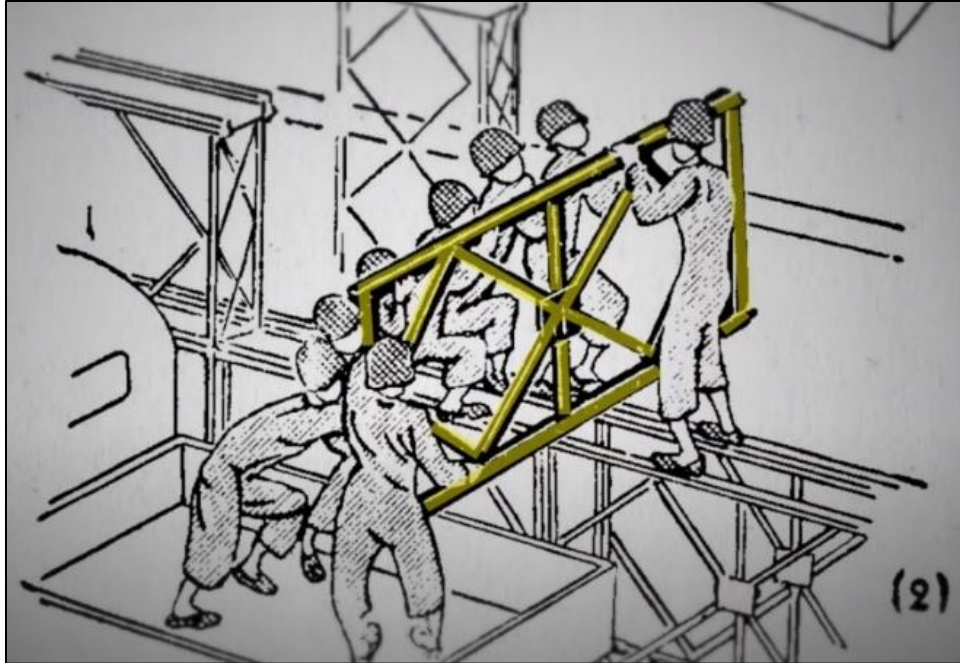


Figure 3-11 Assembly reference. www.vox.com

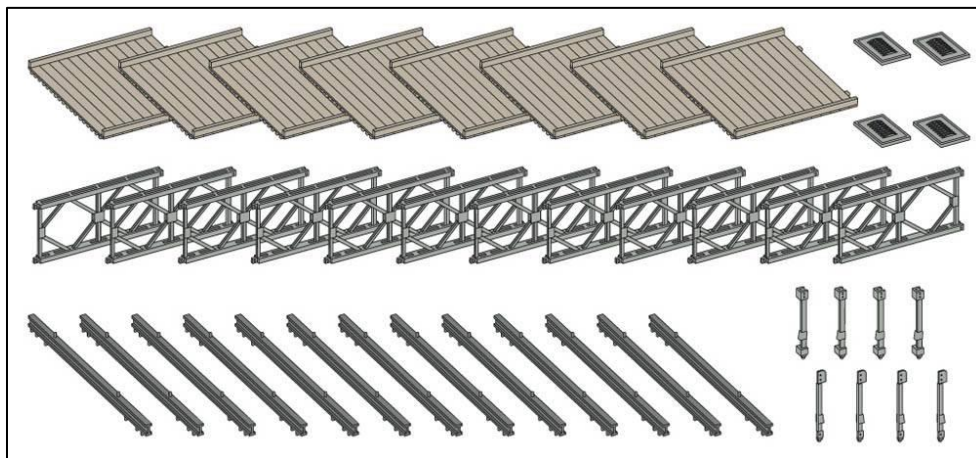


Figure 3-12 Assembly reference. www.vox.com

With over 4000 Bailey bridges erected between 1943 and 1944 alone, these constructions became an indispensable factor that contributed to shortening the course of war (Joiner, 2011). This historical event further highlights the impact of bridges in times of both, peace and war.

3.4 Composite Bridge

The choice of bridge type is not a decision that can be concluded directly. In most cases, the development and deployment of new bridges is accompanied yet by newer roads to the existing transportation network. Subsequently contributing to the overall project cost. The process with which, the bridge type is selected can be a function of multiple factors; these factors are not weighted equally and cannot be generalized for all projects, as each bridge presents a unique case with its own constraints and limitations:

- The overall distance to be bridged: For spans up to 40 m, a girder bridge is recommended. For spans ranging between 40 m and 61 m, both girder & arch bridges may be recommended (Narendra, 2014).
- Underpass clearance: Existing site conditions may limit girder selection to a shorter profile.
- Road geometry: Horizontal curvature or the lack of curvature.
- Aesthetics of surrounding environment.
- Environmental concerns.
- Traffic volume.
- Material availability: Supply chain disruptions such that of the years 2020-2021 could lead to a significant cost additions.

This paper focuses solely on the girder type bridge. The following terms are all used interchangeably to reference this bridge type:

- Beam bridge / girder bridge
- Slab-on-girder bridge
- Composite bridge
- Composite steel plate bridge
- Slab-steel bridge
- Orthotropic steel bridges

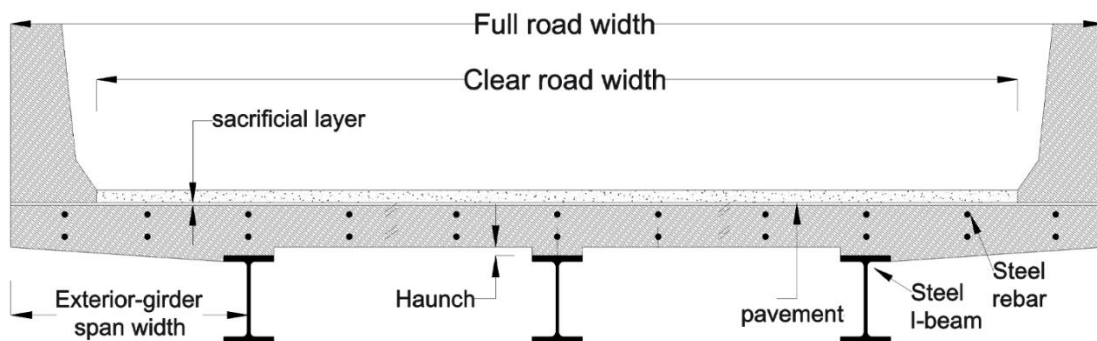


Figure 3-13 Typical cross-section for a composite bridge

The reasoning behind the selection of this bridge type is the fact that this design is mostly suitable for short-to-medium span crossings, spanning up to 90 m. Given the typical traffic network, these bridges represent a prime candidate when it comes to bridging an overpass over the typical two-lane two-way urban highways. Furthermore, the ubiquity of this bridge in our daily commute calls for further attention and care.

The shift to this bridge type for highway overpasses can be attributed to the following:

- **Simple design:** It should be noted that simplicity is a relative term. Especially when compared with available bridge arrangements. The design procedure presents a typical structural analysis process that, for the most part, does not lay new and out of the ordinary problems and issues to solve. In fact, with rigorous and meticulous planning, initial profile sections can be accurately obtained without the use of high-end design methods like finite element method and wind simulators.
- **Construction process:** Available codes permit the use of unshored construction for girder bridges. The structural contribution from unshored construction is a point that will be discussed in later sections. However, the general premise is that during construction, beams require no falsework.
- **Uniformity:** Uniformity lays fertile ground for standardization potential. Thereby streamlining the design process. Right from the very outset of the project, design constraints and limitations would be loud and clear, courtesy of available codes.



Figure 3-14 Composite overpass in Al Madinah, Saudi Arabia.
www.Constructionweekonline.com

Design of composite bridges is not restricted to certain girder types or materials, enabling the design to benefit from steel girders or precast prestressed concrete beams. Apart from this, the use of both, hot rolled steel profiles and plate girders (built-up profiles) is permitted. In fact, a design combination of a hot rolled section with additional plates welded to the flanges has been deployed before (Narendra, 2014).

The provision of shear studs along the length of the top flange ensures that both materials, concrete and steel will act in unison in resisting dead loads as well as vehicular live loads.

Additionally, construction sequence stipulates that the steel girders be unshored, making them fully subjected to their own dead load as well as the load of the freshly poured concrete deck. Once hardened, the resulting composite section (steel girders + hardened concrete) begins contributing to the bridge's structural integrity by bearing live vehicular loads and any subsequently added loads, such as that of the wearing surface (asphalt).

Deviations from the shoring stipulation and construction sequence are permitted. However, the provided equations and provisions are no longer valid and different equations should be derived to reflect the actual construction sequence.

3.5 Design Code

Nowadays, the design of almost all structural elements is a process that is heavily regulated by government or municipal agencies, bridges are no exception to this rule. One of the most prominent design codes for bridges is the AASHTO LRFD Bridge Design Specifications (AASHTO, 2017). This is a probabilistic code that regulates the design of bridges. Used not only in the United States, but also in many other countries here in the region.

For example, the Ministry of Municipal & Rural Affairs in Saudi Arabia is the governing agency that overlooks the design of bridges, and it has published its own design manual, which adopts many excerpt & provisions from the AASHTO code (Ministry of municipal & Rural Affairs, 2013). While outside the scope of this paper, brief skimming of this document reveals that the live loads used in the Saudi release are twice as high as the ones in AASHTO code.

Moving onwards, “AASHTO LRFD Design Specification” and “AASHTO code” will be used interchangeably.

Lastly, comprehensive understanding and being able to navigate through the code’s provisions are necessary skillsets required by anyone who wants to take up bridge engineering. The design procedure followed in this paper conforms to the 8th edition of the AASHTO code which follows the imperial system. Units have been transformed to their SI equivalents, which explains the lack of whole numbers in the presented design problem.

3.6 Design Philosophy

When it comes to evaluating the capacity of a structure under stress, there are two main schools of thought:

1. ASD (Allowable Stress Design): also known as the Working Stress Design (WSD). This design philosophy assumes that the material is linearly elastic. The allowable stress under this theory is computed by dividing the material strength by a factor of safety. This method was mainly used for reinforced concrete structures from the early 1900s until the early 1960s (Narendra, 2014). By the year 2007, the use of this approach became history (Zhao & Tonia, 2017).
2. LRFD (Load and Resistance Factor Design): This approach strives towards a ductile failure, that is a predictable failure that can be observed ahead of total collapse. This is achieved by utilizing the in-elastic portion of the stress-strain curve, where the entire material cross section has yielded. This method addresses the different failure conditions based on the reliability theory (probability based method). Where each condition is referred to as a limit state. Moreover, uncertainties in both, applied loads and material are addressed separately using different load factors. The LRFD design philosophy is the method used in the AASHTO code.

The LRFD method recognizes 4 different limit states that should be checked for every structure member.

- **Strength:** directly related to the overall integrity and safety of the structure. Violating this limit state implies the bridge is unstable and unsafe for use.
- **Service:** often referred to as serviceability limit state. Addresses concerns that may not be detrimental to the structural integrity of the bridge. Among these concerns are:
 - a) **Deflection:** excessive deflection conveys the perception of failure to pedestrians, despite the bridge being structurally sound.
 - b) **Vibration:** excessive vibration is undesirable, especially for bridges that carry pedestrian traffic. Vibration is indirectly mitigated by deflection limits.
- **Fatigue:** repeated cyclic loading can lead to member failure even when the load is well below the ultimate load. This limit state is presented in detail in the upcoming chapter.
- **Extreme event:** refers to the survivability of the structure in events of vessel collision, ice flow and extreme earthquakes.

Under all limit states, the total factored force effect is taken as

$Q = \sum \eta_i \gamma_i Q_i$	AASHTO eq. 3.4.1-1
--------------------------------	--------------------

Where:

- η_i = load modifier related to the structure's ductility. Taken as $\eta_i = 1$ for most bridges.
- γ_i = load factor, given in AASHTO table 3.4.1-1.
- Q = force effect.

Upcoming chapter presents an AASHTO LRFD design example highlighting processes that are unique to bridge engineering.

3.7 Literature Review

The interest in bridge optimization can be traced back to the mid 60's. Where possibly one of the earliest papers that covered this topic has been released, (Torres, Brotchie, & Cornell, 1966). The authors tackled cost optimization of a single-span prestressed concrete bridge. The paper presented an all-inclusive objective function covering construction, material, erection and transportation costs, while also adhering to the AASHTO provisions. The written program made use of the Piecewise linear optimization method, with no direct mention of the coding language used.

Whereas (D. Goldberg, 1986) is considered to be the first to make use of the genetic algorithm for structural engineering, showcasing that this approach is capable of converging to near optimum solutions only by exploring a fraction of the population space.

Few decades later and the term “optimization” has become a branch, of which multiple subfields and disciplines have emerged. Research progressed to a degree where new methods are conceived with the intent of replicating natural phenomena or the behavior of different animals and colonies.

(Mona & Saka, 2019) is an example that made use of 4 different metaheuristic algorithms to optimize the design of two types of bridges. Namely, I-beam (composite) and tied-arch bridges according to AASHTO LRFD specifications. The table below shows the different algorithms with the respective computation time for optimizing the I-beam bridge.

Table 3-1 Algorithm & computation time. (Mona & Saka, 2019)

<i>Algorithm</i>	<i>Time (minutes)</i>
<i>Artificial bee colony algorithm (ABC)</i>	1254
<i>Biogeography-based optimization algorithm (BBO)</i>	2613
<i>Exponential big bang-big crunch algorithm (EBB-BC)</i>	1211
<i>Symbiotic organisms search algorithm (SOS),</i>	5273
<i>Enhanced artificial bee colony algorithm (EABC)</i>	Not applicable

The author made use of application-programming interface (API) functionality within SAP2000, which acted as a direct link to MATLAB, where the algorithms have been written. This approach was successful in tackling a number of constraints that ranged between 13 and 62, based on the bridge model. Finally, the proposed method showed a 13.06% and 13.20% reduction in the bridge weight for both, I-beam and tied-arch bridges.

Another publication that is highly related is a paper by (Faluyi & Arum, 2012), where performance of the generalized reduced gradient algorithm (GRG) within Excel Solver, was compared with the constrained artificial bee colony algorithm (CABC), for optimizing a plate girder. Key note for this reference is the fact that this paper investigated design of plate girders as independent beams subjected to predefined loading scenarios, not as a part of a bridge structure. Paper concluded with a 7.44% and 7.25% reduction in girder cross sectional area for (GRG) and (CABC) respectively.

While outside the scope of bridge engineering, it is no surprise that other fields made use of optimization and its widespread use cases. Even more specifically by implementing Solver tool. The work of (Briones, Morales, Iglesias, & Morales, 2019) has shown the potential of using Solver in the field of chemical engineering to find the optimum distillation sequences that minimize the overall operational costs. The paper highlighted the applicability of non-specialized software. Namely, Solver.

Aspects unique to this paper that sets it apart from available literature include the overall scale of the operation. There is yet to be a documented example making use of the commercially available Excel Solver tool as way of optimizing entire bridge superstructures. (Mona & Saka, 2019)'s paper makes similar remarks, highlighting the fewer number of publications in the field of engineering. Up to this point, Solver was never allowed to be the brain behind optimizing a full structure.

To sum up, much of the endeavors made here, are in a way, an extension to all of the literature above.

Chapter 4

Design Example

Chapter 4 Design Example

The objective of this chapter is to showcase the AASHTO LRFD structural design procedure using an example that has been selected from (Kim, Kim, & Eberle, 2013). Design concepts unique to bridge engineering will be presented in detail whereas repeated & conventional processes will be supplanted as an appendix.

4.1 Problem Parameters

The design problem presents a 12.2 m single-span composite steel I-girder bridge with a full width of 14.2 m, which is to be designed according to the AASHTO LRFD provisions. 6 steel girders with the profile W24x76 have been selected. Bridge cross section is presented in Figure 4-1. Further design parameters are listed in Table 4-1

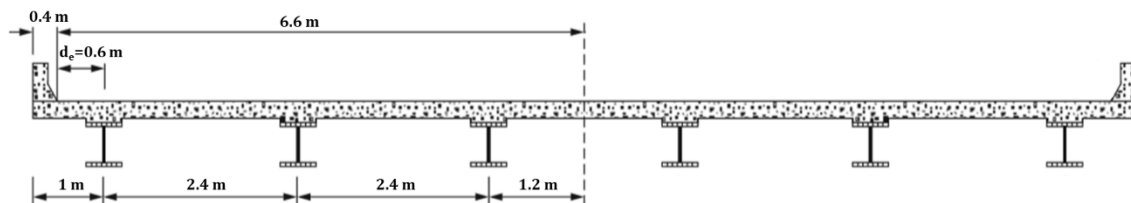


Figure 4-1 Bridge cross-section. (Kim, Kim, & Eberle, 2013)

Table 4-1 Assigned design parameters. (Kim, Kim, & Eberle, 2013)

Variable	Description	Value
L	Span length	12.2 m
BW	Side-barrier weight	7.30 kN/m
f'_c	Concrete strength	31.0 MPa
ADTT	Average daily truck traffic in one direction	2500
W_{FWS}	Future wearing surface load (asphalt)	0.172 MPa
d_e	Distance from the centerline of the exterior girder to the interior edge of curb or traffic barrier	0.61 m
S	Girder spacing	2.44 m
W_c	Concrete unit weight	2400 kg/m ³
f_y	Specified minimum yield strength of steel	414 MPa
t_s	Slab thickness	203 mm
E_s	Modulus of elasticity for steel	200 Gpa
E_c	Modulus of elasticity for concrete	26.4 Gpa
	Load of stay-in-place metal forms	0.335 kN/m ²
	Number of cross-frames	3
	Design fatigue life	75 year
	Steel profile	W24 x 76
	Haunch height	50.8 mm

4.2 Proportional Limits

The proportional limits are a set of rules stipulated by AASHTO Art.6.10.2. These rules aim to guide and regulate the geometry limits for the steel profiles. In particular for situations where built-up sections are used instead of hot-rolled profiles. Figure 4-2 Showcases two profiles made up of the typical elements that comprise an I-beam. Namely, top flange, bottom flange and a web. However, due to their extreme proportions, they no longer behave like an I-beam.

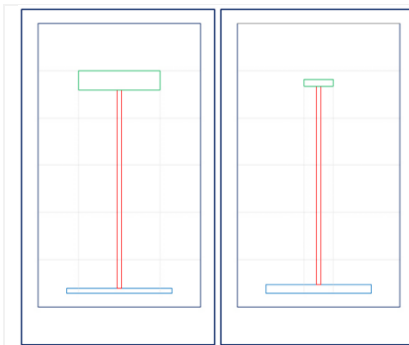


Figure 4-2 I-beams with extreme proportions

W24 × 76
 $t_f = 17 \text{ mm}$
 $b_f = 229 \text{ mm}$
 $t_w = 11 \text{ mm}$
 $d = 607 \text{ mm}$
 $A = 14452 \text{ mm}^2$

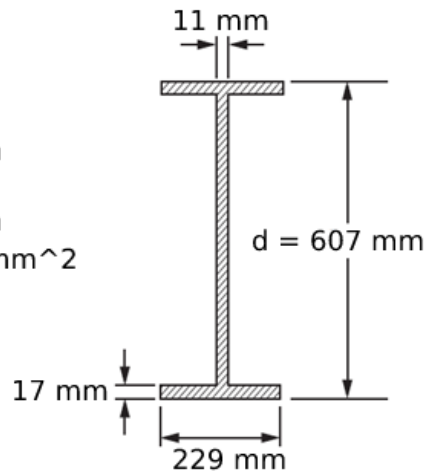


Figure 4-3 W24x76 steel profile. (Kim, Kim, & Eberle, 2013)

For the profile W24x76 shown in Figure 4-3:

- Web proportions: $\frac{D}{t_w} \leq 150$ for webs without longitudinal stiffeners. This design example does not incorporate longitudinal stiffeners.

$51.22 \leq 150$

AASHTO eq.6.10.2.1.1-1

- Flange proportions: $\frac{b_f}{2*t_f} \leq 12$ for both flanges. Both flanges are identical.

$6.61 \leq 12$

AASHTO eq.6.10.2.2-1

- Flange proportions: $b_f \geq D/6$ for all flanges. Both flanges are identical.

$229 \geq 101$

AASHTO eq.6.10.2.2-2

- Flange proportions: $t_f \geq 1.1 * t_w$ for all flanges. Both flanges are identical.

$17 \geq 12.1$

AASHTO eq.6.10.2.2-3

- Flange proportions: $0.1 \geq \frac{I_{yc}}{I_{yt}} \geq 10$. Where I_{yc}, I_{yt} are moments of inertia of the compression & tensions flanges of the steel section about the vertical axis in the plane of the web. Both flanges are identical.

$\frac{I_{yc}}{I_{yt}} = 1$

AASHTO eq.6.10.2.2-4

The selected W24 x 76 meets all proportional limits successfully.

4.3 Section Properties

Performed according to AASHTO Art.4.6.2.6.

Breaking down the bridge length wise enables the analysis of the different loading scenarios in a much more controlled manner. This is done by isolating the loading share applied to interior and exterior girders separately. Figure 4-4. showcases a 3-D view of the composite bridge.

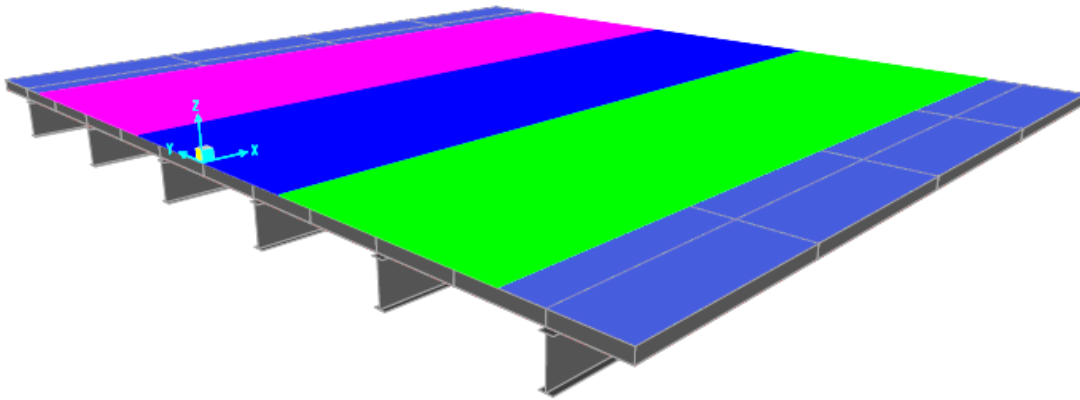


Figure 4-4 Three-dimensional view of the composite bridge. (Mona & Saka, 2019)

The effective flange width, also known as the tributary width, $b_{e,int}$ for interior beams represents the girder's share of concrete deck. Since beams are equally spaced, the effective width is equal to that of the beam spacing.

$b_{e,int} = 2.44 \text{ m}$. With the aid of the bridge cross section Figure 4-5, effective flange width for exterior girders can be deduced as $b_{e,ext} = 2.21 \text{ m}$

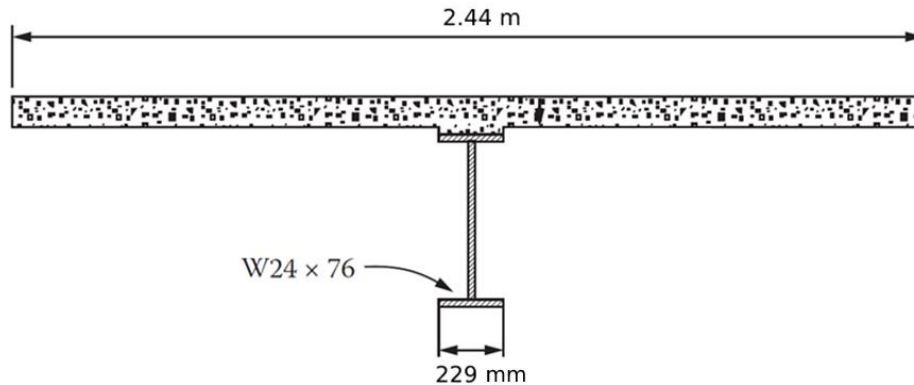


Figure 4-5 Composite section for interior girder. (Kim, Kim, & Eberle, 2013)

One unique aspect in bridge engineering has to do with the different profile sections considered. AASHTO LRFD design procedure concerns itself with three profiles, each with its own unique aspects. These profiles come into effect throughout the bridge lifecycle, beginning with the non-composite section (steel only), followed by the short-term composite section and finally, the long-term composite section.

1. None-composite section (steel girder): This section depicts the state of the bridge during the early construction stages. Only the steel girder is considered. Section properties are readily available in conventional steel design manuals (American Institute of Steel Construction , 2011). Alternatively, given Figure 4-6, required properties can be evaluated with the use of the section geometry.

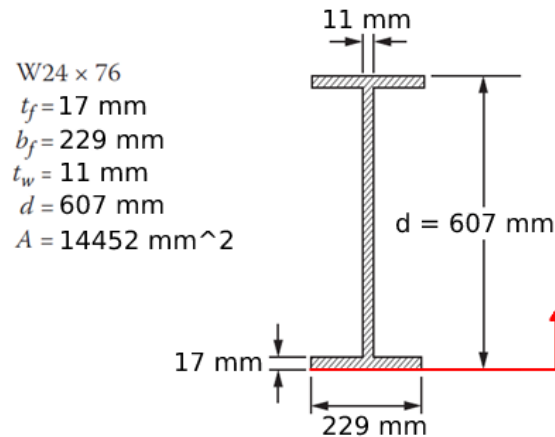


Figure 4-6 Non-composite section

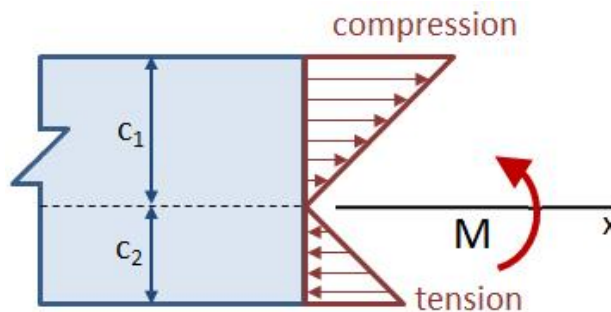


Figure 4-7 Stress profile for a typical simply supported beam

- Neutral axis $\bar{Y} = 303.5 \text{ mm}$. Measured from the bottom datum, shown in red in Figure 4-6.
- Depth of web subjected to compression

$$D_c = Y - t_f = 286 \text{ mm}$$

- By referring to the stress theory Figure 4-7, the elastic section modulus (S_x). Defined as the ratio of the moment of inertia and the distance from the neutral axis to any given point. In this case, the interest is in computing the plastic section modulus at the extreme fibers for both, tension and compression. Elastic section moduli are commonly used in the design of members subjected to bending moment. They aid in determining the bending capacity, which will be shown in later subsections.

$$S_{x.top.steel} = \frac{I}{C_1} = 2838895 \text{ mm}^3$$

$$S_{x.bottom.steel} = \frac{I}{C_2} = 2838895 \text{ mm}^3$$

2. Short-term composite section: The same section properties need to be evaluated. However, the fact that we are not dealing with a homogenous section (made of a single material), the flexure formula, $f = \frac{M \cdot C}{I}$, is no longer valid. As a result, the use of the transformed section is implemented. Thereby transforming all sectional areas other than steel into equivalent steel area. This is done by dividing the effective flange width by the modular ratio.

$$n = \frac{E_s}{E_c} = 7.56 = 8$$

AASHTO eq.6.10.1.1.1b-1

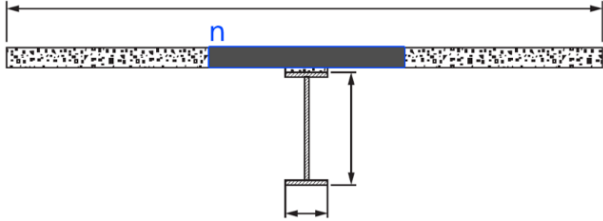
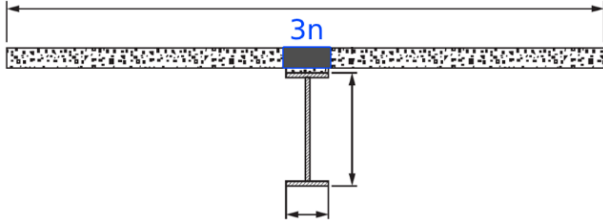
3. Long-term composite section: The same concept of using the transformed section is followed, except for one major difference. The modular ratio is multiplied by a factor of 3 so that:

$$n = 3 * n$$

AASHTO Art. 6.10.1.1.1.

The long-term composite section takes a conservative approach by decreasing the concrete area in order to account for creep effects that occur over time, The increased modular ratio implies an increased stress in the steel girder. See Table 4-2.

Table 4-2 Short/long-term composite section properties

	SHORT-TERM		LONG-TERM	
				
	INTERIOR	EXTERIOR	INTERIOR	EXTERIOR
Modular ratio, n	8	8	$8 \cdot 3 = 21$	$8 \cdot 3 = 21$
Effective width	2.4 m	2.225 m	2.4 m	2.225 m
Neutral axis \bar{Y}	0.674 m	0.667 m	0.573 m	0.563 m
I_{x-x}	0.003489 m^4	0.00342 m^4	0.002688 m^4	0.002616 m^4
S_x at top concrete fiber	0.018648 m^3	0.0177 m^3	0.00933 m^3	0.00876 m^3
S_x at top steel fiber	0.05215 m^3	0.05679 m^3	0.07876 m^3	0.05904 m^3
S_x at bottom steel fiber	0.005177 m^3	0.0051358 m^3	0.0046926 m^3	0.0046486 m^3

4.4 Unfactored Dead Loads

Interior girders are guaranteed to have the highest dead load, given their effective width of 2.44 m as opposed to 2.225 m for exterior girders. Hence, interior girders are used to control the dead load design.

Total dead load per unit length: $W_D = DC1 + DC2 + DW$

1. *DC1*: dead load acting on the steel section (non-composite section), see Figure 4-8. Considered after pouring of concrete and it includes:

- Girder weight (red).
- Concrete (green + blue).
- Stay-in-place forms. Forms are permanently left in place after concrete casting.
- Additional 5% of the steel weight is allocated for miscellaneous details.

$$DC1 = 13.875 \text{ kN/m}$$

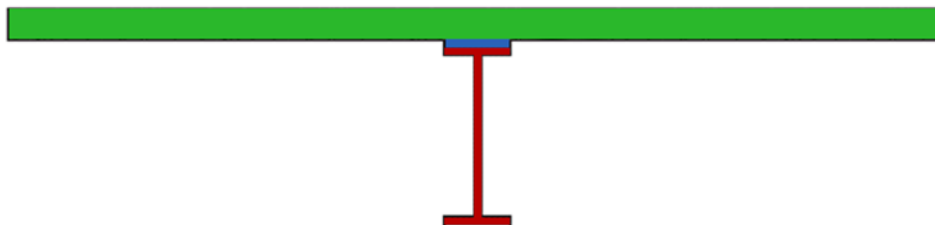


Figure 4-8 DC1 dead load components for interior girder

2. *DC2*: dead load acting on steel & concrete (long-term composite section).

Considered after the concrete deck is fully cured and it includes:

- Side-walk.
- Mid/ side barriers (red), Figure 4-9. Weight is divided on all 6 girders equally.
- Light poles.
- Utility provisions along the bridge.

$$DC2 = 2.44 \text{ kN/m}$$

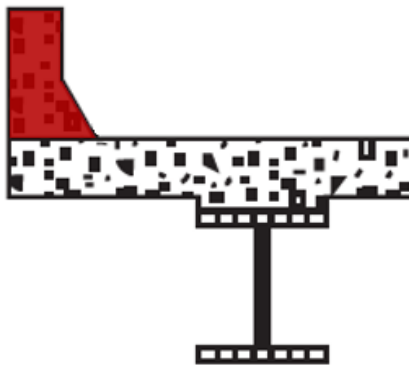


Figure 4-9 Side barrier

3. *DW*: dead load due to the wearing surface (asphalt). Similar to *DC2*, acts on the long-term composite section.

$$DW = 2.67 \text{ kN/m}$$

After DC1, DC2 & DW have been calculated per unit length (kN/m). Moment & shear values are evaluated throughout the bridge length at 10% intervals. Refer to the figures and tables below.

Table 4-3 Moment due to DC1, DC2 & DW

x	x/L	DC1	DC2	DW
m	.	kN.m	kN.m	kN.m
0	0	0	0	0
1.2	0.1	91.4	16.3	17.9
2.4	0.2	162.4	29	31.9
3.7	0.3	213.1	38	41.9
4.9	0.4	243.6	43.5	47.9
6.1	0.5	253.8	45.3	49.9
7.3	0.6	243.6	43.5	47.9
8.5	0.7	213.1	38.1	41.9
9.8	0.8	162.4	29	31.9
11	0.9	91.2	16.3	17.9
12.2	1	0	0	0

Table 4-4 Table 4-5 Shear due to DC1, DC2 & DW

x	x/L	DC1	DC2	DW
m	.	kN	kN	kN
0	0	83.2	14.7	16
1.2	0.1	66.3	11.6	12.9
2.4	0.2	49.8	8.9	9.8
3.7	0.3	32.9	5.8	6.2
4.9	0.4	16.5	2.7	3.1
6.1	0.5	0	0	0
7.3	0.6	-16.5	-2.7	-3.1
8.5	0.7	-32.9	-5.8	-6.2
9.8	0.8	-49.8	-8.9	-9.8
11	0.9	-66.3	-11.6	-12.9
12.2	1	-83.2	-14.7	-16

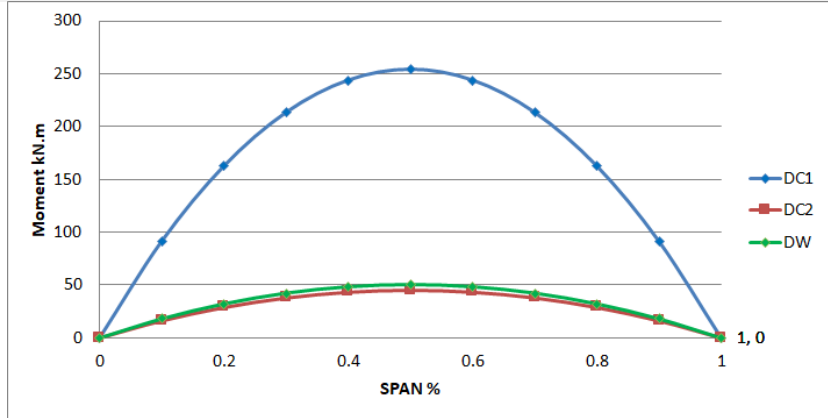


Figure 4-10 Moment diagram due to DC1, DC2 & DW

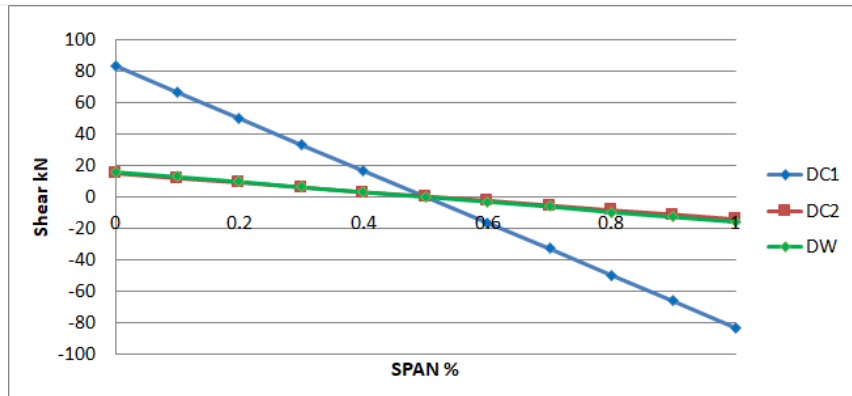


Figure 4-11 Shear diagram due to DC1, DC2 & DW

4.5 Unfactored Live Loads

While this section concerns itself with live loads, we should take a step back and talk about dead loads in hindsight and see where we stand from there.

As much material imperfection as there might be, we can still estimate small discrepancy when it comes to the calculated dead loads. That is simply due to the fact of how definite geometry and unit weights are. Dead loads should encompass every stationary tangible element that is part of the bridge, no exceptions. This eliminates any reasonable doubt of loads that could have been omitted. In short, dead loads are objective.

On the other hand, live loads are subjective and open for dispute. While the term itself “live load” is not unique to bridges, the methodology with which we deal with it here, is what sets it apart. It would not be an understatement to say that there are infinite possibilities and ways to load a bridge span. Considering the number of lanes, the bridge length, combination of vehicles occupying the bridge, axle loads, axle spacing, vehicle speed, bridge geometry (straight, curved) & more. All these variables go hand in hand in presenting a problem, so unique, that it calls for an equally unique method for solving it.

The term live load implies a transient load, usually short-lived, that moves across the length of the bridge span. By this definition, a person walking across a bridge would be of interest to the designing engineering. However, the induced loads by this person or even a group of individuals remain insignificant and are barely of interest to the design of your average highway overpass. Even by excluding non-vehicular live loads, a wide array of possible vehicles remains open for dispute.

Take the case where one engineer might consider a loading scenario where all design lanes are occupied by concrete-mixer trucks as the maximum load that a bridge should withstand. A second opinion might question the plausibility of this scenario on his country-side small river crossing. Even within the same country, different regions and different area designations call for different daily traffic. As a result, a notional (theoretical) truck is presented in the AASHTO code in order to serve as the basic loading unit for the different scenarios.

The history behind the development of this model is outside the scope of this paper. Suffice to say, the first proposed live load model was proposed and used by Squire Whipple in 1846, which gives a sense of scale of how long this problem has been on the mind of engineers (Narendra, 2014).

AASHTO LRFD specifications present a live load module comprised of 3 components:

1. HL-93 Design truck: Consisting of 3 moving point loads, each depicting an axle. Spacing between the first axle pair is fixed at 4.27 m. Whereas the spacing between the last pair is varied between 4.27 - 9.14 m, depending on the bridge span configuration. The aim is to introduce the highest moments and shears. This stipulates that the axle loads be as close to each other as possible for simply supported spans. See Figure 4-12 & Figure 4-13.

AASHTO Art. 3.6.1.2.2

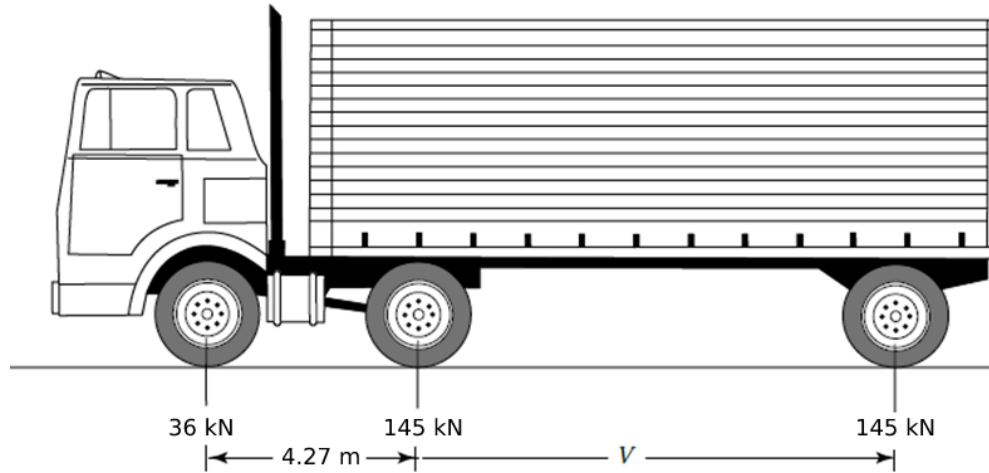


Figure 4-12 HL-93 design truck, longitudinal position. (AASHTO, 2017)

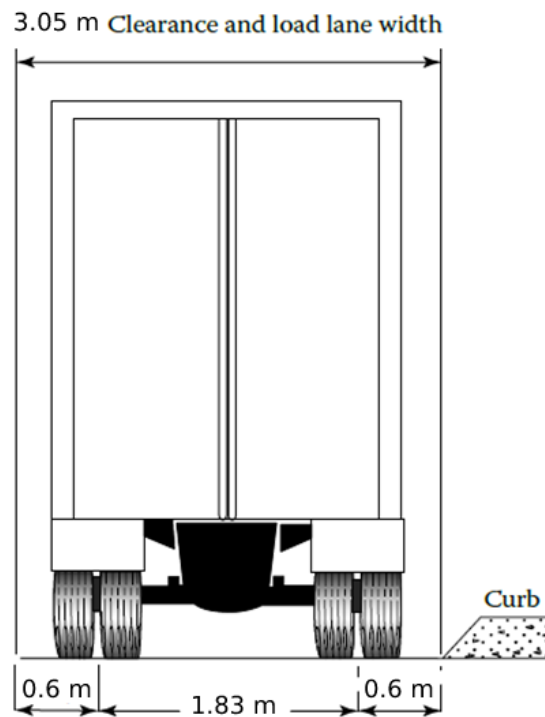


Figure 4-13 HL-93 design truck, transverse position. (AASHTO, 2017)

- Special fatigue configuration: subsequent fatigue checks make use of the same HL-93 design truck. However, the variable axle spacing (V) is fixed at 9.14m.

For the design example, rear axle spacing was fixed at 4.27m as to increase the induced truck load. The truck is incrementally moved across the bridge and respective moment and shear values across the bridge length are calculated. For Figure 4-14 and Figure 4-15, the X-axis (bridge length) is segmented into 10 parts at 10% intervals. Whereas the Y-axis (time) is segmented into 50 parts. Unit of time is not subject of interest as it does not contribute to the calculations.

Similarly, Figure 4-16 and Figure 4-17 present moment & shear diagrams due to design truck under fatigue configuration. Most notable are the two summits in the moment diagram. Note that the code stipulate the spacing of 2nd axis for fatigue truck to be fixed at 9.14m. As a result, high stresses no longer concentrate at the span's mid section. Instead, they alternate position between two different spots.

	0	0.1	0.2	0.3	0.4	0.5	0.6	0.7	0.8	0.9	1
0	0	0	0	0	0	0	0	0	0	0	0
1	0	13.3	11.8	10.3	8.9	7.4	5.9	4.4	3	1.5	0
2	0	26.6	23.6	20.7	17.7	14.8	11.8	8.9	5.9	3	0
3	0	39	35.4	31	26.6	22.1	17.7	13.3	8.9	4.4	0
4	0	37.5	47.2	41.3	35.4	29.5	23.6	17.7	11.8	5.9	0
5	0	36	59	51.6	44.3	36.9	29.5	22.1	14.8	7.4	0
6	0	34.5	69.1	62	53.1	44.3	35.4	26.6	17.7	8.9	0
7	0	33.1	66.1	72.3	62	51.6	41.3	31	20.7	10.3	0
8	0	31.6	63.2	82.6	70.8	59	47.2	35.4	23.6	11.8	0
9	0	30.1	60.2	90.3	79.7	66.4	53.1	39.8	26.6	13.3	0
10	0	28.6	57.3	85.9	88.5	73.8	59	44.3	29.5	14.8	0
11	0	64.6	87.6	110.6	122.3	102	81.6	61.2	40.8	20.4	0
12	0	116.3	131.9	147.5	163.1	138.8	111.1	83.3	55.5	27.8	0
13	0	167.9	176.1	184.4	192.6	175.7	140.6	105.4	70.3	35.1	0
14	0	174.4	220.4	221.3	222.1	212.6	170.1	127.6	85	42.5	0
15	0	167	264.7	258.1	251.6	245.1	199.6	149.7	99.8	49.9	0
16	0	159.7	308.9	295	281.1	267.3	229.1	171.8	114.5	57.3	0
17	0	152.3	304.6	331.9	310.6	289.4	258.6	193.9	129.3	64.6	0
18	0	144.9	289.8	368.8	340.1	311.5	282.9	216.1	144	72	0
19	0	137.5	275.1	405.7	369.6	333.6	297.6	238.2	158.8	79.4	0
20	0	130.2	260.3	390.5	399.1	355.8	312.4	260.3	173.5	86.8	0
21	0	144.6	265	385.4	443.2	390	336.8	283.7	193.2	96.6	0
22	0	190.4	297.5	404.5	508.1	441.7	375.2	308.7	219.7	109.9	0
23	0	236.1	329.9	423.7	517.5	493.3	413.6	333.8	246.3	123.1	0
24	0	254.1	362.4	442.9	523.4	544.9	451.9	358.9	265.9	136.4	0
25	0	240.8	394.8	462.1	529.3	596.6	490.3	384	277.7	149.7	0
26	0	227.5	427.3	481.2	535.2	589.2	528.6	409	289.5	163	0
27	0	214.2	428.5	500.4	541.1	581.8	567	434.1	301.3	168.4	0
28	0	201	401.9	519.6	547	574.4	601.8	459.2	313.1	166.9	0
29	0	187.7	375.4	538.8	552.9	567	581.2	484.3	324.9	165.5	0
30	0	175.3	350.6	525.8	562.3	564	565.7	515.4	343.6	171.8	0
31	0	163.5	327	490.4	574.1	564	553.9	543.9	367.2	183.6	0
32	0	151.7	303.4	455	585.9	564	542.1	520.3	390.8	195.4	0
33	0	139.9	279.8	419.6	559.5	564	530.3	496.7	414.4	207.2	0
34	0	128.1	256.1	384.2	512.3	564	518.5	473.1	427.6	219	0
35	0	116.3	232.5	348.8	465.1	564	506.7	449.5	392.2	230.8	0
36	0	104.5	208.9	313.4	417.9	522.4	494.9	425.9	356.8	242.6	0
37	0	92.7	185.3	278	370.7	463.4	483.1	402.3	321.4	240.5	0
38	0	80.9	161.7	242.6	323.5	404.4	471.3	378.7	286	193.3	0
39	0	69.1	138.1	207.2	276.3	345.3	414.4	355.1	250.6	146.1	0
40	0	59	118	177	236	295	354	343.6	229.1	114.5	0
41	0	53.1	106.2	159.3	212.4	265.5	318.6	361.3	240.9	120.4	0
42	0	47.2	94.4	141.6	188.8	236	283.2	330.4	252.7	126.3	0
43	0	41.3	82.6	123.9	165.2	206.5	247.8	289.1	264.5	132.2	0
44	0	35.4	70.8	106.2	141.6	177	212.4	247.8	276.3	138.1	0
45	0	29.5	59	88.5	118	147.5	177	206.5	236	144	0
46	0	23.6	47.2	70.8	94.4	118	141.6	165.2	188.8	149.9	0
47	0	17.7	35.4	53.1	70.8	88.5	106.2	123.9	141.6	155.8	0
48	0	11.8	23.6	35.4	47.2	59	70.8	82.6	94.4	106.2	0
49	0	5.9	11.8	17.7	23.6	29.5	35.4	41.3	47.2	53.1	0
50	0	0	0	0	0	0	0	0	0	0	0

Figure 4-14 Moment (kN.m) values due to design truck

	0	0.1	0.2	0.3	0.4	0.5	0.6	0.7	0.8	0.9	1
0	0	0	0	0	0	0	0	0	0	0	0
1	34.4	-1.2	-1.2	-1.2	-1.2	-1.2	-1.2	-1.2	-1.2	-1.2	-1.2
2	33.2	-2.4	-2.4	-2.4	-2.4	-2.4	-2.4	-2.4	-2.4	-2.4	-2.4
3	32	32	-3.6	-3.6	-3.6	-3.6	-3.6	-3.6	-3.6	-3.6	-3.6
4	30.7	30.7	-4.8	-4.8	-4.8	-4.8	-4.8	-4.8	-4.8	-4.8	-4.8
5	29.5	29.5	-6	-6	-6	-6	-6	-6	-6	-6	-6
6	28.3	28.3	28.3	-7.3	-7.3	-7.3	-7.3	-7.3	-7.3	-7.3	-7.3
7	27.1	27.1	27.1	-8.5	-8.5	-8.5	-8.5	-8.5	-8.5	-8.5	-8.5
8	25.9	25.9	25.9	-9.7	-9.7	-9.7	-9.7	-9.7	-9.7	-9.7	-9.7
9	24.7	24.7	24.7	24.7	-10.9	-10.9	-10.9	-10.9	-10.9	-10.9	-10.9
10	23.5	23.5	23.5	23.5	-12.1	-12.1	-12.1	-12.1	-12.1	-12.1	-12.1
11	161.2	18.9	18.9	18.9	-16.7	-16.7	-16.7	-16.7	-16.7	-16.7	-16.7
12	155.1	12.8	12.8	12.8	12.8	-22.8	-22.8	-22.8	-22.8	-22.8	-22.8
13	149.1	6.8	6.8	6.8	6.8	-28.8	-28.8	-28.8	-28.8	-28.8	-28.8
14	143	143	0.7	0.7	0.7	-34.9	-34.9	-34.9	-34.9	-34.9	-34.9
15	137	137	-5.3	-5.3	-5.3	-5.3	-40.9	-40.9	-40.9	-40.9	-40.9
16	130.9	130.9	-11.4	-11.4	-11.4	-11.4	-47	-47	-47	-47	-47
17	124.9	124.9	124.9	-17.4	-17.4	-17.4	-53	-53	-53	-53	-53
18	118.9	118.9	118.9	-23.5	-23.5	-23.5	-23.5	-59.1	-59.1	-59.1	-59.1
19	112.8	112.8	112.8	-29.5	-29.5	-29.5	-29.5	-65.1	-65.1	-65.1	-65.1
20	106.8	106.8	106.8	106.8	-35.6	-35.6	-35.6	-71.2	-71.2	-71.2	-71.2
21	241	98.7	98.7	98.7	-43.6	-43.6	-43.6	-43.6	-79.2	-79.2	-79.2
22	230.2	87.8	87.8	87.8	-54.5	-54.5	-54.5	-54.5	-90.1	-90.1	-90.1
23	219.3	76.9	76.9	76.9	76.9	-65.4	-65.4	-65.4	-101	-101	-101
24	208.4	208.4	66	66	66	-76.3	-76.3	-76.3	-76.3	-112	-112
25	197.5	197.5	55.2	55.2	55.2	55.2	-87.2	-87.2	-87.2	-123	-123
26	186.6	186.6	44.3	44.3	44.3	44.3	-98.1	-98.1	-98.1	-134	-134
27	175.7	175.7	175.7	33.4	33.4	33.4	-109	-109	-109	-109	-145
28	164.8	164.8	164.8	22.5	22.5	22.5	22.5	-120	-120	-120	-155
29	153.9	153.9	153.9	11.6	11.6	11.6	11.6	-131	-131	-131	-166
30	143.8	143.8	143.8	143.8	1.4	1.4	1.4	-141	-141	-141	-141
31	134.1	134.1	134.1	134.1	-8.3	-8.3	-8.3	-8.3	-151	-151	-151
32	124.4	124.4	124.4	124.4	-17.9	-17.9	-17.9	-17.9	-160	-160	-160
33	114.7	114.7	114.7	114.7	114.7	-27.6	-27.6	-27.6	-170	-170	-170
34	105	105	105	105	105	-37.3	-37.3	-37.3	-37.3	-180	-180
35	95.4	95.4	95.4	95.4	95.4	-47	-47	-47	-47	-189	-189
36	85.7	85.7	85.7	85.7	85.7	85.7	-56.6	-56.6	-56.6	-199	-199
37	76	76	76	76	76	76	-66.3	-66.3	-66.3	-66.3	-209
38	66.3	66.3	66.3	66.3	66.3	66.3	-76	-76	-76	-76	-218
39	56.6	56.6	56.6	56.6	56.6	56.6	56.6	-85.7	-85.7	-85.7	-228
40	48.4	48.4	48.4	48.4	48.4	48.4	48.4	-93.9	-93.9	-93.9	-93.9
41	43.6	43.6	43.6	43.6	43.6	43.6	43.6	-98.8	-98.8	-98.8	-98.8
42	38.7	38.7	38.7	38.7	38.7	38.7	38.7	38.7	-104	-104	-104
43	33.9	33.9	33.9	33.9	33.9	33.9	33.9	33.9	-109	-109	-109
44	29	29	29	29	29	29	29	29	-113	-113	-113
45	24.2	24.2	24.2	24.2	24.2	24.2	24.2	24.2	24.2	-118	-118
46	19.4	19.4	19.4	19.4	19.4	19.4	19.4	19.4	19.4	-123	-123
47	14.5	14.5	14.5	14.5	14.5	14.5	14.5	14.5	14.5	-128	-128
48	9.7	9.7	9.7	9.7	9.7	9.7	9.7	9.7	9.7	9.7	-133
49	4.8	4.8	4.8	4.8	4.8	4.8	4.8	4.8	4.8	4.8	-138
50	0	0	0	0	0	0	0	0	0	0	0

Figure 4-15 Shear (kN) values due to design truck

	0	0.1	0.2	0.3	0.4	0.5	0.6	0.7	0.8	0.9	1
0	0	0	0	0	0	0	0	0	0	0	0
1	0	16.4	14.6	12.8	10.9	9.1	7.3	5.5	3.6	1.8	0
2	0	32.8	29.2	25.5	21.9	18.2	14.6	10.9	7.3	3.6	0
3	0	37.9	43.7	38.3	32.8	27.3	21.9	16.4	10.9	5.5	0
4	0	36.1	58.3	51	43.7	36.4	29.2	21.9	14.6	7.3	0
5	0	34.3	68.5	63.8	54.7	45.6	36.4	27.3	18.2	9.1	0
6	0	32.5	64.9	76.5	65.6	54.7	43.7	32.8	21.9	10.9	0
7	0	30.6	61.3	89.3	76.5	63.8	51	38.3	25.5	12.8	0
8	0	28.8	57.6	86.4	87.5	72.9	58.3	43.7	29.2	14.6	0
9	0	70.7	92.8	115	127.6	106.3	85	63.8	42.5	21.3	0
10	0	134.5	147.5	160.5	173.5	151.8	121.5	91.1	60.7	30.4	0
11	0	177.4	202.2	206.1	210	197.4	157.9	118.4	79	39.5	0
12	0	168.3	256.8	251.6	246.4	241.2	194.4	145.8	97.2	48.6	0
13	0	159.2	311.5	297.2	282.9	268.6	230.8	173.1	115.4	57.7	0
14	0	150.1	300.2	342.7	319.3	295.9	267.3	200.4	133.6	66.8	0
15	0	141	282	388.3	355.8	323.2	290.7	227.8	151.8	75.9	0
16	0	131.9	263.8	395.7	392.2	350.6	308.9	255.1	170.1	85	0
17	0	122.8	245.6	368.3	428.6	377.9	327.1	276.4	188.3	94.1	0
18	0	113.7	227.3	341	454.7	405.2	345.3	285.5	206.5	103.3	0
19	0	104.6	209.1	313.7	418.2	432.6	363.6	294.6	224.7	112.4	0
20	0	95.4	190.9	286.3	381.8	459.9	381.8	303.7	225.6	121.5	0
21	0	86.3	172.7	259	345.3	431.7	400	312.8	225.6	130.6	0
22	0	77.2	154.5	231.7	308.9	386.1	418.2	321.9	225.6	129.3	0
23	0	68.1	136.2	204.3	272.5	340.6	408.7	331	225.6	120.2	0
24	0	59.4	118.7	178.1	237.4	296.8	356.1	342.6	228.4	114.2	0
25	0	52.1	104.1	156.2	208.3	260.3	312.4	364.4	243	121.5	0
26	0	44.8	89.5	134.3	179.1	223.9	268.6	313.4	257.5	128.8	0
27	0	90.6	122.2	153.8	185.3	216.9	248.5	280.1	283.9	142	0
28	0	148.9	165.9	182.9	199.9	216.9	233.9	250.9	267.9	156.5	0
29	0	176	209.6	212.1	214.5	216.9	219.4	221.8	224.2	171.1	0
30	0	161.4	253.4	241.2	229.1	216.9	204.8	192.6	180.5	168.3	0
31	0	146.8	293.6	270.4	243.7	216.9	190.2	163.5	136.8	110	0
32	0	132.2	264.5	299.5	258.2	216.9	175.6	134.3	93	51.7	0
33	0	123.9	247.8	347.4	297.8	248.2	198.5	148.9	99.3	49.6	0
34	0	116.6	233.2	349.9	341.5	284.6	227.7	170.8	113.8	56.9	0
35	0	109.3	218.7	328	385.3	321.1	256.8	192.6	128.4	64.2	0
36	0	102	204.1	306.1	408.2	357.5	286	214.5	143	71.5	0
37	0	94.8	189.5	284.3	379	393.9	315.2	236.4	157.6	78.8	0
38	0	87.5	174.9	262.4	349.9	430.4	344.3	258.2	172.2	86.1	0
39	0	80.2	160.4	240.5	320.7	400.9	373.5	280.1	186.7	93.4	0
40	0	72.9	145.8	218.7	291.6	364.4	402.6	302	201.3	100.7	0
41	0	65.6	131.2	196.8	262.4	328	393.6	323.8	215.9	107.9	0
42	0	58.3	116.6	174.9	233.2	291.6	349.9	345.7	230.5	115.2	0
43	0	51	102	153.1	204.1	255.1	306.1	357.2	245	122.5	0
44	0	43.7	87.5	131.2	174.9	218.7	262.4	306.1	259.6	129.8	0
45	0	36.4	72.9	109.3	145.8	182.2	218.7	255.1	274.2	137.1	0
46	0	29.2	58.3	87.5	116.6	145.8	174.9	204.1	233.2	144.4	0
47	0	21.9	43.7	65.6	87.5	109.3	131.2	153.1	174.9	151.7	0
48	0	14.6	29.2	43.7	58.3	72.9	87.5	102	116.6	131.2	0
49	0	7.3	14.6	21.9	29.2	36.4	43.7	51	58.3	65.6	0
50	0	0	0	0	0	0	0	0	0	0	0

Figure 4-16 Moment (kN.m) values due to fatigue design truck

	0	0.1	0.2	0.3	0.4	0.5	0.6	0.7	0.8	0.9	1
0	0	0	0	0	0	0	0	0	0	0	0
1	34.1	-1.5	-1.5	-1.5	-1.5	-1.5	-1.5	-1.5	-1.5	-1.5	-1.5
2	32.6	-3	-3	-3	-3	-3	-3	-3	-3	-3	-3
3	31.1	31.1	-4.5	-4.5	-4.5	-4.5	-4.5	-4.5	-4.5	-4.5	-4.5
4	29.6	29.6	-6	-6	-6	-6	-6	-6	-6	-6	-6
5	28.1	28.1	28.1	-7.5	-7.5	-7.5	-7.5	-7.5	-7.5	-7.5	-7.5
6	26.6	26.6	26.6	-9	-9	-9	-9	-9	-9	-9	-9
7	25.1	25.1	25.1	-10.5	-10.5	-10.5	-10.5	-10.5	-10.5	-10.5	-10.5
8	23.6	23.6	23.6	23.6	-12	-12	-12	-12	-12	-12	-12
9	160.5	18.1	18.1	18.1	18.1	-17.4	-17.4	-17.4	-17.4	-17.4	-17.4
10	153	10.7	10.7	10.7	10.7	-24.9	-24.9	-24.9	-24.9	-24.9	-24.9
11	145.5	145.5	3.2	3.2	3.2	-32.4	-32.4	-32.4	-32.4	-32.4	-32.4
12	138.1	138.1	-4.3	-4.3	-4.3	-4.3	-39.9	-39.9	-39.9	-39.9	-39.9
13	130.6	130.6	-11.7	-11.7	-11.7	-11.7	-47.3	-47.3	-47.3	-47.3	-47.3
14	123.1	123.1	123.1	-19.2	-19.2	-19.2	-54.8	-54.8	-54.8	-54.8	-54.8
15	115.6	115.6	115.6	-26.7	-26.7	-26.7	-26.7	-62.3	-62.3	-62.3	-62.3
16	108.2	108.2	108.2	108.2	-34.2	-34.2	-34.2	-69.7	-69.7	-69.7	-69.7
17	100.7	100.7	100.7	100.7	-41.6	-41.6	-41.6	-41.6	-77.2	-77.2	-77.2
18	93.2	93.2	93.2	93.2	93.2	-49.1	-49.1	-49.1	-84.7	-84.7	-84.7
19	85.8	85.8	85.8	85.8	85.8	-56.6	-56.6	-56.6	-92.2	-92.2	-92.2
20	78.3	78.3	78.3	78.3	78.3	-64.1	-64.1	-64.1	-64.1	-99.6	-99.6
21	70.8	70.8	70.8	70.8	70.8	70.8	-71.5	-71.5	-71.5	-107	-107
22	63.3	63.3	63.3	63.3	63.3	63.3	-79	-79	-79	-79	-115
23	55.9	55.9	55.9	55.9	55.9	55.9	55.9	-86.5	-86.5	-86.5	-122
24	48.7	48.7	48.7	48.7	48.7	48.7	48.7	-93.7	-93.7	-93.7	-93.7
25	42.7	42.7	42.7	42.7	42.7	42.7	42.7	42.7	-99.6	-99.6	-99.6
26	36.7	36.7	36.7	36.7	36.7	36.7	36.7	36.7	-106	-106	-106
27	168.2	25.9	25.9	25.9	25.9	25.9	25.9	25.9	-116	-116	-116
28	156.3	13.9	13.9	13.9	13.9	13.9	13.9	13.9	13.9	-128	-128
29	144.3	144.3	2	2	2	2	2	2	2	-140	-140
30	132.4	132.4	-10	-10	-10	-10	-10	-10	-10	-10	-152
31	120.4	120.4	120.4	-21.9	-21.9	-21.9	-21.9	-21.9	-21.9	-21.9	-164
32	108.5	108.5	108.5	-33.9	-33.9	-33.9	-33.9	-33.9	-33.9	-33.9	-176
33	101.6	101.6	101.6	-40.7	-40.7	-40.7	-40.7	-40.7	-40.7	-40.7	-40.7
34	95.6	95.6	95.6	95.6	-46.7	-46.7	-46.7	-46.7	-46.7	-46.7	-46.7
35	89.7	89.7	89.7	89.7	-52.7	-52.7	-52.7	-52.7	-52.7	-52.7	-52.7
36	83.7	83.7	83.7	83.7	83.7	-58.6	-58.6	-58.6	-58.6	-58.6	-58.6
37	77.7	77.7	77.7	77.7	77.7	-64.6	-64.6	-64.6	-64.6	-64.6	-64.6
38	71.7	71.7	71.7	71.7	71.7	-70.6	-70.6	-70.6	-70.6	-70.6	-70.6
39	65.8	65.8	65.8	65.8	65.8	65.8	-76.6	-76.6	-76.6	-76.6	-76.6
40	59.8	59.8	59.8	59.8	59.8	59.8	59.8	-82.6	-82.6	-82.6	-82.6
41	53.8	53.8	53.8	53.8	53.8	53.8	53.8	-88.5	-88.5	-88.5	-88.5
42	47.8	47.8	47.8	47.8	47.8	47.8	47.8	-94.5	-94.5	-94.5	-94.5
43	41.8	41.8	41.8	41.8	41.8	41.8	41.8	41.8	-101	-101	-101
44	35.9	35.9	35.9	35.9	35.9	35.9	35.9	35.9	-107	-107	-107
45	29.9	29.9	29.9	29.9	29.9	29.9	29.9	29.9	-112	-112	-112
46	23.9	23.9	23.9	23.9	23.9	23.9	23.9	23.9	23.9	-118	-118
47	17.9	17.9	17.9	17.9	17.9	17.9	17.9	17.9	17.9	-124	-124
48	12	12	12	12	12	12	12	12	12	12	-130
49	6	6	6	6	6	6	6	6	6	6	-136
50	0	0	0	0	0	0	0	0	0	0	0

Figure 4-17 Shear (kN) values due to fatigue design truck

2. Tandem: Similar to the design truck, tandem load represents 2 moving point loads. This component depicts loads induced due to a tandem trailer having 2 axles, 1.22 m apart. See Figure 4-18 and Figure 4-19.

Similar procedure is repeated for for the tandem load. Where both point loads are simulated to to cross the bridge. Moment & shear values respectively are calculated in Figure 4-20 & Figure 4-21.

AASHTO Art. 3.6.1.2.3

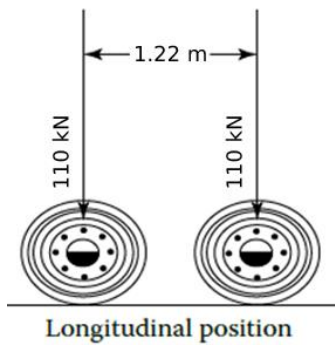


Figure 4-18 Tandem load configuration.

(AASHTO, 2017)



Figure 4-19 Real-life tandem trailer

	0	0.1	0.2	0.3	0.4	0.5	0.6	0.7	0.8	0.9	1
0	0	0	0	0	0	0	0	0	0	0	0
1	0	26.8	23.9	20.9	17.9	14.9	11.9	8.9	6	3	0
2	0	53.7	47.7	41.8	35.8	29.8	23.9	17.9	11.9	6	0
3	0	80.5	71.6	62.6	53.7	44.7	35.8	26.8	17.9	8.9	0
4	0	107.4	95.4	83.5	71.6	59.7	47.7	35.8	23.9	11.9	0
5	0	132.9	130.2	113.9	97.6	81.3	65.1	48.8	32.5	16.3	0
6	0	156.7	177.9	155.6	133.4	111.2	88.9	66.7	44.5	22.2	0
7	0	180.6	225.6	197.4	169.2	141	112.8	84.6	56.4	28.2	0
8	0	204.5	273.3	239.2	205	170.8	136.7	102.5	68.3	34.2	0
9	0	228.3	321.1	280.9	240.8	200.7	160.5	120.4	80.3	40.1	0
10	0	225.1	341.7	322.7	276.6	230.5	184.4	138.3	92.2	46.1	0
11	0	219.1	359.6	364.4	312.4	260.3	208.3	156.2	104.1	52.1	0
12	0	213.1	377.5	406.2	348.2	290.1	232.1	174.1	116.1	58	0
13	0	207.2	395.4	448	384	320	256	192	128	64	0
14	0	201.2	402.4	478.9	419.8	349.8	279.8	209.9	139.9	70	0
15	0	195.2	390.5	490.8	455.5	379.6	303.7	227.8	151.8	75.9	0
16	0	189.3	378.5	502.7	491.3	409.5	327.6	245.7	163.8	81.9	0
17	0	183.3	366.6	514.7	527.1	439.3	351.4	263.6	175.7	87.9	0
18	0	177.3	354.7	526.6	562.9	469.1	375.3	281.5	187.6	93.8	0
19	0	171.4	342.7	514.1	574.3	498.9	399.1	299.4	199.6	99.8	0
20	0	165.4	330.8	496.2	580.3	528.8	423	317.3	211.5	105.8	0
21	0	159.4	318.9	478.3	586.2	558.6	446.9	335.2	223.4	111.7	0
22	0	153.5	307	460.4	592.2	588.4	470.7	353.1	235.4	117.7	0
23	0	147.5	295	442.5	590	610.1	494.6	370.9	247.3	123.6	0
24	0	141.5	283.1	424.6	566.2	610.1	518.5	388.8	259.2	129.6	0
25	0	135.6	271.2	406.7	542.3	610.1	542.3	406.7	271.2	135.6	0
26	0	129.6	259.2	388.8	518.5	610.1	566.2	424.6	283.1	141.5	0
27	0	123.6	247.3	370.9	494.6	610.1	590	442.5	295	147.5	0
28	0	117.7	235.4	353.1	470.7	588.4	592.2	460.4	307	153.5	0
29	0	111.7	223.4	335.2	446.9	558.6	586.2	478.3	318.9	159.4	0
30	0	105.8	211.5	317.3	423	528.8	580.3	496.2	330.8	165.4	0
31	0	99.8	199.6	299.4	399.1	498.9	574.3	514.1	342.7	171.4	0
32	0	93.8	187.6	281.5	375.3	469.1	562.9	526.6	354.7	177.3	0
33	0	87.9	175.7	263.6	351.4	439.3	527.1	514.7	366.6	183.3	0
34	0	81.9	163.8	245.7	327.6	409.5	491.3	502.7	378.5	189.3	0
35	0	75.9	151.8	227.8	303.7	379.6	455.5	490.8	390.5	195.2	0
36	0	70	139.9	209.9	279.8	349.8	419.8	478.9	402.4	201.2	0
37	0	64	128	192	256	320	384	448	395.4	207.2	0
38	0	58	116.1	174.1	232.1	290.1	348.2	406.2	377.5	213.1	0
39	0	52.1	104.1	156.2	208.3	260.3	312.4	364.4	359.6	219.1	0
40	0	46.1	92.2	138.3	184.4	230.5	276.6	322.7	341.7	225.1	0
41	0	40.1	80.3	120.4	160.5	200.7	240.8	280.9	321.1	228.3	0
42	0	34.2	68.3	102.5	136.7	170.8	205	239.2	273.3	204.5	0
43	0	28.2	56.4	84.6	112.8	141	169.2	197.4	225.6	180.6	0
44	0	22.2	44.5	66.7	88.9	111.2	133.4	155.6	177.9	156.7	0
45	0	16.3	32.5	48.8	65.1	81.3	97.6	113.9	130.2	132.9	0
46	0	11.9	23.9	35.8	47.7	59.7	71.6	83.5	95.4	107.4	0
47	0	8.9	17.9	26.8	35.8	44.7	53.7	62.6	71.6	80.5	0
48	0	6	11.9	17.9	23.9	29.8	35.8	41.8	47.7	53.7	0
49	0	3	6	8.9	11.9	14.9	17.9	20.9	23.9	26.8	0
50	0	0	0	0	0	0	0	0	0	0	0

Figure 4-20 Moment (kN.m) values due tandem load

	0	0.1	0.2	0.3	0.4	0.5	0.6	0.7	0.8	0.9	1
0	0	0	0	0	0	0	0	0	0	0	0
1	108.8	-2.4	-2.4	-2.4	-2.4	-2.4	-2.4	-2.4	-2.4	-2.4	-2.4
2	106.3	-4.9	-4.9	-4.9	-4.9	-4.9	-4.9	-4.9	-4.9	-4.9	-4.9
3	103.9	-7.3	-7.3	-7.3	-7.3	-7.3	-7.3	-7.3	-7.3	-7.3	-7.3
4	101.4	-9.8	-9.8	-9.8	-9.8	-9.8	-9.8	-9.8	-9.8	-9.8	-9.8
5	209.1	97.9	-13.3	-13.3	-13.3	-13.3	-13.3	-13.3	-13.3	-13.3	-13.3
6	204.2	93	-18.2	-18.2	-18.2	-18.2	-18.2	-18.2	-18.2	-18.2	-18.2
7	199.3	88.1	-23.1	-23.1	-23.1	-23.1	-23.1	-23.1	-23.1	-23.1	-23.1
8	194.4	83.2	-28	-28	-28	-28	-28	-28	-28	-28	-28
9	189.5	78.3	-32.9	-32.9	-32.9	-32.9	-32.9	-32.9	-32.9	-32.9	-32.9
10	184.6	184.6	73.4	-37.8	-37.8	-37.8	-37.8	-37.8	-37.8	-37.8	-37.8
11	179.7	179.7	68.5	-42.7	-42.7	-42.7	-42.7	-42.7	-42.7	-42.7	-42.7
12	174.8	174.8	63.6	-47.6	-47.6	-47.6	-47.6	-47.6	-47.6	-47.6	-47.6
13	169.9	169.9	58.7	-52.5	-52.5	-52.5	-52.5	-52.5	-52.5	-52.5	-52.5
14	165	165	165	53.8	-57.4	-57.4	-57.4	-57.4	-57.4	-57.4	-57.4
15	160.1	160.1	160.1	48.9	-62.3	-62.3	-62.3	-62.3	-62.3	-62.3	-62.3
16	155.2	155.2	155.2	44	-67.2	-67.2	-67.2	-67.2	-67.2	-67.2	-67.2
17	150.3	150.3	150.3	39.1	-72.1	-72.1	-72.1	-72.1	-72.1	-72.1	-72.1
18	145.4	145.4	145.4	34.2	-77	-77	-77	-77	-77	-77	-77
19	140.6	140.6	140.6	140.6	29.4	-81.8	-81.8	-81.8	-81.8	-81.8	-81.8
20	135.7	135.7	135.7	135.7	24.5	-86.7	-86.7	-86.7	-86.7	-86.7	-86.7
21	130.8	130.8	130.8	130.8	19.6	-91.6	-91.6	-91.6	-91.6	-91.6	-91.6
22	125.9	125.9	125.9	125.9	14.7	-96.5	-96.5	-96.5	-96.5	-96.5	-96.5
23	121	121	121	121	121	9.8	-101	-101	-101	-101	-101
24	116.1	116.1	116.1	116.1	116.1	4.9	-106	-106	-106	-106	-106
25	111.2	111.2	111.2	111.2	111.2	0	-111	-111	-111	-111	-111
26	106.3	106.3	106.3	106.3	106.3	-4.9	-116	-116	-116	-116	-116
27	101.4	101.4	101.4	101.4	101.4	-9.8	-121	-121	-121	-121	-121
28	96.5	96.5	96.5	96.5	96.5	96.5	-14.7	-126	-126	-126	-126
29	91.6	91.6	91.6	91.6	91.6	91.6	-19.6	-131	-131	-131	-131
30	86.7	86.7	86.7	86.7	86.7	86.7	-24.5	-136	-136	-136	-136
31	81.8	81.8	81.8	81.8	81.8	81.8	-29.4	-141	-141	-141	-141
32	77	77	77	77	77	77	77	-34.2	-145	-145	-145
33	72.1	72.1	72.1	72.1	72.1	72.1	72.1	-39.1	-150	-150	-150
34	67.2	67.2	67.2	67.2	67.2	67.2	67.2	-44	-155	-155	-155
35	62.3	62.3	62.3	62.3	62.3	62.3	62.3	-48.9	-160	-160	-160
36	57.4	57.4	57.4	57.4	57.4	57.4	57.4	-53.8	-165	-165	-165
37	52.5	52.5	52.5	52.5	52.5	52.5	52.5	52.5	-58.7	-170	-170
38	47.6	47.6	47.6	47.6	47.6	47.6	47.6	47.6	-63.6	-175	-175
39	42.7	42.7	42.7	42.7	42.7	42.7	42.7	42.7	-68.5	-180	-180
40	37.8	37.8	37.8	37.8	37.8	37.8	37.8	37.8	-73.4	-185	-185
41	32.9	32.9	32.9	32.9	32.9	32.9	32.9	32.9	32.9	-78.3	-190
42	28	28	28	28	28	28	28	28	28	-83.2	-194
43	23.1	23.1	23.1	23.1	23.1	23.1	23.1	23.1	23.1	-88.1	-199
44	18.2	18.2	18.2	18.2	18.2	18.2	18.2	18.2	18.2	-93	-204
45	13.3	13.3	13.3	13.3	13.3	13.3	13.3	13.3	13.3	-97.9	-209
46	9.8	9.8	9.8	9.8	9.8	9.8	9.8	9.8	9.8	9.8	-101
47	7.3	7.3	7.3	7.3	7.3	7.3	7.3	7.3	7.3	7.3	-104
48	4.9	4.9	4.9	4.9	4.9	4.9	4.9	4.9	4.9	4.9	-106
49	2.4	2.4	2.4	2.4	2.4	2.4	2.4	2.4	2.4	2.4	-109
50	0	0	0	0	0	0	0	0	0	0	0

Figure 4-21 Shear (kN) values due to tandem load

3. Lane load: As opposed to the design truck & tandem load, the lane load is a uniformly continuous load applied to entire bridge. Value is fixed at 9.34 kN/m , Figure 4-22.

It should be noted that the lane load is also introduced incrementally until it covers the entire bridge span. The process would have to be done from both ends in case this was a continuous bridge. For simply supported beams, maximum results would be mirrored across the mid-span. Moment & shear are presented in Figure 4-23 and Figure 4-24

AASHTO Art. 3.6.1.2.4

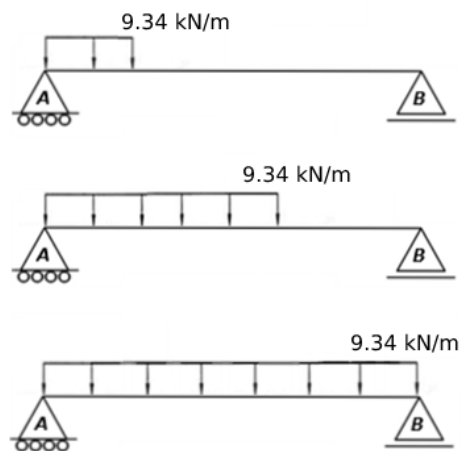


Figure 4-22 Incremental introduction of lane load

	0	0.1	0.2	0.3	0.4	0.5	0.6	0.7	0.8	0.9	1
0	0	0	0	0	0	0	0	0	0	0	0
1	0	0.2	0.2	0.2	0.2	0.1	0.1	0.1	0.1	0	0
2	0	1	0.9	0.8	0.7	0.6	0.4	0.3	0.2	0.1	0
3	0	2.2	2	1.7	1.5	1.2	1	0.7	0.5	0.2	0
4	0	4	3.6	3.1	2.7	2.2	1.8	1.3	0.9	0.4	0
5	0	6.2	5.6	4.9	4.2	3.5	2.8	2.1	1.4	0.7	0
6	0	8.7	8	7	6	5	4	3	2	1	0
7	0	11.1	10.9	9.5	8.2	6.8	5.4	4.1	2.7	1.4	0
8	0	13.5	14.2	12.4	10.7	8.9	7.1	5.3	3.6	1.8	0
9	0	15.8	18	15.7	13.5	11.2	9	6.7	4.5	2.2	0
10	0	18	22.2	19.4	16.7	13.9	11.1	8.3	5.6	2.8	0
11	0	20.2	26.6	23.5	20.2	16.8	13.4	10.1	6.7	3.4	0
12	0	22.4	30.9	28	24	20	16	12	8	4	0
13	0	24.5	35	32.8	28.2	23.5	18.8	14.1	9.4	4.7	0
14	0	26.5	39.1	38.1	32.7	27.2	21.8	16.3	10.9	5.4	0
15	0	28.5	43	43.7	37.5	31.2	25	18.7	12.5	6.2	0
16	0	30.4	46.9	49.5	42.6	35.5	28.4	21.3	14.2	7.1	0
17	0	32.2	50.6	55.1	48.1	40.1	32.1	24.1	16	8	0
18	0	34	54.2	60.5	54	45	36	27	18	9	0
19	0	35.8	57.7	65.7	60.1	50.1	40.1	30.1	20	10	0
20	0	37.5	61.1	70.8	66.6	55.5	44.4	33.3	22.2	11.1	0
21	0	39.1	64.4	75.7	73.2	61.2	49	36.7	24.5	12.2	0
22	0	40.7	67.5	80.5	79.5	67.2	53.8	40.3	26.9	13.4	0
23	0	42.2	70.6	85	85.6	73.4	58.8	44.1	29.4	14.7	0
24	0	43.7	73.5	89.5	91.5	80	64	48	32	16	0
25	0	45.1	76.4	93.7	97.2	86.8	69.4	52.1	34.7	17.4	0
26	0	46.5	79.1	97.8	102.6	93.6	75.1	56.3	37.5	18.8	0
27	0	47.8	81.7	101.7	107.8	100.1	81	60.7	40.5	20.2	0
28	0	49	84.2	105.5	112.8	106.3	87.1	65.3	43.5	21.8	0
29	0	50.2	86.6	109	117.6	112.3	93.4	70.1	46.7	23.4	0
30	0	51.4	88.9	112.5	122.2	118	100	75	50	25	0
31	0	52.5	91	115.7	126.5	123.4	106.5	80.1	53.4	26.7	0
32	0	53.5	93.1	118.8	130.6	128.6	112.6	85.3	56.9	28.4	0
33	0	54.5	95	121.7	134.5	133.4	118.5	90.7	60.5	30.2	0
34	0	55.4	96.9	124.5	138.2	138	124	96.3	64.2	32.1	0
35	0	56.2	98.6	127	141.6	142.3	129.1	102	68	34	0
36	0	57	100.2	129.4	144.8	146.3	133.9	107.7	72	36	0
37	0	57.8	101.7	131.7	147.8	150.1	138.4	112.9	76	38	0
38	0	58.5	103.1	133.8	150.6	153.6	142.6	117.8	80.2	40.1	0
39	0	59.1	104.3	135.7	153.2	156.7	146.4	122.3	84.5	42.2	0
40	0	59.7	105.5	137.4	155.5	159.7	149.9	126.3	88.9	44.4	0
41	0	60.2	106.6	139	157.6	162.3	153.1	130	93.1	46.7	0
42	0	60.7	107.5	140.4	159.5	164.7	155.9	133.3	96.9	49	0
43	0	61.1	108.3	141.7	161.2	166.7	158.4	136.3	100.2	51.3	0
44	0	61.5	109.1	142.8	162.6	168.5	160.6	138.8	103.1	53.8	0
45	0	61.8	109.7	143.7	163.8	170.1	162.4	140.9	105.5	56.2	0
46	0	62	110.2	144.4	164.8	171.3	163.9	142.7	107.5	58.5	0
47	0	62.2	110.6	145	165.6	172.3	165.1	144	109.1	60.2	0
48	0	62.4	110.8	145.4	166.2	173	165.9	145	110.2	61.5	0
49	0	62.4	111	145.7	166.5	173.4	166.4	145.6	110.8	62.2	0
50	0	62.5	111.1	145.8	166.6	173.5	166.6	145.8	111.1	62.5	0

Figure 4-23 Moment (kN.m) values due design lane

	0	0.1	0.2	0.3	0.4	0.5	0.6	0.7	0.8	0.9	1
0	0	0	0	0	0	0	0	0	0	0	0
1	2.3	0	0	0	0	0	0	0	0	0	0
2	4.5	-0.1	-0.1	-0.1	-0.1	-0.1	-0.1	-0.1	-0.1	-0.1	-0.1
3	6.6	-0.2	-0.2	-0.2	-0.2	-0.2	-0.2	-0.2	-0.2	-0.2	-0.2
4	8.7	-0.4	-0.4	-0.4	-0.4	-0.4	-0.4	-0.4	-0.4	-0.4	-0.4
5	10.8	-0.6	-0.6	-0.6	-0.6	-0.6	-0.6	-0.6	-0.6	-0.6	-0.6
6	12.8	1.5	-0.8	-0.8	-0.8	-0.8	-0.8	-0.8	-0.8	-0.8	-0.8
7	14.8	3.4	-1.1	-1.1	-1.1	-1.1	-1.1	-1.1	-1.1	-1.1	-1.1
8	16.8	5.4	-1.5	-1.5	-1.5	-1.5	-1.5	-1.5	-1.5	-1.5	-1.5
9	18.7	7.3	-1.8	-1.8	-1.8	-1.8	-1.8	-1.8	-1.8	-1.8	-1.8
10	20.5	9.1	-2.3	-2.3	-2.3	-2.3	-2.3	-2.3	-2.3	-2.3	-2.3
11	22.3	10.9	-0.5	-2.8	-2.8	-2.8	-2.8	-2.8	-2.8	-2.8	-2.8
12	24	12.7	1.3	-3.3	-3.3	-3.3	-3.3	-3.3	-3.3	-3.3	-3.3
13	25.8	14.4	3	-3.8	-3.8	-3.8	-3.8	-3.8	-3.8	-3.8	-3.8
14	27.4	16	4.6	-4.5	-4.5	-4.5	-4.5	-4.5	-4.5	-4.5	-4.5
15	29	17.6	6.3	-5.1	-5.1	-5.1	-5.1	-5.1	-5.1	-5.1	-5.1
16	30.6	19.2	7.8	-3.6	-5.8	-5.8	-5.8	-5.8	-5.8	-5.8	-5.8
17	32.1	20.7	9.4	-2	-6.6	-6.6	-6.6	-6.6	-6.6	-6.6	-6.6
18	33.6	22.2	10.8	-0.5	-7.4	-7.4	-7.4	-7.4	-7.4	-7.4	-7.4
19	35	23.7	12.3	0.9	-8.2	-8.2	-8.2	-8.2	-8.2	-8.2	-8.2
20	36.4	25.1	13.7	2.3	-9.1	-9.1	-9.1	-9.1	-9.1	-9.1	-9.1
21	37.8	26.4	15	3.6	-7.8	-10	-10	-10	-10	-10	-10
22	39.1	27.7	16.3	4.9	-6.5	-11	-11	-11	-11	-11	-11
23	40.3	28.9	17.6	6.2	-5.2	-12	-12	-12	-12	-12	-12
24	41.5	30.2	18.8	7.4	-4	-13.1	-13.1	-13.1	-13.1	-13.1	-13.1
25	42.7	31.3	19.9	8.5	-2.8	-14.2	-14.2	-14.2	-14.2	-14.2	-14.2
26	43.8	32.4	21	9.7	-1.7	-13.1	-15.4	-15.4	-15.4	-15.4	-15.4
27	44.9	33.5	22.1	10.7	-0.7	-12	-16.6	-16.6	-16.6	-16.6	-16.6
28	45.9	34.5	23.1	11.8	0.4	-11	-17.9	-17.9	-17.9	-17.9	-17.9
29	46.9	35.5	24.1	12.7	1.3	-10	-19.2	-19.2	-19.2	-19.2	-19.2
30	47.8	36.4	25.1	13.7	2.3	-9.1	-20.5	-20.5	-20.5	-20.5	-20.5
31	48.7	37.3	25.9	14.6	3.2	-8.2	-19.6	-21.9	-21.9	-21.9	-21.9
32	49.6	38.2	26.8	15.4	4	-7.4	-18.8	-23.3	-23.3	-23.3	-23.3
33	50.4	39	27.6	16.2	4.8	-6.6	-18	-24.8	-24.8	-24.8	-24.8
34	51.1	39.7	28.3	16.9	5.6	-5.8	-17.2	-26.3	-26.3	-26.3	-26.3
35	51.8	40.4	29	17.6	6.3	-5.1	-16.5	-27.9	-27.9	-27.9	-27.9
36	52.5	41.1	29.7	18.3	6.9	-4.5	-15.9	-27.2	-29.5	-29.5	-29.5
37	53.1	41.7	30.3	18.9	7.5	-3.8	-15.2	-26.6	-31.2	-31.2	-31.2
38	53.7	42.3	30.9	19.5	8.1	-3.3	-14.7	-26.1	-32.9	-32.9	-32.9
39	54.2	42.8	31.4	20	8.6	-2.8	-14.1	-25.5	-34.6	-34.6	-34.6
40	54.7	43.3	31.9	20.5	9.1	-2.3	-13.7	-25.1	-36.4	-36.4	-36.4
41	55.1	43.7	32.3	20.9	9.5	-1.8	-13.2	-24.6	-36	-38.3	-38.3
42	55.5	44.1	32.7	21.3	9.9	-1.5	-12.8	-24.2	-35.6	-40.2	-40.2
43	55.8	44.4	33	21.7	10.3	-1.1	-12.5	-23.9	-35.3	-42.1	-42.1
44	56.1	44.7	33.3	22	10.6	-0.8	-12.2	-23.6	-35	-44.1	-44.1
45	56.4	45	33.6	22.2	10.8	-0.6	-12	-23.3	-34.7	-46.1	-46.1
46	56.6	45.2	33.8	22.4	11	-0.4	-11.8	-23.1	-34.5	-45.9	-48.2
47	56.7	45.3	34	22.6	11.2	-0.2	-11.6	-23	-34.4	-45.8	-50.3
48	56.8	45.5	34.1	22.7	11.3	-0.1	-11.5	-22.9	-34.3	-45.6	-52.5
49	56.9	45.5	34.1	22.8	11.4	0	-11.4	-22.8	-34.2	-45.6	-54.7
50	56.9	45.5	34.2	22.8	11.4	0	-11.4	-22.8	-34.2	-45.5	-56.9

Figure 4-24 Shear (kN) values due to design lane

4.6 Live load summary

While the moment & shear tables from the previous section are a pleasure to look at, they fall short in conveying the results in a direct and brief manner. One further step has been taken better summarize and manage live load calculations done so far.

At increments of 10% of span length, the maximum moment and shear values are noted down respectively. Note that there is no negative moment for the design example, given that this is a simply supported span.

In simple terms, at mid-span $x = 6.1$ m the maximum applied moment at the bridge section due to the design truck is calculated to be 596.2 kN.m. Highest shear value due to design truck has been documented at supports to be 241 kN See Table-4-6 & Table-4-7 below.

Table 4-6 Moment summary due to live load

x	x/L	Truck		Tandem		Lane	
m	.	kN.m		kN.m		kN.m	
0	0	0	0	0	0	0	0
1.2	0.1	253.9	0	228.2	0	62.4	0
2.4	0.2	428.2	0	402.2	0	111	0
3.7	0.3	543.6	0	526.3	0	145.7	0
4.9	0.4	601.5	0	591.9	0	166.5	0
6.1	0.5	596.2	0	609.8	0	173.4	0
7.3	0.6	601.5	0	591.9	0	166.5	0
8.5	0.7	543.6	0	526.3	0	145.7	0
9.8	0.8	428.2	0	402.2	0	111	0
11	0.9	253.9	0	228.2	0	62.4	0
12.2	1	0	0	0	0	0	0

Table 4-7 Shear summary due to live load

x	x/L	Truck		Tandem		Lane	
m	.	kN		kN		kN	
0	0	241	0	209.1	0	56.9	0
1.2	0.1	208.4	-9.7	184.6	-9.8	46.1	-0.6
2.4	0.2	175.7	-24.2	165	-32.9	36.4	-2.3
3.7	0.3	143.8	-38.7	140.6	-52.5	27.9	-5.1
4.9	0.4	114.7	-56.6	121	-77	20.5	-9.1
6.1	0.5	85.7	-85.7	96.5	-96.5	14.2	-14.2
7.3	0.6	56.6	-114.7	77	-121	9.1	-20.5
8.5	0.7	38.7	-143.8	52.5	-140.6	5.1	-27.9
9.8	0.8	24.2	-175.7	32.9	-165	2.3	-36.4
11	0.9	9.7	-208.4	9.8	-184.6	0.6	-46.1
12.2	1	0	-241	0	-209.1	0	-56.9

4.7 Dynamic Load Allowance

The greatest of the following loading scenarios is taken as the controlling live load value (LL):

• Case 1	$LL = LL_{truck} * (1 + \%IM) + LL_{Lane}$
• Case 2	$LL = LL_{Tandem} * (1 + \%IM) + LL_{Lane}$
	AASHTO Art. 3.6.1.3.1

Case 1 & case 2 are applied for both, moment and shear independently. Where (IM) is the impact factor, also known as the dynamic load allowance. A factor used to increase live loads by accounting for centrifugal & braking forces, also known as the impact factor. Applied only for the design truck and tandem load. IM is given by Table 4-8 below.

Table 4-8 AASHTO LRFD specifications, table 3.6.2.1-1

Component	<i>IM</i>
Deck Joints—All Limit States	75%
All Other Components	
• Fatigue and Fracture Limit State	15%
• All Other Limit States	33%

Considering our design example at X= 6.1 m (mid-span).

• Case 1	$LL = 967 \text{ kN.m}$
• Case 2	$LL = 985 \text{ kN.m}$

The same procedure is repeated across all span intervals. See Table 4-9 & Table 4-10 for the load summary including the impact factor. Case 1 can be seen in this example to be the controlling case.

Table 4-9 Moment summary due to live load including impact factor

x	x/L	Truck		Tandem		Lane		Case 1		Case 2	
m	.	kN.m		kN.m		kN.m		kN.m		kN.m	
0	0	0	0	0	0	0	0	0	0	0	0
1.2	0.1	253.9	0	228.2	0	62.4	0	400.1	0	365.9	0
2.4	0.2	428.2	0	402.2	0	111	0	680.5	0	645.9	0
3.7	0.3	543.6	0	526.3	0	145.7	0	868.6	0	845.6	0
4.9	0.4	601.5	0	591.9	0	166.5	0	966.5	0	953.7	0
6.1	0.5	596.2	0	609.8	0	173.4	0	966.4	0	984.4	0
7.3	0.6	601.5	0	591.9	0	166.5	0	966.5	0	953.7	0
8.5	0.7	543.6	0	526.3	0	145.7	0	868.6	0	845.6	0
9.8	0.8	428.2	0	402.2	0	111	0	680.5	0	645.9	0
11	0.9	253.9	0	228.2	0	62.4	0	400.1	0	365.9	0
12.2	1	0	0	0	0	0	0	0	0	0	0

Table 4-10 Shear summary due to live load including impact fact

x	x/L	Truck		Tandem		Lane		Case 1		Case 2	
m	.	kN		kN		kN		kN		kN	
0	0	241	0	209.1	0	56.9	0	377.5	0	335	0
1.2	0.1	208.4	-9.7	184.6	-9.8	46.1	-0.6	323.3	-13.4	291.6	-13.6
2.4	0.2	175.7	-24.2	165	-32.9	36.4	-2.3	270.1	-34.5	255.9	-46.1
3.7	0.3	143.8	-38.7	140.6	-52.5	27.9	-5.1	219.1	-56.6	214.8	-74.9
4.9	0.4	114.7	-56.6	121	-77	20.5	-9.1	173.1	-84.5	181.4	-111.5
6.1	0.5	85.7	-85.7	96.5	-96.5	14.2	-14.2	128.2	-128.2	142.6	-142.6
7.3	0.6	56.6	-114.7	77	-121	9.1	-20.5	84.5	-173.1	111.5	-181.4
8.5	0.7	38.7	-143.8	52.5	-140.6	5.1	-27.9	56.6	-219.1	74.9	-214.8
9.8	0.8	24.2	-175.7	32.9	-165	2.3	-36.4	34.5	-270.1	46.1	-255.9
11	0.9	9.7	-208.4	9.8	-184.6	0.6	-46.1	13.4	-323.3	13.6	-291.6
12.2	1	0	-241	0	-209.1	0	-56.9	0	-377.5	0	-335

4.8 Live Load Distribution Factors

In the previous sections, live loads have been estimated. However, it should not be forgotten that the bridge deck is an element composed of different materials. Each material with its own behavior, interactions and set of rules. Not to mention the wide array of possible cross sections. These individual parts cease to behave independently. Instead, they act as single integrated unit. Depicting the behavior of this newly integrated element is a complex affair. We would be doing this topic injustice by generalizing the behavior of one material for the rest of the structure.

Imagine a truck traveling the length of simple wooden bridge, the effect is immediately noted on the girder directly below it, in terms of creaking and arching as it carries the majority of the truck's weight. Neighboring girders and members should also contribute by drawing some of the load to them, given how connected the entire bridge system is. In other words, truck load is resisted by multiple girders, but the loads are not shared equally. Now, how much of the truck's load is transmitted to each girder is a question whose answer is laid down in AASHTO LRFD Art.4.6.2 & 4.6.3. Both articles concern themselves with laying down procedures and methods with which, the live load share on each girder can be approximated.

- Approximate method AASHTO Art.4.6.2: calculated live loads (moment & shear) are multiplied by a dimensionless factor called distribution factor (DF). A total of 4 factors are needed. Two pairs for moment and shear for interior girders and another pair for exterior girders.
- Refined methods AASHTO Art.4.6.3: the most prominent of them is the finite element analysis.

Upcoming subsection lays down the procedure for acquiring live load distribution factors using the approximate method.

4.8.1 Approximate Method

K_g : Defined as the longitudinal stiffness parameter and is given by:

$K_g = n(I + A * e_g^2)$	AASHTO eq.4.6.2.2.1-1
--------------------------	-----------------------

Where e_g is the distance between the center of gravity of the steel girder and deck center. See Figure 4-25.

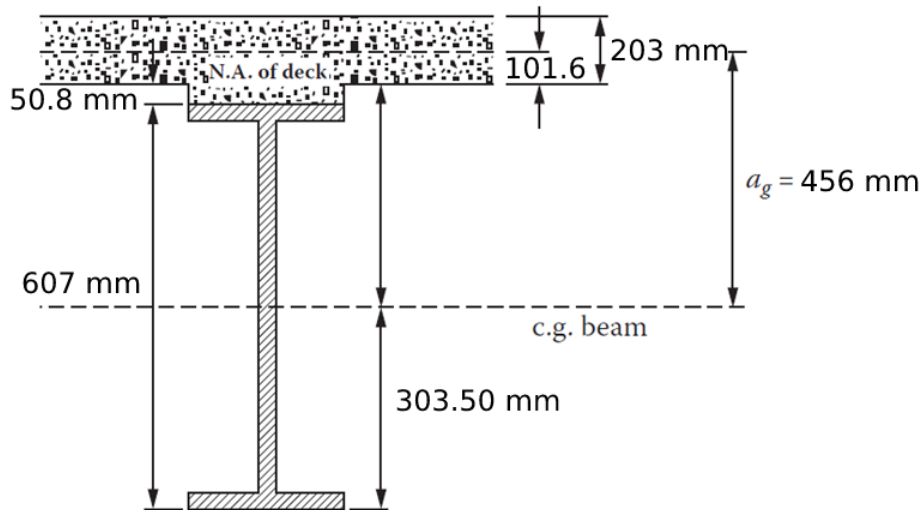
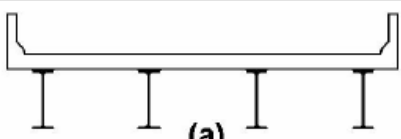


Figure 4-25 Section geometry showing e_g

Code provisions designate type (a) for this design example. Subsequent equations used should match the designated bridge type. Refer to Table 4-12.

Table 4-11 Excerpt from AASHTO Table 4.6.2.2.1-1

Supporting Components	Type of Deck	Typical Cross-Section
Steel Beam	Cast-in-place concrete slab, precast concrete slab, steel grid, glued/spiked panels, stressed wood	 <p>(a)</p>

The tables below present a summary for evaluating the live load distribution factors for moment and shear at interior and exterior girders for type (a) bridge designation. The procedure considers two loading scenarios; One for the case where only a single lane is loaded, the second considers two or more lanes are loaded.

Table 4-12 Live load distribution factor summary (interior). AASHTO Tables 4.6.2.2.2b-1 & 4.6.2.2.3a-1

FORCE TYPE	LANE LOADING	DISTRIBUTION FACTOR	APPLICABILITY CONDITIONS
MOMENT	1	$0.06 + \left(\frac{S}{4300}\right)^{0.4} \left(\frac{S}{L}\right)^{0.3} \left(\frac{K_g}{Lt_s^3}\right)^{0.1}$ $= 0.4973$	$1100 \leq S \leq 4900$ $110 \leq t_s \leq 300$ $6000 \leq L \leq 73\ 000$ $N_b \geq 4$ $4 \times 10^9 \leq K_g \leq 3 \times 10^{12}$
	≥ 2	$0.075 + \left(\frac{S}{2900}\right)^{0.6} \left(\frac{S}{L}\right)^{0.2} \left(\frac{K_g}{Lt_s^3}\right)^{0.1}$ $= 0.6546 \text{ controlling for moment}$	
SHEAR	1	$0.36 + \frac{S}{7600} = 0.68$	$1100 \leq S \leq 4900$ $6000 \leq L \leq 73\ 000$ $110 \leq t_s \leq 300$ $N_b \geq 4$
	≥ 2	$0.2 + \frac{S}{3600} - \left(\frac{S}{10\ 700}\right)^{2.0}$ $= 0.814 \text{ controlling for shear}$	

Table 4-13 Table 4.10 Live load distribution factor summary (exterior). AASHTO Tables 4.6.2.2.2d-1 & 4.6.2.2.3b-1

FORCE TYPE	LANE LOADING	DISTRIBUTION FACTOR	APPLICABILITY CONDITIONS
MOMENT	1	<ul style="list-style-type: none"> Lever rule. Detailed below $= 0.75 \text{ controlling for moment}$	$-300 \leq d_e \leq 1700$
	≥ 2	$g = e g_{interior}$ $e = 0.77 + \frac{d_e}{2800}$ $= 0.648$	
SHEAR	1	<ul style="list-style-type: none"> Lever rule. Detailed below $= 0.75 \text{ controlling for shear}$	
	≥ 2	$g = e g_{interior}$ $e = 0.6 + \frac{d_e}{3000}$ $= 0.6512$	

In case the applicability conditions were not met, refined structural analysis using finite element may be needed. This example meets all applicability conditions.

The lever rule is an additional requirement for exterior girders in beam-slab bridges. The goal of this procedure is to determine the support reaction assuming the first interior support is a hinge. First wheel is located 0.61 m from the barrier base. Second wheel is located 1.82 m from the first wheel. In case the second wheel is located beyond the first interior beam, then the load of this wheel is not considered, Figure 4-26.

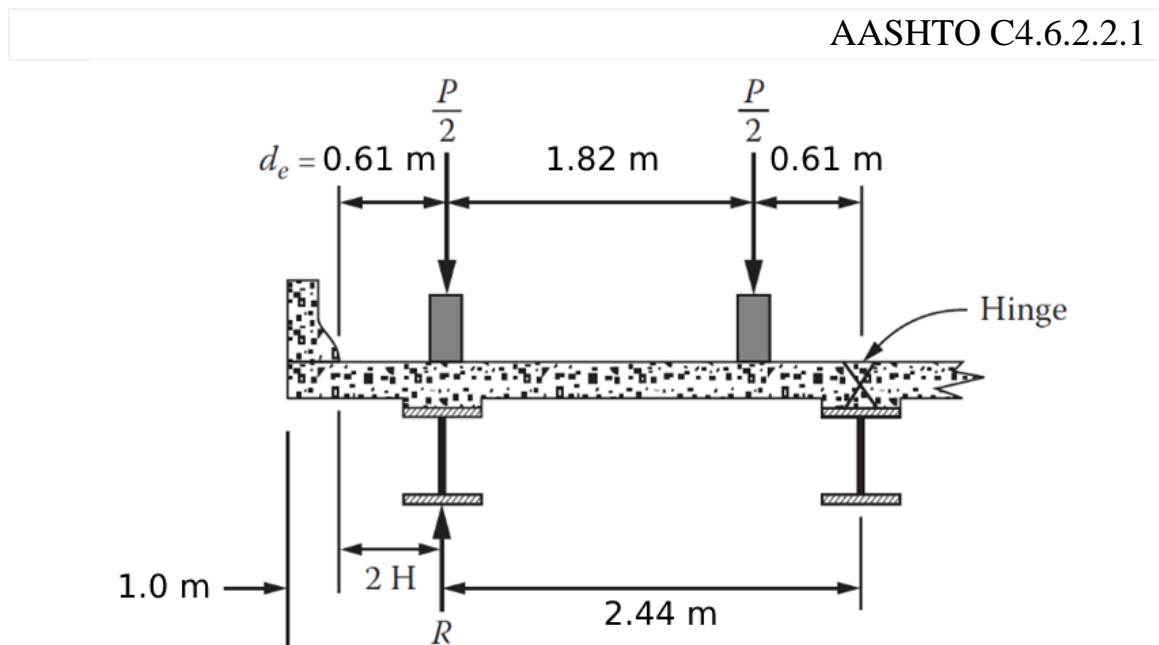


Figure 4-26 Lever rule configuration

Using simple statistics, the support reaction at the first exterior girder is calculated as $R = 0.625$.

The distribution factor for exterior girders calls for an additional multiplier called the multiple presence factor, (m). Given by Table 4-14

Table 4-14 Multiple presence factor - AASHTO Table 3.6.1.1.2-1

Number of Loaded Lanes	Multiple Presence Factors, <i>m</i>
1	1.20
2	1.00
3	0.85
>3	0.65

- Live load distribution factor for moment for exterior girders with one lane loaded is given by $DF = R * m = 0.625 * 1.2 = 0.75$.
- Live load distribution factor for shear for exterior girders with one loaded lane is similar to that of the moment, $DF = R * m = 0.75$.

AASHTO Art.3.6.1.1.2 states that for the fatigue limit state, the multiple presence factor (*m*) should not be considered. Therefore, cases where single lane is loaded are considered and are divided by their respective multiple presence factor. Note that fatigue design only considers loading due to a single truck:

- Fatigue distribution factor for interior girders for moment where one lane is loaded is **$0.4973/1.2 = 0.4144$**
- Fatigue distribution factor for interior girders for shear where one lane is loaded is **$0.0.68/1.2 = 0.5667$**
- Fatigue distribution factor for exterior girders for moment where one lane is loaded **$0.75/1.2 = 0.625$**
- Fatigue distribution factor for exterior girders for shear where one lane is loaded **$0.75/1.2 = 0.625$**

Table 4-16 Shear summary due to live load

x	x/L	Truck		Tandem		Lane		Case 1		Case 2		INT (LL+IM)		EXT (LL+IM)	
m	.	kN		kN		kN		kN		kN		kN		kN	
0	0	241	0	209.1	0	56.9	0	377.5	0	335	0	307.4	0	283.3	0
1.2	0.1	208.4	-9.7	184.6	-9.8	46.1	-0.6	323.3	-13.4	291.6	-13.6	263.3	-11.1	242.4	-10.2
2.4	0.2	175.7	-24.2	165	-32.9	36.4	-2.3	270.1	-34.5	255.9	-46.1	220.2	-37.4	202.4	-34.7
3.7	0.3	143.8	-38.7	140.6	-52.5	27.9	-5.1	219.1	-56.6	214.8	-74.9	178.4	-60.9	164.1	-56
4.9	0.4	114.7	-56.6	121	-77	20.5	-9.1	173.1	-84.5	181.4	-111.5	147.7	-90.7	136.1	-83.6
6.1	0.5	85.7	-85.7	96.5	-96.5	14.2	-14.2	128.2	-128.2	142.6	-142.6	116.1	-116.1	106.8	-106.8
7.3	0.6	56.6	-114.7	77	-121	9.1	-20.5	84.5	-173.1	111.5	-181.4	90.7	-147.7	83.6	-136.1
8.5	0.7	38.7	-143.8	52.5	-140.6	5.1	-27.9	56.6	-219.1	74.9	-214.8	60.9	-178.4	56	-164.1
9.8	0.8	24.2	-175.7	32.9	-165	2.3	-36.4	34.5	-270.1	46.1	-255.9	37.4	-220.2	34.7	-202.4
11	0.9	9.7	-208.4	9.8	-184.6	0.6	-46.1	13.4	-323.3	13.6	-291.6	11.1	-263.3	10.2	-242.4
12.2	1	0	-241	0	-209.1	0	-56.9	0	-377.5	0	-335	0	-307.4	0	-283.3

Given Table 4-15 & Table 4-16, Columns for case-1 & case-2 (marked with blue arrows) represent live load applied in kN.m per design lane. On the other hand, the newly added columns (marked with red arrows) represent the live load applied in kN.m per girder.

The entire goal in the beginning has been to answer one question. For a truck moving across a bridge, how much of its load is transmitted to neighboring girders? The proportioned live load value is referred to as (LL+IM). Implying that the impact factor has already been added.

At $X = 6.1$ m (mid-span), the maximum moment due to live load for interior girders is given by

$$\max(966.4, 984.4) * 0.6546 = 649.9 \text{ kN.m}$$

Where:

- 966.4 kN.m is due to case-1.
- 984.4 kN.m is due to case 2.
- 0.6546 is the live load distribution factor for moment for interior girders.

This marks the end of live load calculations. Subsequent section will make use of the resulting (LL+IM) values present in Table 4-13 & Table 4-14.

4.10 Permanent Deformations

Performed according to AASHTO Art.6.10.4.2 at the service II limit state.

The objective of this check is to ensure that objectionable deformations due to severe traffic would not compromise the structure. Procedure is performed for both flanges, top and bottom, for interior and exterior girders. Resulting in a total of 4 passing checks. Moreover, service II limit state aims to limit yielding of steel components and to control slippage of slip-critical connections.

Flanges should satisfy the following requirements:

$f_f \leq 0.95 * Rh * F_{yf}$ for top flanges	AASHTO 6.10.4.2.2-1
$f_f + f_l/2 \leq 0.95 * Rh * F_{yf}$ for bottom flanges	AASHTO 6.10.4.2.2-2

Where

$F_{yf} = f_y = 414 \text{ MPa}$	
f_l : flange lateral bending stress at the section under consideration due to the Service II loads. $f_l = 0$ for skewless bridges.	
Rh : hybrid factor. $Rh = 1$	AASHTO 6.10.1.10.1
f_f : flange stress due to the Service II.	

Intuition would have us believe that by using the stress equation $f = M_u / S_x$, the entire applied moment on the section would have to be divided by a single elastic modulus, S_x . More specifically, S_x of the bridge as it stands during service in its composite state (steel + concrete).

The uniqueness of bridge engineering shines as it presents a rather different way of considering stresses applied. Instead, f_f is computed as the incremental stresses due to loads applied throughout the bridge's lifecycle, where each load is applied on its respective cross section.

The incremental stresses are:

- Stresses due to the moment induced by DC1, applied on the non-composite section (steel only).
- Stresses due to the moment induced by (DC2+DW), applied on the long-term composite section.
- Stresses due to the moment induced by (LL+IM), applied on the short-term composite section.

For service II limit state, maximum moment is given by

$$M_u = \eta[M_{DC} + M_{DW} + 1.3 * (LL + IM)] \quad \text{AASHTO Table 3.4.1-1}$$

Where: $\eta=1$

f_f is computed as:

$$f_f = \frac{M_{DC1}}{S_{x, non-composite}} + \frac{M_{DC2} + M_{DW}}{S_{x, composite-long-term}} + \frac{1.3 * (LL + IM)}{S_{x, composite-short-term}}$$

Table 4-17 showcases the 4 different checks performed. Top & bottom flanges for both, interior and exterior girders successfully meet the permanent deformation provisions at service II limit state.

Table 4-18 Permanent deformations calculation summary

Variable	INTERIOR		EXTERIOR	
	TOP	BOTTOM	TOP	BOTTOM
Moment _{DC1}	253.6 kN.m			
Moment _{DC2}	45.3 kN.m			
Moment _{DW}	49.9 kN.m			
Moment (LL+IM)	644.3 kN.m		738.34 kN.m	
S_x . non-composite section	Refer to Table 4-2 Short/long-term composite section properties			
S_x . composite-long-term				
S_x . composite-short-term				
f_t	107 MPa	272 MPa	108 MPa	297 MPa
f_f ≤ 0.95 * 1 * 60 = 393 MPa	✓	✓	✓	✓

4.11 Plastic Moment of Composite Section

Computed according to AASHTO Appendix D6.

The plastic moment, M_p , is defined as the moment at which the entire composite section has reached its yield stress.

Unlike the previously evaluated neutral axis for the short- & long-term composite sections, the plastic moment is evaluated about a different neutral axis. Namely, the plastic neutral axis, PNA. Investigating PNA's location is the first step towards obtaining the plastic moment. See Figure 4-27.

Forces governing PNA's location are as follows:

$P_s = 0.85 * f'_c * b_e * t_s$	Plastic compressive force in concrete deck, equals 13064 kN, 11923 kN for interior & exterior girders respectively. This expression is based on a rectangular stress block.
$P_{rb} = P_{rt}$	Plastic compressive force in slab reinforcement top & bottom layers. Conservatively neglected.
$P_c = F_{yc} * b_c * t_c$	plastic force in compression flange, equals 1633 kN for interior & exterior girders.
$P_w = F_{yw} * D * t_w$	plastic force in web, equals 2646 kN for interior & exterior girders.
$P_t = F_{yt} * b_t * t_t$	plastic force in tension flange, equals 1633 kN for interior & exterior girders.

Assuming PNA is somewhere within the concrete slab and by means of force equilibrium, PNA's location can be computed by using the following expression for interior and exterior girders respectively:

$$\bar{Y} * (0.85 * f'_c * b_e) = P_c + P_w + P_t$$

$$\bar{Y} = 91.95\text{mm}, 100.8\text{ mm}$$

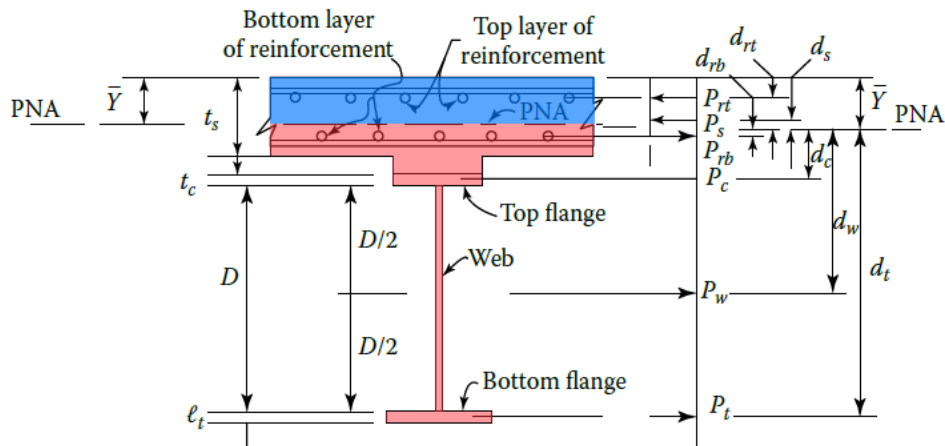


Figure 4-27 Cross section showing location of PNA

\bar{Y} is measured from the top of the composite section as seen in Figure 4-27. Resulting values are in accordance with deck height. Note that, although the slab is partially in tension. Only the compression component is considered. Concrete is assumed to have no contribution in tension. The same goes for reinforcement bars within the concrete. In case \bar{Y} resulted in a value greater than slab height (203 mm), it implies that the initial assumption was misplaced.

Alternatively, code provisions lay down detailed systematic procedure comprising 7 different cases for PNA's location. These cases would have to be checked in the right order, stopping at the first case that meets its respective conditions.

Algebraically, M_p is the sum of all plastic forces multiplied by their arm length to PNA.

$$M_p = \left(\frac{\bar{Y}^2}{2}\right) * (0.85 * f'_c * b_e) + [P_c * d_c + P_w * d_w + P_t * d_t]$$
$$M_p = 3025 \text{ kN.m}, 2999 \text{ kN.m}$$

for interior & exterior girders respectively.

Acquiring M_p is an indispensable part for ensuring a bridge's structural integrity. Subsequent design steps will make use of the computed plastic moment.

4.12 Flexural Resistance of Composite Section

Performed according to AASHTO Art.6.10.6.2 at Strength I limit state.

Procedure breakdown is summarized in Figure 4-28 below.

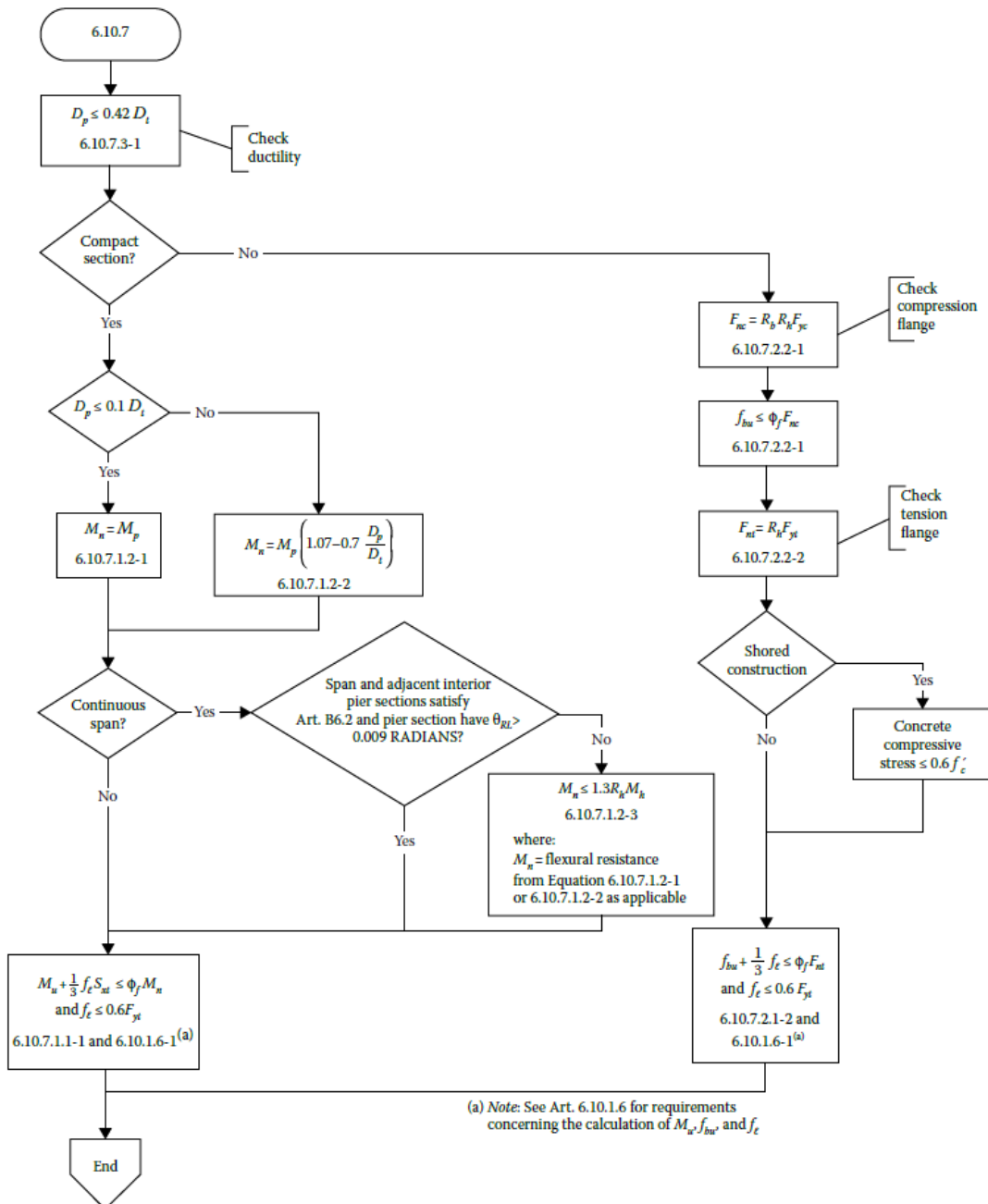


Figure 4-28 Flowchart for AASHTO LRFD Art.6.10.7

Flexural resistance of composite sections is conditioned on whether the section is compact or non-compact. For checking compactness, the following conditions should be satisfied:

- Minimum yield strength of flanges $F_y = 414 < 485 \text{ MPa}$. Condition is met for interior & exterior girders.
- Web should satisfy AASHTO Art.6.10.2.1.1 requirements, $\frac{D}{t_w} = 51.2 < 150$. Condition is met for interior & exterior girders.
- $\frac{2 \cdot D_{cp}}{t_w} \leq 3.76 * \sqrt{\frac{E}{F_{yc}}}$, where D_{cp} is the depth of web in compression at the plastic state. PNA has been shown to be located in the concrete deck. Hence, $D_{cp} = 0$. Condition is met for interior & exterior girders. AASHTO eq. 6.10.6.2.2-1.

Compactness of the composite section is thereby confirmed. See Table-18 for subsequent calculations summary.

Table 4-19 Calculation summary for flexural resistance of composite section

ITEM	DEFINITION	GIRDER TYPE	
		INTERIOR	EXTERIOR
D_p	Distance from top of concrete slab to PNA. $D_p = \bar{Y}$.	92 mm	100.7 mm
D_t	Full depth of composite section.	861 mm	
$0.1 * D_t$		86.1 mm	
M_n	if $D_p \leq 0.1 * D_t$	$M_n = M_p$	
M_n	if $D_p > 0.1 * D_t$ Governs.	$M_n = M_p * (1.07 - 0.7 * \frac{D_p}{D_t})$	
		3010.8 kN.m	2961.5 kN.m
M_u at strength I limit state	<ul style="list-style-type: none"> $M_u = \eta[1.25 * M_{DC} + 1.5 * M_{DW} + 1.75 * (LL + IM)]$ $\eta = 1$ 	1575.86 kN.m	1740.5 kN.m
Check	<ul style="list-style-type: none"> $M_u + \frac{1}{3} * f_l * S_{xt} \leq \Phi_f * M_n$ For skew-less bridges $f_l = 0$. Resistance factor $\Phi = 1$. 	✓	✓
$D_p \leq 0.42 D_t$	Additional requirement, AASHTO Art.6.10.7.3. Safeguard concrete slab from premature crushing	✓	✓

The last check, $D_p \leq 0.42 D_t$, is a ductility requirement that aims to protect the concrete deck from premature cracking.

Moreover, the algebraic expression M_u/M_n can be referred to as the performance indicator or performance ratio. This ratio gives an indication of the overall performance of the conducted limit state check. M_u/M_n is calculated to be 0.524, 0.588 for interior and exterior girders respectively. For a design to be considered cost-efficient and economical, the engineer responsible for the profile selection should strive for a design that pushes the performance ratios as close as possible to the value of 1.0.

4.13 Shear Design

Performed according to AASHTO Art.6.10.9 at Strength I limit state. Procedure breakdown is summarized in Figure 4-29 below.

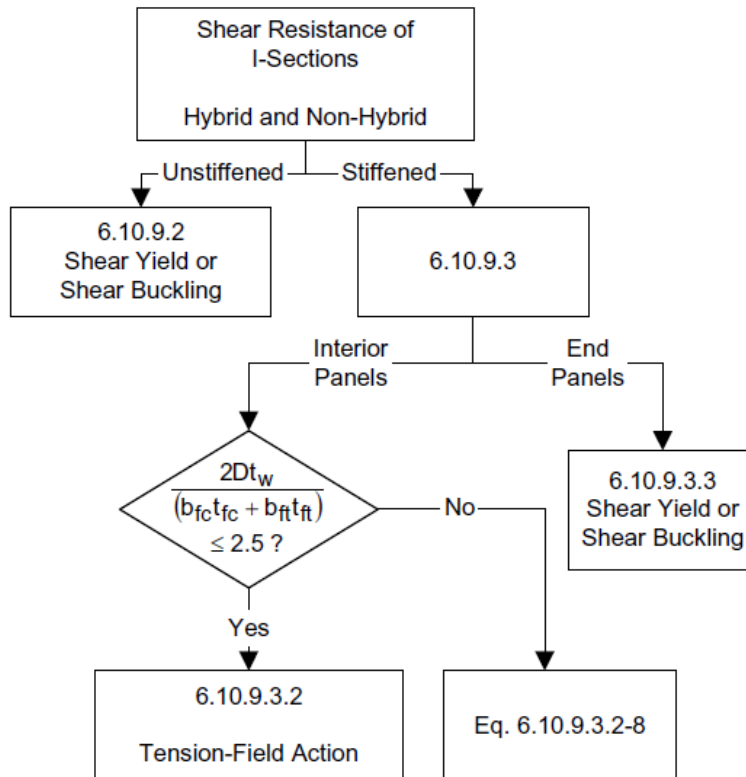


Figure 4-29 Flowchart for Shear Design of I-Sections. AASHTO C6.10.9.1-1

The shear resistance of a bridge is predominantly a function of the web's stiffness. In cases where the web has been shown to have inadequate stiffness, the addition of supporting ribs becomes imperative. This applies when the factored shear load exceeds the unstiffened web capacity. These supporting ribs are referred to as stiffeners and they may be added in two forms:

- Transverse stiffeners: comprising a steel plate fixed vertically at the beams' web from either side, Figure 4-30. The plate is fixed by means of welding, note that the plate should also be welded to the compression flange and it may be short of the tension flange (Zhao & Tonias, 2017). Transverse stiffeners themselves are divided into two categories depending on their location.
 1. Bearing stiffeners: also known as end stiffeners, located at bridge supports.
 2. Intermediate stiffeners: located anywhere between the bridge supports.Maximum spacing between transverse stiffeners is shown in Figure 4-31. Shear resistance is calculated based on the resulting panels, either end or interior panel.
- Longitudinal stiffeners: comprising a steel plate placed horizontally at the web along the beam's length from either side, Figure 4-30. When used in conjunction with transverse stiffeners, the longitudinal stiffener should extend uninterrupted. Therefore, it is advisable that they should be placed on the opposite side of the web from transverse stiffeners. Longitudinal stiffeners are typically used for long-span bridges (Narendra, 2014).

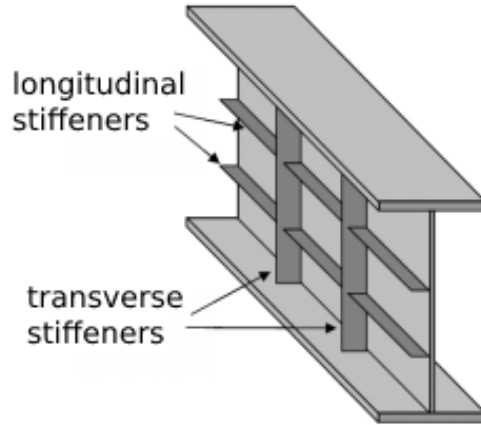


Figure 4-30 Longitudinal & transverse stiffeners

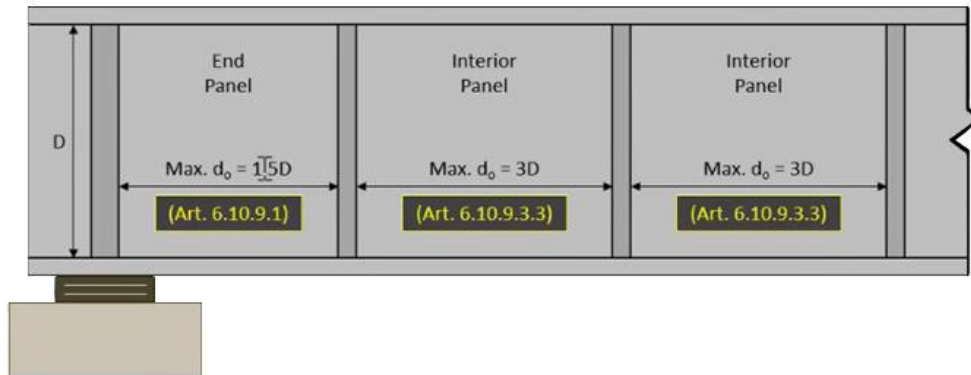


Figure 4-31 Maximum spacing of transverse stiffeners

Although the AASHTO LRFD shear provision 6.10.9 permits the use of an unstiffened design, the addition of stiffeners is rewarding to the overall economy of the steel profile as it permits the use of deep thinner webs.

This design example makes use of transverse stiffeners. Furthermore, subsequent calculations summary for the shear design makes use of the assumed stiffeners spacing only. Whereas, exact geometry of the stiffeners takes no direct part this AASHTO section.

Shear resistance is given by

$V_u \leq \Phi_v * V_n$	AASHTO 6.10.9.1-1
-------------------------	-------------------

Where:

- V_u : shear in the web at the section under consideration. As calculated in earlier sections of this chapter.
- Φ_v : resistance factor for shear, given by AASHTO Art.6.5.4.2.
- V_n : nominal shear resistance of unstiffened webs. Calculated according to AASHTO 6.10.9.3. Detailed procedure breakdown is shown below in Table 4-19 & Table 4-20

Table 4-20 Calculation summary for nominal shear resistance. Part-1

VARIABLE	DEFINITION	Equation	Reference	Value
V_p	Plastic shear force	<ul style="list-style-type: none"> $V_p = 0.58 * F_{yw} * D * T_w$ T_w: Web thickness D: Web height 	6.10.9.3.3-2	1535 kN
d_o	Maximum spacing used between all transverse stiffeners	<ul style="list-style-type: none"> $d_{o.end} = 1.5 * D$ 	6.10.9.3.3	859 mm
k	Shear-buckling coefficient	$k = 5 + 5/(d_o/D)^2$	6.10.9.3.2-7	7.22
Φ_v	Shear resistance factor		6.5.4.2	1
V_u	Ultimate shear at Strength I limit state	<ul style="list-style-type: none"> $V_u = \eta[1.25 * V_{DC} + 1.5 * V_{DW} + 1.75 * (LL + IM)]$ $V_{u.ext} = 644 \text{ kN}$ $V_{u.int} = 685 \text{ kN}$ $V_u = \max(V_{u.ext}, V_{u.int})$ 		685 kN
C	Ratio of shear buckling resistance to shear-yield strength. For web slenderness case (1)	<ul style="list-style-type: none"> if $\frac{D}{T_w} \leq 1.2 * \sqrt{\frac{E*k}{F_{yw}}}$ then $C = 1$ ✓ (controls) 	6.10.9.3.2-4	1
	Web slenderness case (2)	<ul style="list-style-type: none"> if $1.12 * \sqrt{\frac{E*k}{F_{yw}}} \leq \frac{D}{T_w} \leq 1.4 * \sqrt{\frac{E*k}{F_{yw}}}$ then $C = \frac{1.12}{\frac{D}{T_w}} * \sqrt{\frac{E*k}{F_{yw}}}$ ✗ 	6.10.9.3.2-5	1.94
	Web slenderness case (3)	<ul style="list-style-type: none"> if $\frac{D}{T_w} > 1.4 * \sqrt{\frac{E*k}{F_{yw}}}$ then $C = \frac{1.57}{\left(\frac{D}{T_w}\right)^2} * \left(\frac{E*k}{F_{yw}}\right)$ ✗ 	6.10.9.3.2-6	4.71

Table 4-21 Calculation summary for nominal shear resistance. Part-2

End panel				
VARIABLE	DEFINITION	Equation	Reference	Value
V_n	Nominal shear resistance	$V_n = V_{cr} = C * V_p$	6.10.9.2-1	1535 kN
	Check	$V_u \leq (\Phi_v * V_n)$	6.10.9.1-1	✓
Interior panel				
VARIABLE	DEFINITION	Equation	Reference	Value
V_n	Nominal shear resistance	<ul style="list-style-type: none"> • if $\frac{2*D*T_w}{b_{fc}*t_{fc}+b_{ft}*t_{ft}} \leq 2.5$ • then $V_n = V_p * (C + \frac{0.87*(1-C)}{\sqrt{(\frac{d_o}{D})^2}})$ • ✓ • else $V_n = V_p * (C + \frac{0.87*(1-C)}{\sqrt{(\frac{d_o}{D})^2 + (\frac{d_o}{D})}})$ • ✗ 	6.10.9.3.2-1 6.10.9.3.2-2 6.10.9.3.2-8	1535 kN
	Check	$V_u \leq (\Phi_v * V_n)$	6.10.9.1-1	✓

The controlling performance ratio V_u/V_n was calculated to be 0.446, which meets the passing criteria. However, cost-effectiveness of the design in terms of shear design remains highly questionable.

4.14 Fatigue Design

Performed according to AASHTO Art.6.6.1 at Fatigue I limit state.

One unique phenomenon in steel structures is the fact that member failure may occur when subjected to cyclic loading, even when the applied load is well below the ultimate design load.

First described in 1839 by J. V. Poncelet (Poncelet , 1870), fatigue is a detrimental behavior that leads to reduced material strength under repeated loading. This discovery presented a new perspective to the design procedure, shifting the emphasis from the maximum load applied to stress range and load fluctuations. Interestingly enough, steel grade has been shown to carry no significant contribution in resisting fatigue failure. See Figure 4-32.

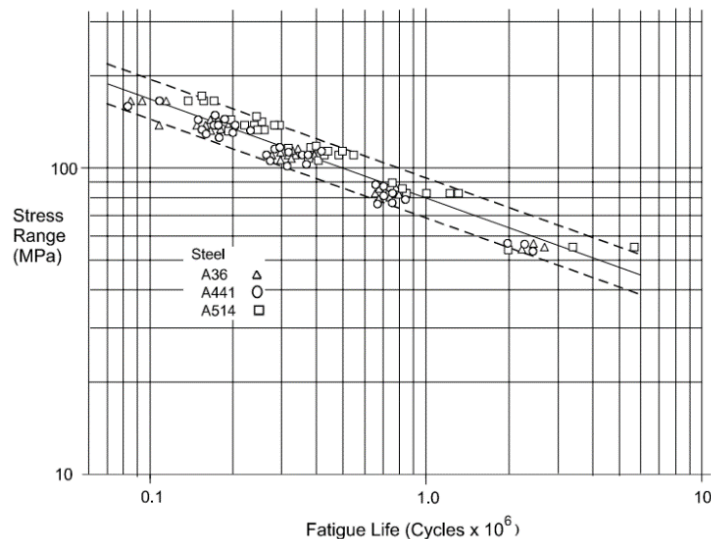


Figure 4-32 Effect of Grade of Steel on Fatigue Life. (Fisher, Kulak, & Smith, 1998)

Notches, sudden changes of cross section, grooves, sharp corners as well as material imperfections at the surface level can result in stress raisers. Additionally, sudden increase in temperature due to welding can lead to the formation of residual stresses. All in all, these locations would be subjected to

higher stress concentrations under normal loading scenarios, rendering it fertile grounds for microscopic cracks to propagate further into the material cross-section (Fisher, Kulak, & Smith, 1998).

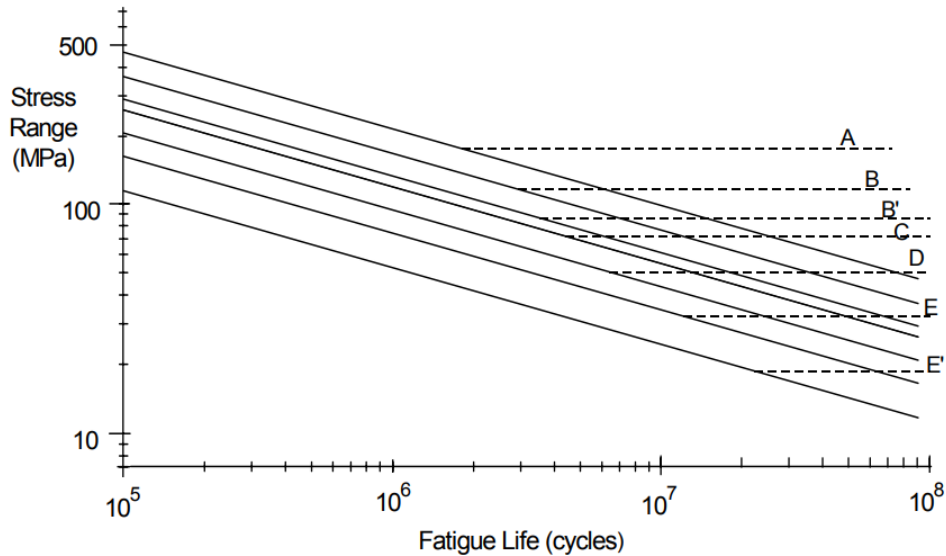


Figure 4-33 Endurance (or S-N) curve. (Fisher, Kulak, & Smith, 1998)

According to Figure 4-33, as the stress range decreases, the higher the number of allowed stress cycles. This increase in the number of stress cycles is valid until a horizontal line is reached, implying that beyond this point, the steel detail in question could be loaded infinitely throughout its theoretical service life without being subjected to fatigue failure.

AASHTO LRFD provisions make use of the endurance curve (S-N) by providing two fatigue limit states. Where design criteria is given by

$\gamma * (\Delta F) \leq \phi \Delta F n$	AASHTO eq. 6.6.1.2.2-1
--	------------------------

The two limit states are as follows:

- Fatigue I (infinite-life): representing the infinite range region. As long as the stress range does not exceed a certain value, the detail in question is able to withstand the applied load an infinite number of times. Traffic volume plays no role in this limit state.

The nominal fatigue resistance here is given by:

$$\Delta F_n = \Delta F_{TH}$$

This expression is checked for the different components as given in AASHTO Table 6.6.1.2.3-1

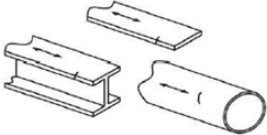
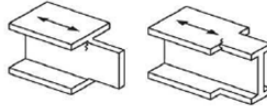
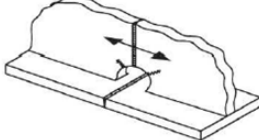
- Fatigue II (finite-life): representing the finite range region. Traffic volume, more specifically, the average daily truck traffic (ADTT) plays a major role in determining the nominal fatigue resistance.

It is worth noting that fatigue checks apply to loading scenarios based on a single design truck. Lane load & tandem load take no part in fatigue considerations.

While Fatigue I is a more conservative design approach, AASHTO LRFD provisions permits designing for Fatigue II given that the average daily truck traffic (ADTT) is within an allowable range. This design example makes use of Fatigue I limit state.

Fatigue provisions constantly make reference to the term “detail” or “design detail”. This term refers to the different bridge components susceptible to fatigue failure. The components are categorized and designated by the following letters: A, B, B’, C, C’, D, E, E’. See Table 4-21 for sample components & descriptions.

Table 4-22 Excerpt from AAHTO Table 6.6.1.2.3-1. Detail Categories for Load-Induced Fatigue

Description	Category	Constant A MPa $\wedge 3$	Threshold $(\Delta F)_{TH}$ MPa	Potential Crack Initiation Point	Illustrative Examples
Section 1—Plain Material away from Any Welding					
1.1 Base metal, except noncoated weathering steel, with rolled or cleaned surfaces. Flame-cut edges with surface roughness value of 1,000 μ -in. or less, but without re-entrant corners.	A	8.21 * 10^{12}	165	Away from all welds or structural connections	
1.2 Noncoated weathering steel base metal with rolled or cleaned surfaces designed and detailed in accordance with FHWA (1989). Flame-cut edges with surface roughness value of 1,000 μ -in. or less, but without re-entrant corners.	B	3.94 * 10^{12}	110	Away from all welds or structural connections	
1.3 Member with re-entrant corners at copes, cuts, block-outs or other geometrical discontinuities made to the requirements of AASHTO/AWS D1.5, except weld access holes.	C	1.44 * 10^{12}	69	At any external edge	
1.4 Rolled cross sections with weld access holes made to the requirements of AASHTO/AWS D1.5, Article 3.2.4.	C	1.44 * 10^{12}	69	In the base metal at the re-entrant corner of the weld access hole	

Detail category (C) represents a very common design detail that covers a wide array of bridge components. Namely, stiffener connections, weld access holes and most importantly shear studs. There is a high likelihood that fatigue design for this detail would control fatigue design, if not the entire bridge design. Calculation summary for Fatigue I limit state is presented below in Table 4-22.

Table 4-23 Calculation summary for Fatigue I limit state

Item	DEFINITION	GIRDER	
		INTERIOR	EXTERIOR
ϕ	Resistance factor	1	
γ	Fatigue load factor	1.75	
Mu	Maximum moment due to fatigue truck	460 kN.m	
IM	Impact factor for single design lane	1.15	
DF.moment	Live load distribution factor for moment	0.414	0.625
m(LL+IM)	$Mu * IM * DF.moment$	218.8 kN.m	330.35 kN.m
$Sx_{st.top}$	Plastic section modulus for the short term at the top of steel	Refer to Table 4-2 Short/long-term composite section properties	
$Sx_{st.bottom}$	Plastic section modulus for the short term at the bottom of steel		
$\Delta F_n (C)$	Nominal fatigue resistance for detail (C)	6.9 MPa	
$\gamma * \Delta F_{top}$	Factored Stress at the top of steel $= \gamma * m(LL+IM) / S_x$	7.3 MPa	10.2 MPa
$\gamma * \Delta F_{bottom}$	Factored stress at the bottom of steel $= \gamma * m(LL+IM) / S_x$	74.0 MPa	112.7 MPa
	Controlling stress value (max)	74.0 MPa	112.7 MPa
	Check $\gamma * (\Delta F) \leq \phi \Delta F_n$	✗	✗

While previous design checks have been far from failing or even being close to fail, Fatigue I limit state for detail (C) has been shown to be a major concern. Exterior girders are shown to have a performance ratio of 1.63. Interior girders do also exceed the permitted allowance at a value of 1.073 although by a short margin. The use of different steel profiles will be explored in upcoming chapters.

4.15 Miscellaneous checks

- Live load deflection

At face value, a beam deflecting due to its own weight or due to an applied load is an expected behavior. Allowing for marginal material imperfections and using preliminary knowledge in mechanics of materials, deflection can be deduced at the design stage with high accuracy. However, undesirable implications can still stem from other secondary members or connections.

Moreover, vibration due to deflection can carry negative psychological effects on both, pedestrians and drivers. High amplitude vibrations can induce unrest & discomfort, similar to that of seasickness (Roeder, Barth, & Bergman, 2002).

Previous AASHTO LRFD provisions carried within it an optional clause that regulated live load beam deflection to a maximum value of

$\frac{L}{800}$	AASHTO Art. 2.5.2.6.2
-----------------	-----------------------

Where L is the span length. This check is nowhere to be mentioned in the more recent AASHTO LRFD editions. However, for the sake of completeness, the check will be incorporated into the design procedure.

Deflection is calculated as the largest of:

1. Deflection due to design truck alone. Dynamic load allowance will be applied.
2. Deflection due to 25% of the deflection due to the design truck plus deflection due to lane load. Dynamic load allowance will not be applied to the lane load.

Below is the calculation summary for the live load deflection check

Table 4-24 Calculation summary for live load deflection

Item	DEFINITION	GIRDER	
		INTERIOR	EXTERIOR
Allowed deflection	Maximum allowed deflection ($L/800$)	15.24 mm	
DF	Live load distribution factor = $m * \left(\frac{\text{Number of lanes}}{\text{Number of girders}} \right)$. m is the multi-presence factor	0.425	
1. Due to design truck	• (Δ) due to the 145kN axis being placed at midspan = $PL^3/EI48$	10.2 mm	10.4 mm
	• (Δ) due to the remaining off-centered axles. 145kN and 35kN	5.6 mm	5.7 mm
	• (Δ_{truck}) Total deflection due to design truck alone	15.8 mm	16.1 mm
	• Total factored deflection due to design truck = $(\Delta_{truck}) * DF$	6.7 mm	6.8 mm
2. Due to lane load + 25% design truck	• (Δ_{lane}) Total deflection due to design lane	3.8 mm	3.9 mm
	• Total factored deflection due to design lane = $(\Delta_{lane}) * DF$	1.6 mm	1.6 mm
	• $(\Delta_{lane}) * DF + 25\%(\Delta_{truck}) * DF$	3.3 mm	3.4 mm
Controlling case	• max(1.,2.)	6.7 mm	6.8 mm
	Check $(L/800) \leq \max(a, b)$	✓	✓

It is worth going over the methodology, with which the deflection was calculated. The design truck comprising 3 axles have been placed in such a way that would yield the highest deflection, that is by placing the 2nd axle (145 kN) directly at mid-span. Deflection of a simply supported beam due to mid-span load or even an off-centered load can be calculated with the aid of deflection equations found in your typical university mechanics of materials textbook. See Figure 4-34.

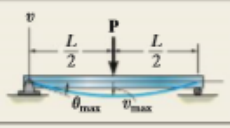
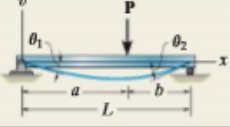
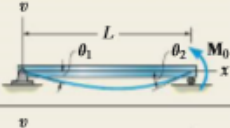
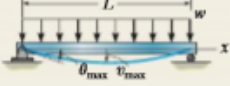
Simply Supported Beam Slopes and Deflections			
Beam	Slope	Deflection	Elastic Curve
	$\theta_{\max} = \frac{-PL^2}{16EI}$	$v_{\max} = \frac{-PL^3}{48EI}$	$v = \frac{-Px}{48EI} (3L^2 - 4x^2)$ $0 \leq x \leq L/2$
	$\theta_1 = \frac{-Pab(L+b)}{6EIL}$ $\theta_2 = \frac{Pab(L+a)}{6EIL}$	$v \Big _{x=a} = \frac{-Pba}{6EIL} (L^2 - b^2 - a^2)$	$v = \frac{-Pbx}{6EIL} (L^2 - b^2 - x^2)$ $0 \leq x \leq a$
	$\theta_1 = \frac{-M_0L}{6EI}$ $\theta_2 = \frac{M_0L}{3EI}$	$v_{\max} = \frac{-M_0L^2}{9\sqrt{3}EI}$ at $x = 0.5774L$	$v = \frac{-M_0x}{6EIL} (L^2 - x^2)$
	$\theta_{\max} = \frac{-wL^3}{24EI}$	$v_{\max} = \frac{-5wL^4}{384EI}$	$v = \frac{-wx}{24EI} (x^3 - 2Lx^2 + L^3)$

Figure 4-34 Slopes and deflection of beams. (Hibbeler, 2014)

The (EI) part of the deflection equation presents an interesting question. For our composite bridge, which modulus of elasticity should be considered? Moreover, which moment of inertia?

Given that this check concerns itself with live load, section properties of the short-term composite section are to be considered. These include an equivalent moment of inertia (I) for the entire section. Earlier subsections in this chapter showcased how the concrete section of the bridge has been transformed into an equivalent area of steel. This enables the use of the modulus of elasticity of steel (E) for deflection equations.

Deflection resulting from each of the truck's 3 axles is summed and multiplied by the live load distribution factor. Final value is compared with the maximum allowed deflection. Similar procedure has been performed for the lane load, which comprises a uniformly distributed load. Both, interior and exterior girders have been shown to exhibit no excessive deflection due to the live load.

4.16 Summary

The presented AASHTO LRFD provisions in this chapter by no means cover the entirety of the design process. They serve only to present aspects of the design that are unique to the field of bridge engineering. Moreover, the intention was to provide the reader with a brief summary on some of the fundamental engineering concepts that take place behind hidden doors in any conventional bridge engineering software. The full design procedure is provided as an appendix that is addressed in the upcoming chapter.

At this point we should address the state of the bridge in terms of conforming to the AASHTO LRFD provisions. Note that, failure to meet any of the limit states requirements dictates that the design is invalid and should be revised.

Fatigue-I limit state has been shown to be a major design flow since it recorded a performance ratio of 1.63. Even if we were to proceed with the assumption that Fatigue-I was too conservative for this design example, and Fatigue II were to be used instead, cost-effectiveness of the design remains questionable.

The performance ratio for Strength I limit state for both, flexural resistance & shear was recorded at 0.588 & 0.446 respectively. These values imply that, when fully loaded, the superstructure is only utilizing 50% of its full potential.

By relying on the conventional method for amending the problem, the selected steel profile would have to be revised and the problem should be solved once again. However, there is no guarantee that the new selected profile won't come to face the same issues, if not even new issues. Especially when considering the near-infinite number of possibilities for the design changes.

Take the scenario where one engineer might decide to go with a wider bottom flange as to address the fatigue failure. Another engineer might consider a shorter section with thicker flanges, in an attempt to address fatigue and cost-effectiveness in a single step. There is also the possibility of considering hot-rolled vs built-up sections and their effect on the bridge economy.

All these questions present the perfect use case for optimization tools as they are able to dynamically search the domain for possible design parameters that meet all presented requirements. Thereby ensuring a design that possibly pushes all performance ratios to their limits.

The upcoming chapter explores a procedure that implements the use of both, Excel solver & AASHRO LRFD specifications with the goal of amending the problem parameters.

Chapter 5

Methods & Procedures

Chapter 5 Methods & Procedures

5.1 Introduction

Early in this paper, Chapter 2 presented the topic of optimization as whole with emphasis on nature inspired methods such as the genetic optimization. This was followed by exploring Excel Solver as a readily-available tool for tackling non-linear engineering problems. Moreover, making the case for Excel and justifying the methodology is a point that was briefly touched upon in Chapter 2. Detailed discussion is presented in the upcoming chapter.

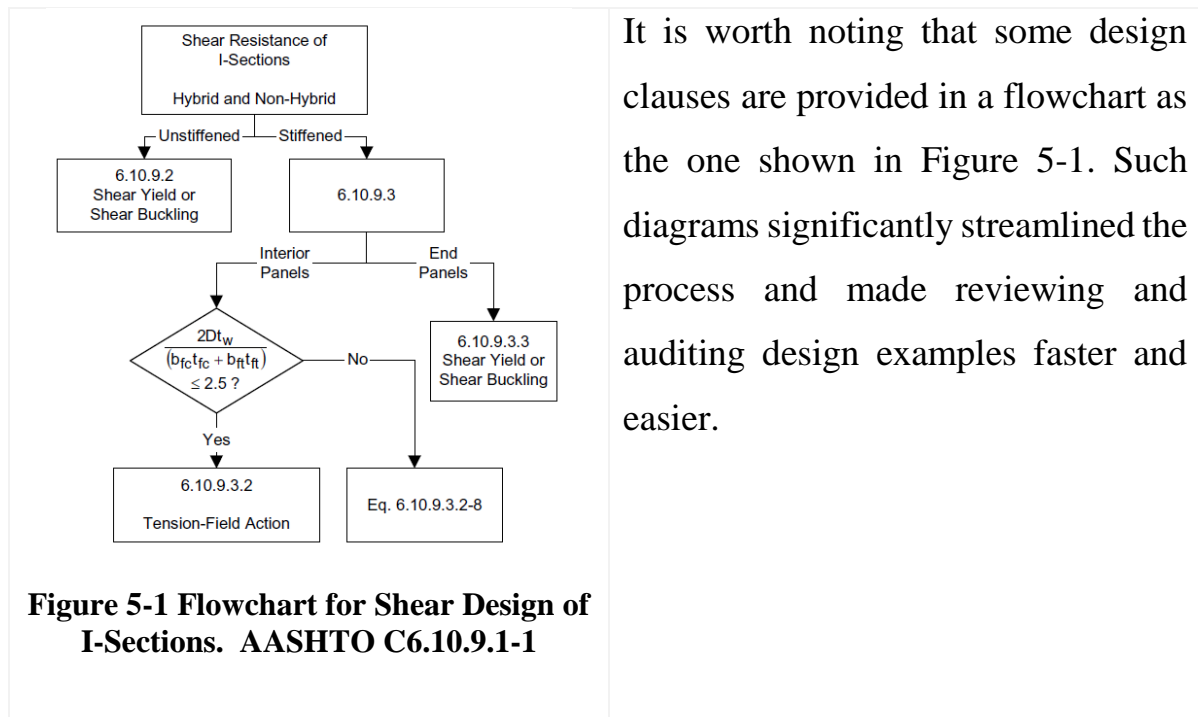
On the other hand, Chapter 4 introduced AASHTO LRFD design procedure for composite plate girder bridges, highlighting design aspects unique to the field of bridge engineering. While the intention was for that chapter to be a brief summary, the reader will come to see how intricate the overall design flow is.

Finally, this chapter is an amalgamation of everything that preceded it. The know-how & empirical equations governing the design procedure will be translated into an Excel module that incorporates genetic optimization using Excel Solver. Different constraints and administrative decisions will be tried and tested and finally compared in upcoming sections.

5.2 The Mapping Process

Mapping down the problem in a spreadsheet in a sequential manner could not be achieved by relying on the AASHTO LRFD provisions alone. AASHTO provisions are laid down in an order that doesn't match how the problem is conventionally solved. Instead, the use of multiple existing design examples had to be followed to ensure no major design steps have been omitted. This is further supplemented by the fact that code provisions are narrated without an accompanying example.

Translating the code's provisions into a spreadsheet module accounted for the majority of the research's time and efforts. This did not come as a surprise since the integrity of any subsequent results and conclusions heavily rely on the module being audited and tested with each new addition to the design process.



It is worth noting that some design clauses are provided in a flowchart as the one shown in Figure 5-1. Such diagrams significantly streamlined the process and made reviewing and auditing design examples faster and easier.

5.3 Excel Setup

By referring to the problem parameters presented in subsection Problem Parameters4.1, a similar section had been created in the spreadsheet to serve as a central reference for all unit weights & geometry parameters for future use. Separation of logic (equations) and data entry is a good practice that ensures the problem parameters can be modified and customized easily without interfering with the problem’s logic. Additionally, it eliminates the need for in-depth onboarding & training for prospective users. Table 5-1 & Table 5-2.

Table 5-1 Girder parameters

<i>Solver Initial Trial</i>	<i>Value</i>	<i>Unit</i>
<i>Selected girder</i>	W24x76	
<i>Top flange width</i>	229	mm
<i>Top flange thk</i>	17.3	mm
<i>Web height</i>	572.5	mm
<i>Web thk</i>	11.2	mm
<i>Bottom flange width</i>	229	mm
<i>Bottom flange thk</i>	17.3	mm
<i>Deck thk</i>	203	mm
<i>Overhang width</i>	1	m
<i>Number of girders</i>	6	
<i>no. of cross frames</i>	3	

-

Table 5-2 General Parameters Setup

<i>Bridge Parameter</i>	<i>Value</i>	<i>Unit</i>
(L) Single span length	12.2	m
Full bridge width	14.2	m
Number of mid-barriers	0	-
Barrier base thickness	0.4	m
Clear road width (Full - 2 * Barrier base)	13.4	m
(n) Modular Ratio	8	-
Top rebar cover	57	mm
Bottom rebar cover	32	mm
Unit weight for SIP	0.335	kN/m ²
Unit weight of Asphalt	1.2	kN/m ²
Density of concrete	2400	kg/ m ³
Density of steel	7850	kg/ m ³
(Fy) Yield strength of steel	414	MPa
(fc') Compressive strength of concrete	31	MPa
Standard width of design lane	3.66	m
Number of design lanes	3	
(S) Effective width of interior girders	2.44	m
Effective width of exterior girders	2.225	m
<i>Related to wind design</i>		
Bridge Location -	<i>Open country</i>	
Vo (Table 3.8.1.1-1)	13.2	mph
Zo (Table 3.8.1.1-1)	0.070	m
Bridge height from low ground	10.67	m
<i>Related to fatigue design</i>		
Average daily truck traffic (ADTT). max ADT of 20 000 *(0.2)	12000	

To further aid the data-entry process, a number of drawings have been created using the built-in X-Y scatter graphs. These graphs have been setup in a way that makes them react dynamically to changes in the bridge geometry. This addition played a major role in the early setup stages. See Figure 5-2, Figure 5-3.

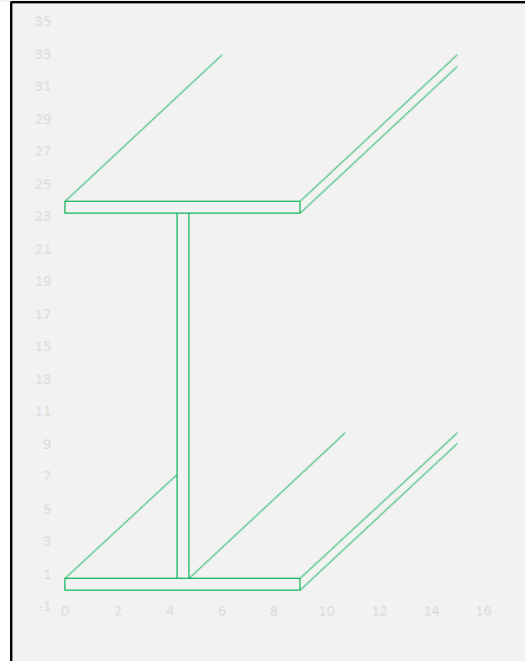


Figure 5-2 X-Y scatter graph of selected girder profile

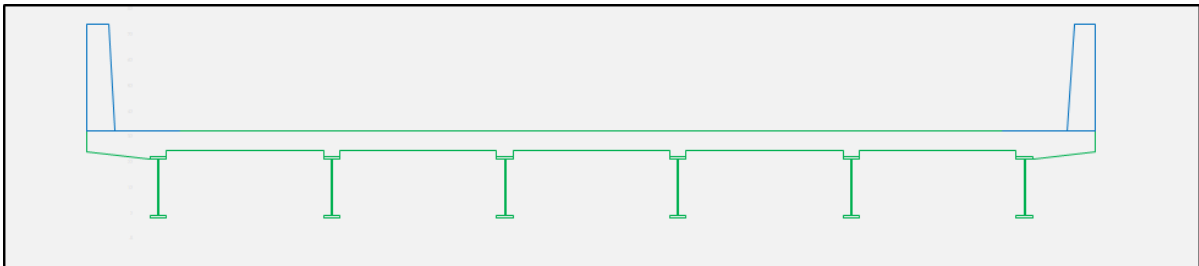


Figure 5-3 X-Y scatter graph of bridge cross section

Admittedly, these 2-D drawings are no match to the typical 3-D models that you would find in many of the bridge engineering software tools, however they remain a welcome visual abstraction from all of the numbers.

5.4 Variables

At this stage, the spreadsheet as a whole can be summarized as being a function where the input parameters correspond to the bridge geometry and the output being the different performance ratios from the design steps. The responsibility and role of improving the output is completely up to the operator. However, by introducing Solver you forgo having to go through the iterative process of testing different input parameters. This requires defining the set of design parameters that are intended to be updated with each iteration.

Design variables have been selected as the following:

- Top flange width.
- Top flange thickness.
- Web height.
- Web thickness.
- Bottom flange width.
- Bottom flange thickness.
- Number of girders.
- Deck overhang width.
- Number of cross frames (diaphragm).

Figure 5-6 showcases the size parameters for a typical bridge girder.

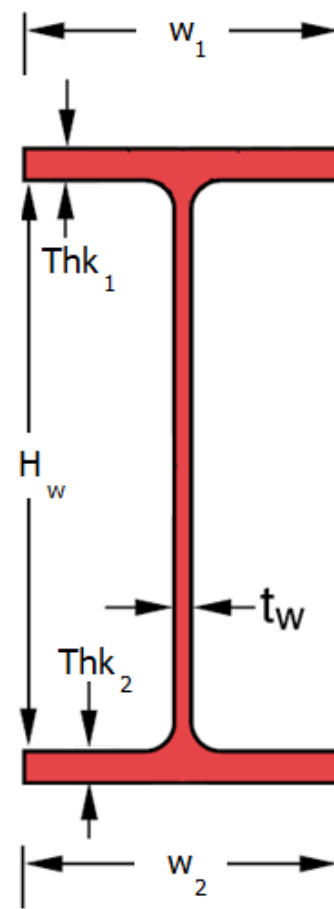


Figure 5-4 I-Girder geometry

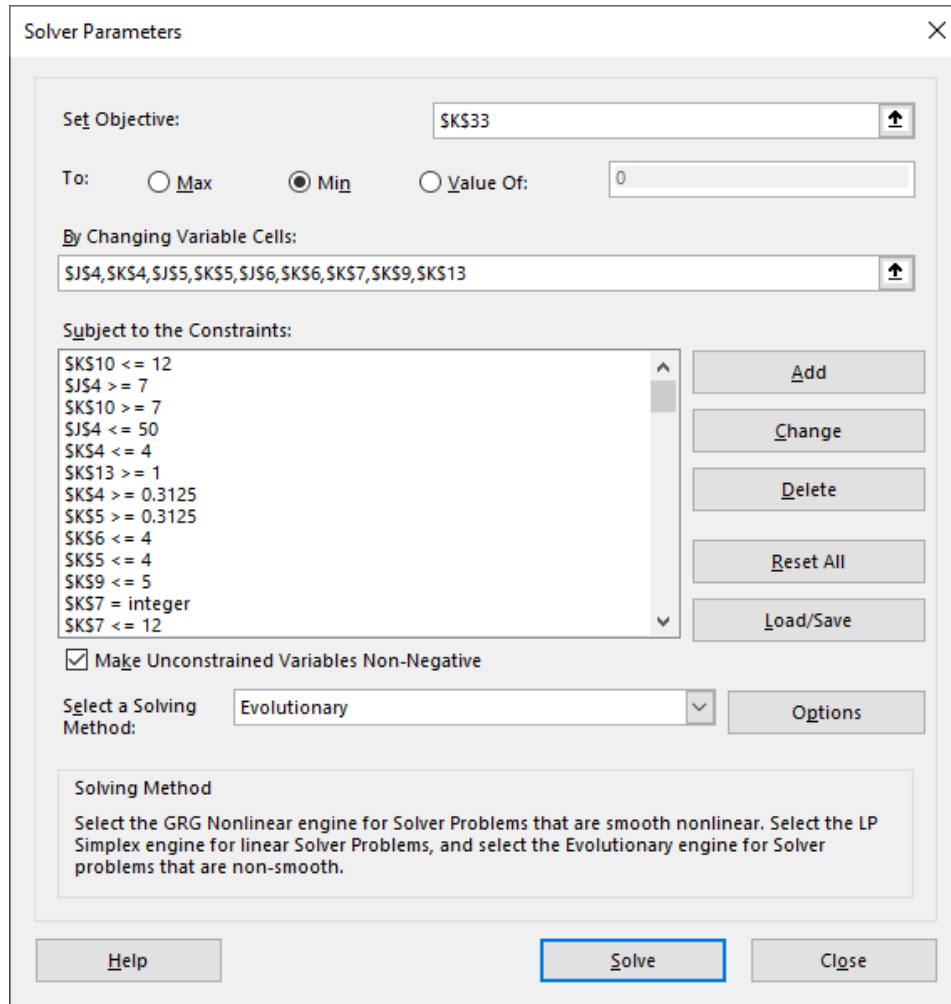


Figure 5-5 Populated Solver dialogue box

Setting up of the design parameters as Solver variables is as simple as writing their reference cell location in the input field titled “By changing variable cells” in Figure 5-5. The setup procedure was discussed previously in

Chapter 2. Additionally, Solver permits the user to restrict some variables to be integers only, this is applicable for the number of girders & cross frames. However, when it comes to the sections that make up the girder, one aspect that should be kept in mind is the market availability of the steel sections. The best way to circumvent this issue is to simply let Solver cycle between any decimal values and then correct the resulting dimensions by rounding to the nearest available thickness.

Another point worth discussing is the intention of using both, built-up sections as well as hot-rolled profiles and possibly comparing both alternatives. In order to capitalize on the built-up section, top and bottom flanges have been setup to be different from one another.



Figure 5-6 Deck overhang & cross frames

www.researchgate.net/profile/Md-Ashiquzzaman-2

Existing resources on bridge engineering provide inadequate background and theory when it comes to the deck overhang. There is little information to make up the case for this component, as the introduction of a cantilever results in the exterior girders being subjected to eccentric loads, especially during concrete casting, see Figure 5-6. As a result, the decision has been made to incorporate this design parameter in the model with the goal of providing a better understanding for this component. Note that the overall bridge width is fixed. The overhang width is simply changed by manipulating the spacing of the girders.

Cross frames, also known as diaphragms, as shown in Figure 5-6 are the lateral components responsible for the torsional rigidity of the bridge, especially during the deck casting stage. The design of this component is left to the engineer as the AASHTO provisions do not make any specific requirements other than the spacing limitation. While an increase in the number of cross frames is directly proportional with the lateral and torsional rigidity of the bridge, it is immediately met with an increase in steel components that need to be fabricated and assembled. As a result, this tradeoff presents a perfect opportunity for being implemented as a design variable in the optimization module.

Finally, Solver is free to present any design configuration as an applicable design, provided all constraints are within the acceptable range. These constraints are discussed in the next subsection.

5.5 Constraints

Problem constraints have been divided into multiple categories with the goal of separating the different topics and scopes that they cover:

Table 5-3 Constraints table 1 / 6

Geometry related		
Constraint	Reference	
Web proportions $\frac{D}{t_w} \leq 150$	Eq. 6.10.2.1.1-1	
Flange proportions (top & bottom) $\frac{b_f}{2*t_f} \leq 12$	Eq.6.10.2.2-1	
Flange proportions (top & bottom) $b_f \geq D/6$	Eq.6.10.2.2-2	
Flange proportions (top & bottom) $t_f \geq 1.1 * t_w$	Eq.6.10.2.2-3	
Flange proportions (top & bottom) $0.1 \geq \frac{I_{yc}}{I_{yt}} \leq 10$	Eq.6.10.2.2-4	
Test flanges not overlapping	Geometry	
Erection consideration $b_{fc} \leq L/85$	C6.10.3.4-1	
Live Load DF. Girder Spacing > 1.06 m	Table 4.6.2.2.2b-1	
Live Load DF. Girder spacing is < 4.88 m		
Live Load DF. (de) > -0.305 m		
Live Load DF. (de) < 1.67 m		
Live Load DF. (de) > 0 m		
Live Load DF. Deck thickness > 114 mm		
Live Load DF. Deck thickness < 305 mm		
Live Load DF. Span length > 6.1m		
Live Load DF. Span length < 73.15 m		
Live Load DF. (kg) > 4 * 10 ⁹		
Live Load DF. (kg) < 3 * 10 ¹²		
Check location of PNA is in web (compact section requirement)		Geometry
(Lb) Cross frame spacing > = 9.14m		CL. 6.7.4.2

Table 5-4 Constraints table 2 / 6

Strength limit state	
Constraint	Reference
Ductility requirement for compact sections (interior & exterior girders)	CL.6.1 0.7.3
Compactness check.1. Composite section in positive flexure	CL.6.10.6.2.2
Compactness check.2. Composite section in positive flexure	
Strength I. Flexure (interior & exterior girders)	Eq.6.10.7.1.1-1
Strength I. Shear (interior & exterior girders)	CL.6.9.10
Strength III. check $f_l < 0.6 F_yf$	CL.6.10.6
Strength III- Flexure (Interior & exterior girders)	
Strength IV- Flexure (Interior & exterior girders)	
Strength V- Flexure (Interior & exterior girders)	
Strength V. check $f_l < 0.6 F_yf$	

Table 5-5 Constraints table 3 / 6

Constructability	
Constraint	Reference
Top Flange (LTB, FLB) Strength-I	CL.6.10.8.2
Top Flange (LTB, FLB). Special Loading	
Top Flange (LTB, FLB). Strength-III	
Top Flange (Flange tip yielding). Strength-I	
Top Flange (Flange tip yielding). Special Loading	
Top Flange (Flange tip yielding). Strength-III	
Bottom Flange (Flange tip yielding). Strength-I	
Bottom Flange (Flange tip yielding). Special Loading	
Bottom Flange (Flange tip yielding). Strength-III	
Web Bend Buckling – Strength-I	CL. 6.10.1.9
Web Bend Buckling - Special loading	
Web Bend Buckling – Strength-III	
Shear. for Stiffened interior panels	CL.6.10.3.3

Note that:

- LTB: lateral torsional buckling
- FLB: frame local buckling

Table 5-6 Constraints table 4 / 6

Deck overhang	
Constraint	Reference
Strength I - Top Flange	CL.6.10.3.2 & CL. 6.10.3.4
Special Loading -Top Flange	
Strength I -Bottom Flange	
Special Loading -Bottom Flange -Deck Over hang Loads	
Strength I AF ≥ 1	
Special loads AF ≥ 1	
Strength III- Top flange - Wind	
Strength III- Bottom flange - Wind	

Table 5-7 Constraints table 5 / 6

Service limit state	
Constraint	Reference
Live Load deflection (interior & exterior girders)	CL.2.5.2.6.2
Permanent Deformations (top & bottom flanges for interior & exterior girders)	CL.6.10.4.2
Web bend buckling during service (interior & exterior girders)	CL. 6.10.1.9

Table 5-8 Constraints table 6 / 6

Fatigue limit state	
Constraint	Reference
Fatigue I of detail C. (Interior & exterior girders)	CL.6.6.1
Fatigue I of detail C. Exterior	CL.6.10.4.2
Special Fatigue requirement for webs (Fatigue I)	CL. 6.10.1.9

While the list above might seem overwhelming, the majority of these constraints have been presented thoroughly in the design procedure in the previous section.

5.6 Objective Function

The intention behind the objective function is to have a unit of measurement, an indicator, capable of evaluating different bridge configurations based on the quantity of steel used in the superstructure. A quick observation and the reader will come to notice that the majority of the selected design parameters have one thing in common. Changing the value of any of them leads directly to a change in the amount of steel in the bridge. That is, they are selected with the steel being the main player in mind. Since this optimization method can only handle a single objective, some administrative decisions should be taken. Among these is the decision to omit the concrete deck thickness from the design parameters.

If that weren't the case, and the deck thickness were to be added as an additional variable, the genetic algorithm would quickly come to notice that increasing the deck thickness enables the selection of thinner steel profiles, and that is free-of-charge. One solution that combines both materials into a single objective would be to do the optimization with all materials being reflected in the module in their respective unit cost. Namely, cost optimization. As opposed to weight optimization. This way multiple materials can be clubbed in a single objective function. However, after some consideration, and given that 8 of the to-be 10 parameters relate to steel, the decision to omit the deck thickness has been taken. Additionally, having the output of this work be reflected in cost basis, can limit the applicability of the conclusion to a very short period of time. Instead, within the allowable deck thickness range, the value will be taken as a ratio to the allowable span length.

The discussion below demonstrates how the objective function came to be. Initially, the objective function has been assigned the value of the total area of the steel girders. Additionally, available resources on bridge engineering approximates the weight of the diaphragms and miscellaneous items to 5% of the girders weight. This estimate is used to account for cases where the chosen diaphragm spacing results in a higher count of diaphragms. All in all, the objective function can be summarized using the following expression:

$$\sum_{i=1}^{N_g} A_g + \left(\sum_{i=1}^{N_g} A_g * 5\% \right) * (D_{add}/D_{optimum})$$

Where: N_g is the number of girders, A_g corresponds to the cross-sectional area of a single girder. D_{add} is a figure used to account for any additional diaphragms. D_{add} is derived from the generic estimate of how much the bare minimum number of diaphragms would weigh, $(\sum_{i=1}^{N_g} A_g * 5\%)$. $D_{optimum}$ is the optimum number of cross frames based on the smallest allowable spacing at 6.1 m. The presented objective function is an arbitrary formulation of how we intend to measure the efficiency of a design combination. The designer is free to add any factors that would reward or otherwise punish the system for taking an un-wanted design approach. Given the above, the unit of this objective function is mm^2 .

To reiterate, a 20% reduction in the objective function does not necessarily translate to a 20% reduction in the consumed steel. The objective function is only relevant within the context with which it was defined. For outsiders, it is an arbitrary, digit that corresponds to how the stakeholders decided to evaluate the bridge. Therefore, it is critical to convey the overall design improvement in a conventional weight or weight per length units.

Chapter 6

Results and Discussions

Chapter 6 Results and Discussions

6.1 Introduction

This chapter presents the design example from (Kim, Kim, & Eberle, 2013) after implementing the optimization process using Solver. The work of (Mona & Saka, 2019) will serve as the main reference for auditing the work of this paper, since it utilized the same design example.

Reference	(Kim, Kim, & Eberle, 2013)	(Mona & Saka, 2019)
Number of girders	6	
Profile	W24x76	W24x62
Type	Hot rolled	
Total cross-sectional area of steel girders	86700 mm ²	70451 mm ²
Concrete deck thickness	203 mm	178 mm
Note	Identifical flanges	

The results of (Mona & Saka, 2019)'s work is considered to be of high fidelity, given the that the output relied on a SAP2000 bridge model. This is further substantiated by the fact that 5 different metaheuristic algorithms yielded the same output. While it's not directly stated, (Kim, Kim, & Eberle, 2013) & (Mona & Saka, 2019) design configurations are assumed to carry the optimum number of cross frames, which results in the objective function matching the total cross-sectional area of the steel girders without any additions. Finally, three different optimization models have been created and are presented in the upcoming pages.

In order to unify Solver's parameters, the following settings have been selected for all optimization models, with the stopping criteria set at 1800 seconds (30-minutes).

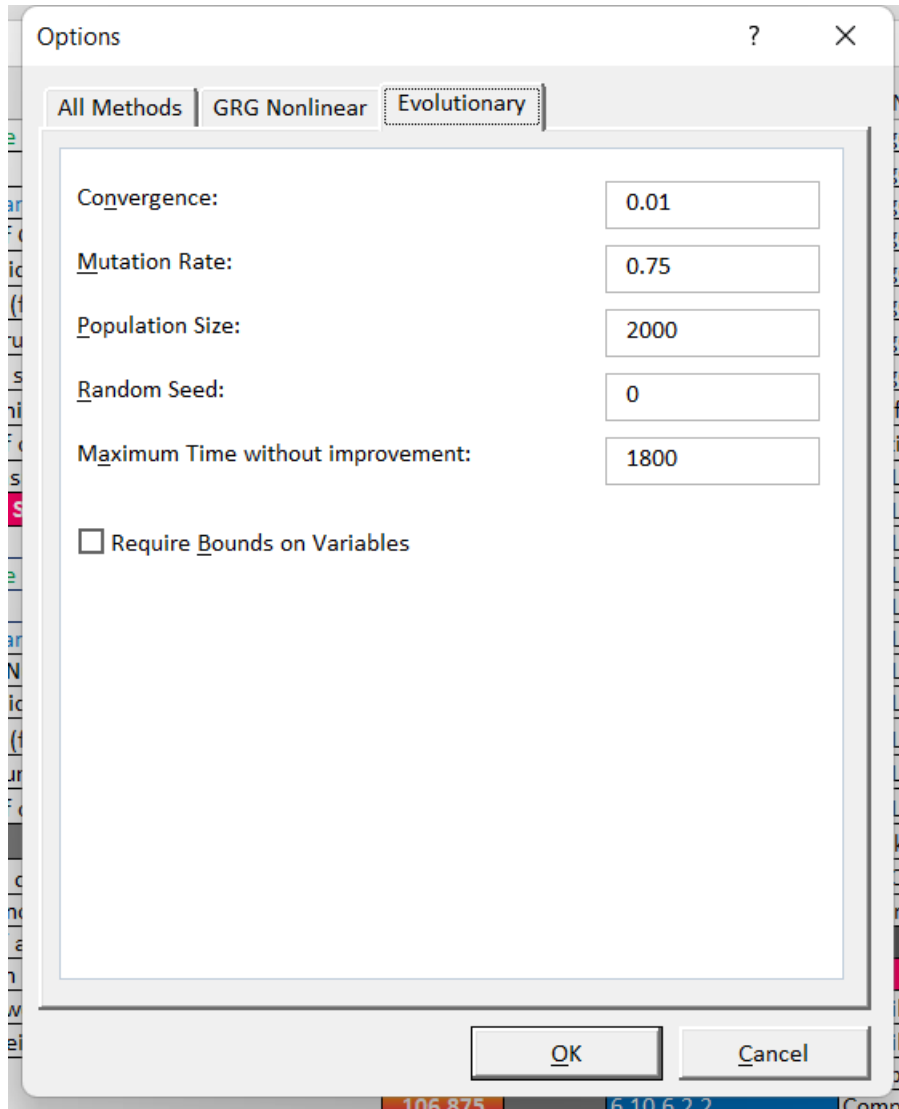


Figure 6-1 Selected Solver settings

6.2 Model 1

6.2.1 Variables

The deck thickness has been set to 178 mm. The girder configuration on the other hand was left open for Solver, this included all of the 9 variables from subsection 5.4.

6.2.2 Expectations

The main objective of this model is to provide Solver with an environment where it can freely cycle between any design configuration for the steel components. As for the deck thickness, the restriction to 178 mm aims primarily to simulate the system of variables that lead to the output produced by (Mona & Saka, 2019) . Additionally, given that this model has the flexibility to select built up profiles, we should expect an output that matches the design efficiency and optimization presented in (Mona & Saka, 2019) as a bare minimum.

Results that comply with these expectations should indicate that the overall setup of the spreadsheet model and AASHTO provisions was successful. On the other hand, results that excessively exceeds the provided datum could carry negative connotations. This paper doesn't aim to dismiss other optimization methods or the commercial market of structural design software. In fact, since this paper aligns itself with the same code provisions, we shouldn't expect a second re-invention of the wheel, and thereby a substantially improved design. The item in question is the mythology and its viability.

6.2.3 Results

After 45 minutes of runtime, the stopping criteria was automatically triggered at 1800 seconds (30 minutes). Meaning that it only took 15 minutes to reach the optimum design and no other improvements took place beyond that. The objective function for this design was calculated at 68950 mm², which corresponds to the total cross sectional area of the steel components while also accounting for additional cross frames. This configuration called for a single cross frame, which matches the optimum number using the maximum allowable spacing of 6.1 m. Therefore the second part of the objective function is 0, leaving only the cross sectional area of the steel girders, $\sum_{i=1}^{N_g} A_g$. Breakdown of the design variables is shown below in Table 6-1.

Table 6-1 Optimization output for model 1

<i>Solver Initial Trial</i>	<i>Value</i>	<i>Unit</i>
<i>Top flange width</i>	266.7	mm
<i>Top flange thk</i>	12.7	mm
<i>Web height</i>	965.2	mm
<i>Web thk</i>	9.53	mm
<i>Bottom flange width</i>	209.6	mm
<i>Bottom flange thk</i>	22.2	mm
<i>Deck thk</i>	178	mm
<i>Overhang width</i>	0.406	m
<i>Number of girders</i>	4	
<i>no. of cross frames</i>	1	

6.2.4 Observations

The resulting design configuration presented a 20.5% reduction in steel from the initial design by (Kim, Kim, & Eberle, 2013). The model also outperformed (Mona & Saka, 2019) by 2.1%, which is right where the model was expected to land as a best-case scenario. The number of girders & overhang width provided the model with additional real-estate that in theory and in practice allowed for a wider search range, leading to a better solution.

Most notably was how the model made use of the number of girders by reducing it from 6 to 4. Moreover, the reduction in the overhang width was apparent. Figure 6-2 & Figure 6-3 show a rough sketch of the original cross-section as well as the new optimized model.

A quick look at the selected flanges will show that the bottom flange has 27% more cross-sectional area than that of the top flange. This design feature is rather typical for a composite bridge. Since the problem presents a simply-supported span, all moment loads induce tension on the lower fibers and compression on top fibers. Having a composite design means that the concrete will aid in resisting the compression on the top flanges, resulting in the need for a smaller top flange.

All in all, the results of this model were in accordance with the prior expectations. Solver was successful in coming up with a unique design that meets all of problem constraints while also outperforming the shown reference.

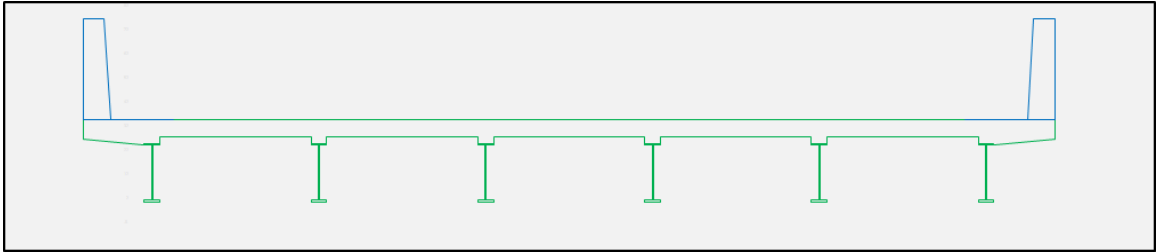


Figure 6-2 X-Y scatter graph of original bridge

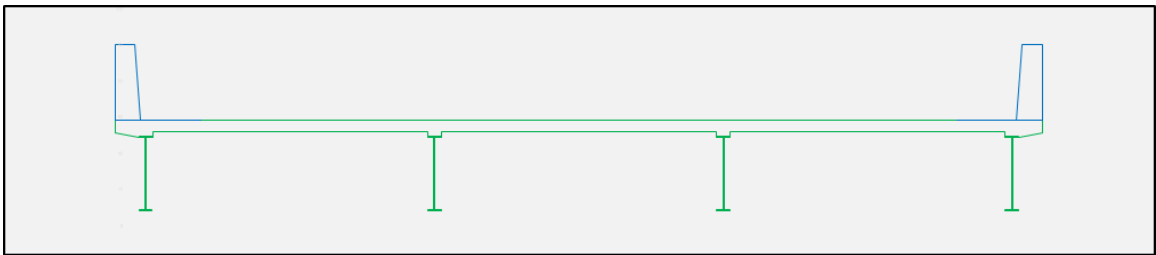


Figure 6-3 X-Y scatter graph of model 1

6.3 Model 2

6.3.1 Variables

The deck thickness has been set to 178mm. The number of girders is fixed at 6 while the 8 remaining variables are left open for Solver.

6.3.2 Expectations

By fixing the number of girders at 6, we would be imposing a restriction that narrows the range of possible solutions. However, the near-infinite set of solutions for model 2 remains a subset of model 1 as shown in Figure 6-4. Every single combination that could be produced in model 2, has already covered by model 1. If both models were to be ran for an infinitely-long period of time, model 2 cannot produce results that outperform that of model 1.

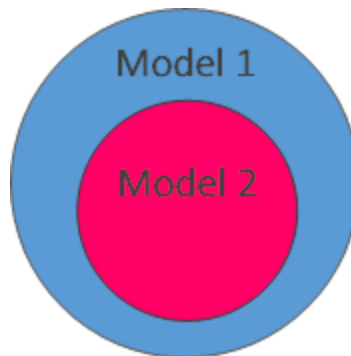


Figure 6-4 Solution range of model 1 & 2

Other runs of the Solver model have been shown to take a very repetitive approach, and that is by almost always reducing the number of girders to the permissible minimum. As a result, the objective of this model is to ensure the fidelity of system by restricting the number of girders, ensuring the system's flexibility to work under different constraints.

6.3.3 Results

This model was allowed to run multiple times even after the stopping criteria was triggered. In total, the model ran for 5 hours (total of 10 runs). The results plateaued after the second hour (4th run). The additional runs were intended to confirm the hypothesis that this model wouldn't be able to outperform the first model. The objective function for this design was calculated at 80260 mm². This value corresponds to the total cross sectional area of the steel components while also accounting for additional cross frames. This configuration called for a single cross frame, which matches the optimum number using the maximum allowable spacing of 6.1 m. Breakdown of the design variables is shown below in Table 6-2.

Table 6-2 Optimization output for model 2

Solver Initial Trial	Value	Unit
Top flange width	260.35	mm
Top flange thk	11.11	mm
Web height	914.4	mm
Web thk	7.92	mm
Bottom flange width	254	mm
Bottom flange thk	12.7	mm
Deck thk	178	mm
Overhang width	0.393	m
Number of girders	6	
no. of cross frames	1	

6.3.4 Observations

It was obvious that this model struggled to make the design improvements at the same pace as the first model, even when the restriction was only imposed on a single variable, namely the number of girders being fixed at 6. Nonetheless, the resulting design configuration presented a 7.44% reduction in steel from the initial design by (Kim, Kim, & Eberle, 2013). However, the model was unsuccessful when it comes to presenting an improvement close to that of (Mona & Saka, 2019), which showed a 18.75% reduction in steel.

On the other hand, the initial assumption that this model would not outperform the first model has been shown to be correct. Especially considering that this model was allowed more runtime than the first model.

When it comes to the geometry of this design, the same trends can be noted. The design included a bottom flange with 11.5% additional cross-sectional area, compared with the top flange. Moreover, the overhang showed the same trend of reduction in width.

To sum up, comparing the behavior of this model with the first model shows similar trends, albeit at a different scale. We shouldn't expect any direct conclusions to be drawn from a two model runs, let alone from two models with different restrictions. As to what could have caused the stagnation, it could be attributed to the pitfalls of metaheuristic approaches becoming stuck in local optimum solutions.

6.4 Model 3

This model represents the bulk of the results. Instead of running the optimization process for a single design configuration, the model will be run for the same bridge at different span length. Ranging from the initial design at 12.2 m up to 60.1 m at 3 m increments.

Each configuration will be allowed a maximum of two runs (total of 1 hour). Note that the first model showed no improvements beyond the first 15 minutes. Moreover, this procedure will be performed in an ascending order, starting at span length of 12.2m. This means that every subsequent design configuration would not be a valid design for the one after it. Ensuring that no exceptional mutations in the design would be carried to the next run.

6.4.1 Variables

The deck thickness has been set to a function that builds on a linear ratio ranging between 178mm and a maximum of 305mm depending on the span length. The girder was left open for Solver, this included all of the 9 variables from subsection 5.4.

6.4.2 Expectations

The main objective of this model is to investigate dominant design behaviors (if any) and to document the relationship between the different components. Moreover, this unrestricted environment should provide a genuine insight on the true shape of the code provisions in the form of the resulting bridge configuration.

Given the results of the first model, it is highly likely that all subsequent runs would lead to the same trend of reducing the number of girders. The added value that comes from additional girders is a by no means a match to the reward that the system gets by increasing the web depth. The flexural resistance of the bridge is directly proportional to the moment of inertia of its components. Namely, the girders. This model, with no restrictions, is nothing but a fertile ground for the web to grow. This growth will be immediately rewarded by a factor of the power 3, given the moment inertia of rectangular shapes at the X-axis, $I = bh^3/12$. Note that the design procedure already incorporates a number of constraints, ensuring webs never go out of proportions. Namely, proportion limits and web bend buckling restrictions.

6.4.3 Results

Results from running model-3 are shown below in tables. Data was split into two tables only due to formatting and fitting concerns. Each column represents the result from two optimization runs (1-hour total), at different span length. All design variables from subsection 5.4 are included. Highlighted in green is the objective function for each run.

Table 6-3 Results of model-3, part 1 of 2

Span length	m	12.2	15.2	18.3	21.3	24.4	27.4	30.5	33.5
Deck thk	mm	178	186	194	202	210	217	225	233
Top flange w	mm	267	260	248	305	311	330	305	381
Top flange thk	mm	13	13	13	13	14	14	14	17
Web h	mm	965	991	1270	1295	1219	1575	1575	1473
Web thk	mm	9.5	9.5	11.1	11.1	11.1	12.7	12.7	12.7
Bottom flange w	mm	210	203	229	267	260	305	279	381
Bottom flange thk	mm	22	32	25	32	51	32	44	44
no. girders		4	4	4	4	4	4	4	4
Overhang width	mm	0.41	0.4	0.4	0.4	0.44	0.41	0.4	0.4
no. cross frames		1	2	3	3	4	4	6	5
Objective function	mm ²	68951	76774	94564	106935	126960	137580	150774	169193
Girder cross sectional area	mm ²	17741	19786	22919	26754	31023	34855	37021	42390
Area of top flange	mm ²	3471	3380	3224	3965	4354	4620	4270	6477
Area of web	mm ²	9650	9910	13970	14245	13409	20475	20475	19149
Area of bottom flange	mm ²	4620	6496	5725	8544	13260	9760	12276	16764

Table 6-4 Results of model-3, part 2 of 2

Span length	m	36.6	39.6	42.7	45.7	48.8	51.8	54.9	57.9	61
Deck thk	mm	241	249	257	265	273	281	289	297	305
Top flange w	mm	362	387	330	387	476	489	527	432	489
Top flange thk	mm	16	21	32	25	25	32	29	44	44
Web h	mm	1880	1778	1702	1930	2007	1981	2235	2210	2286
Web thk	mm	14.3	14.3	14.3	15.9	15.9	15.9	17.5	17.5	17.5
Bottom flange w	mm	419	356	438	381	400	451	578	502	546
Bottom flange thk	mm	29	44	44	44	44	44	32	44	44
no. girders		4	4	4	4	4	4	4	4	4
Overhang width	mm	0.41	0.39	0.41	0.39	0.41	0.4	0.55	0.59	0.47
no. cross frames		6	6	8	8	7	8	8	9	9
Objective function	mm ²	180089	196814	220715	231318	246935	268064	289757	320322	343709
Girder cross sectional area	mm ²	44263	48683	53660	57319	61612	67188	71774	78666	84402
Area of top flange	mm ²	5792	8127	10560	9675	11900	15648	15283	19008	21516
Area of web	mm ²	26320	24892	23828	30880	32112	31696	37995	37570	38862
Area of bottom flange	mm ²	12151	15664	19272	16764	17600	19844	18496	22088	24024

6.4.4 Observations

In order to better evaluate the resulting data, the objective function has been plotted against the span length in Figure 6-5 below. It can be said that the increase of cross-sectional area of girders is linearly proportional to the span length. Applicable for this design case where no limitations on the web height or any other special requirements are dictated. Moreover, this diagram aids in locating instances where the allocated processing time was inadequate. For instance, the configuration at span length of 42.67 m presents a perceptible uptick that doesn't align with other point. This is a direct result of relying on metaheuristic approaches, where there is no guarantee of consistency, especially for short runs.

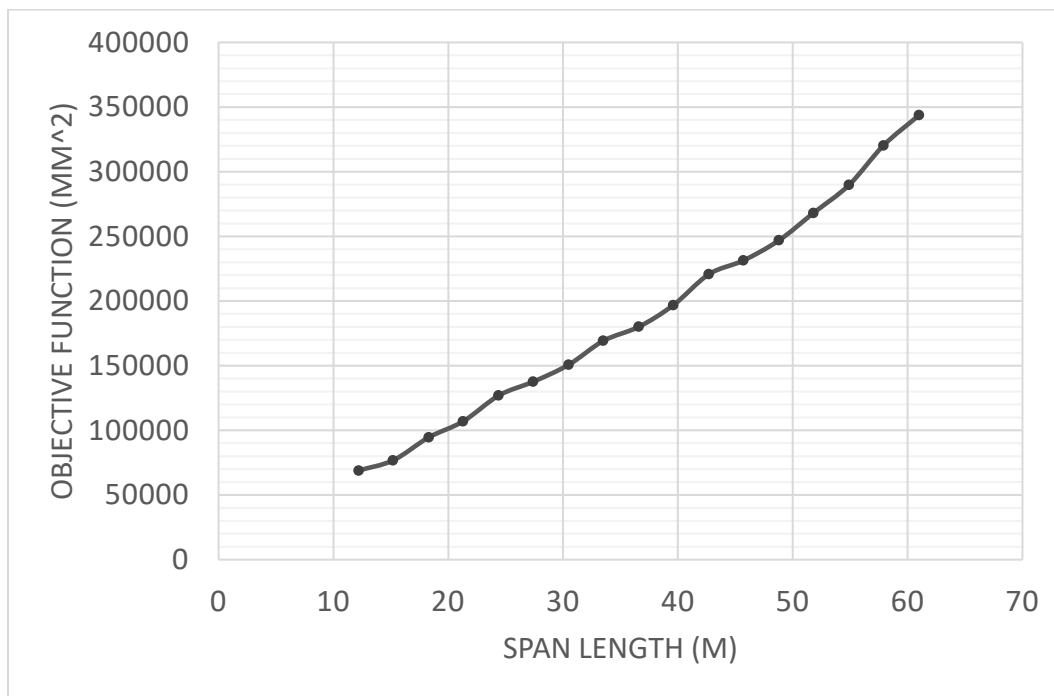


Figure 6-5 Span length (m) VS objective function (mm²)

Secondly, the resulting number of girders for all spans does align with the initial hypothesis that the design is highly rewarded when it increases the web depth as opposed to adding additional girders. In other words, site conditions permitting the use of deep webs will yield the highest return on investment in terms of capturing the highest resistance for the least amount of material.

Given the significance of the web, the graphs below show the rate of increase of the web's height & thickness as the bridge span increases. By referring to manufacturing documents and brochures published by steel mills, we can confirm the resulting dimensions are within what can be readily manufactured. In fact, mills are capable of processing segments having a width of 3.05 m, (Garrell, 2011). Moreover, the resulting trendlines provide historical bases which can guide in providing initial design configurations. Furthermore, this data can be fed back to the same optimization model as new constraints that limit the web height and thickness to values within a certain margin of the trendline, based on the span length.

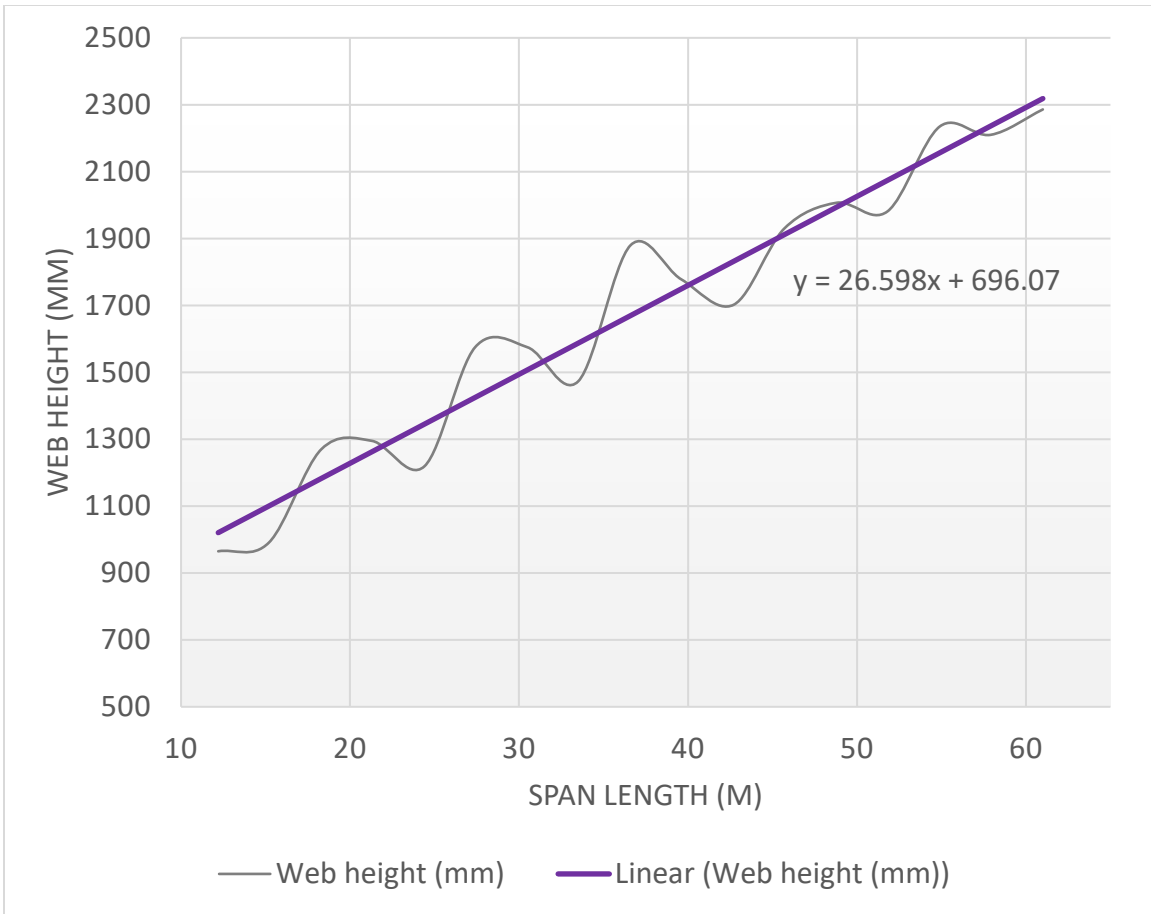


Figure 6-6 Span length (m) VS web height (mm)

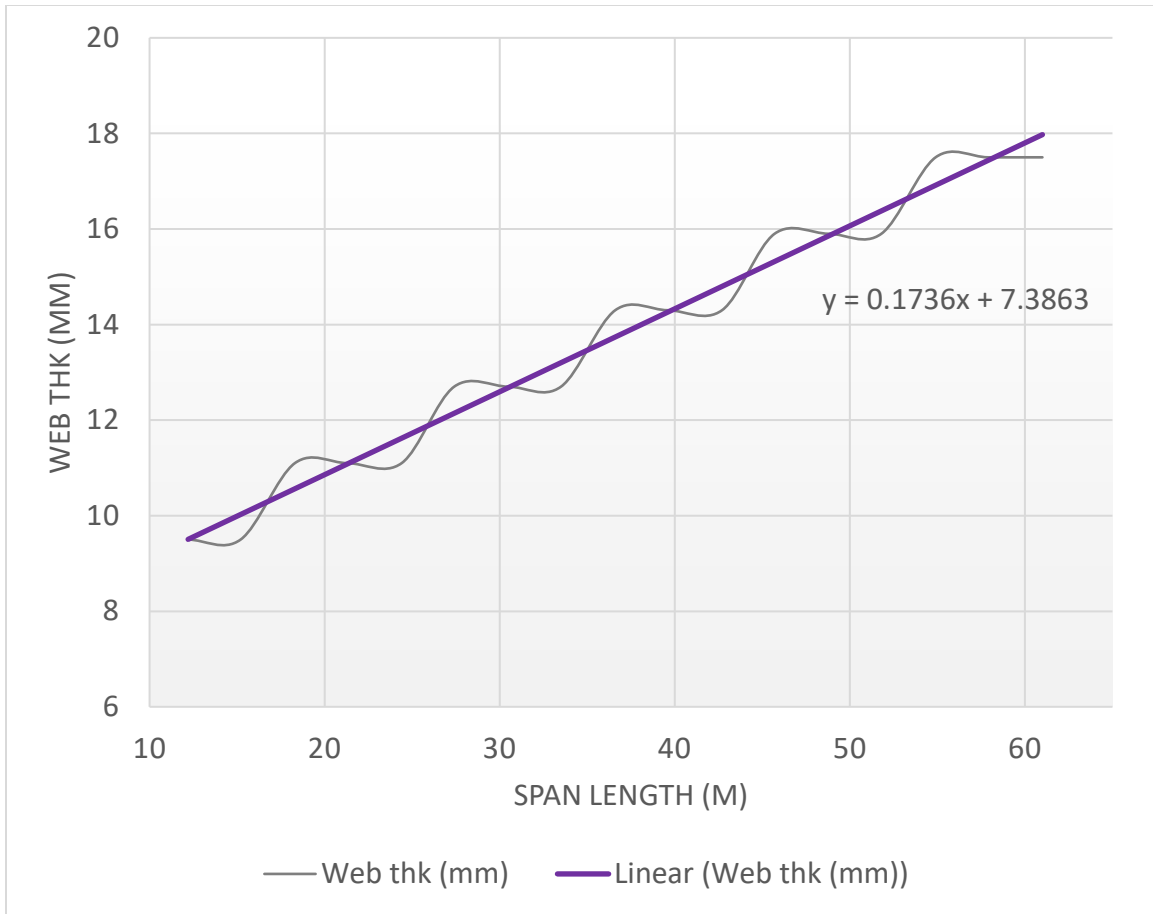


Figure 6-7 Span length (m) VS web thickness (mm)

A different overview of the results can be concluded by graphing the span length against the cross-sectional area of each of the girder's components, Figure 6-8. The resulting wave-shaped line is a response that can be on one hand attributed to the metaheuristic nature of this approach, swinging between solutions. On the other hand, there remains the likelihood of the design being stuck in a local optimum configuration, where closing this discrepancy between local and global optimum could lead to smoother lines.

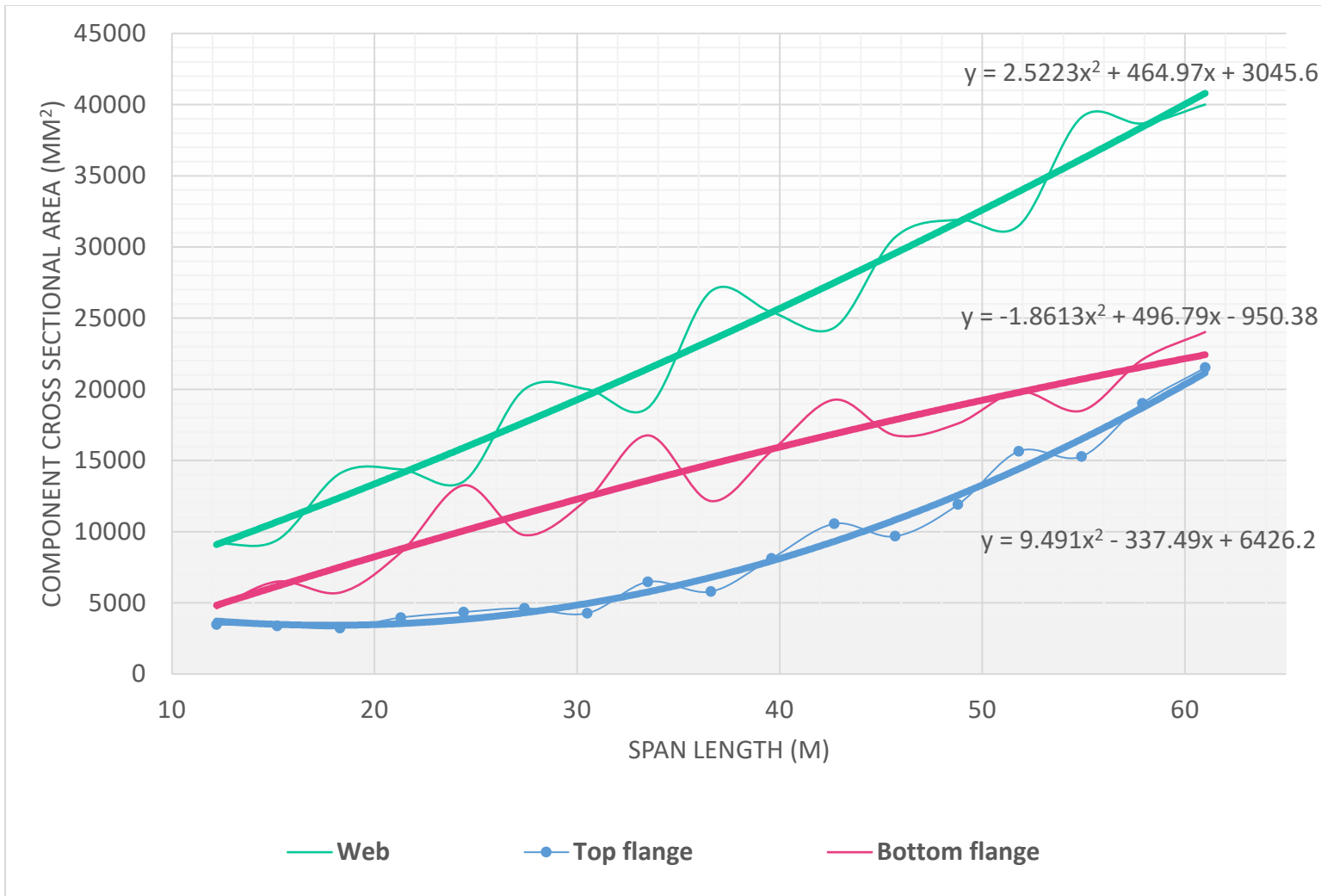


Figure 6-8 Span length (m) vs cross-sectional area of the different girder components (mm²)

Additionally, based on knowledge acquired throughout this research and given the natural response of composite plate girder bridges to loads. We know that the design is highly unlikely to be controlled by the top flange. Especially considering the design philosophy where the entire compression force is assumed to be resisted by the concrete deck without any contribution from the top flange, that is at the composite state. In contrast, the constructability checks are in place to ensure that bottom flanges don't fail during construction. Making them the likely suspect in controlling the overall design. With these facts in mind, we can state that variables with higher effect on the objective function will tend to have higher fluctuations, as seen in Figure 6-8. In a way, the short running time for this model gave insight on variables and their weights in the overall model.

Another aspect that aids in validating the data can be noted in the same figure. Any uptick in the cross-sectional area of the web (in green) is met by a downtick in the area of the bottom flange (in red), and vice versa. This implies that Solver already made the connection between the two parts. It means, there are no scenarios where increasing the dimensions of the top flange and the web at the same time, would lead to weight savings, even when the system tried to compensate by reducing size of the bottom flange.

While the top and bottom flanges are independent from one another, they both exhibited similar upticks and downticks trends. This is likely to have been caused by a single set of rules and equations. Namely, the proportional limits.

The overhang width exhibited consistent results up until the 54.9 m mark, where it showed a sudden increase in its value. Reviewing the AASHTO LRFD spread sheet revealed no discrete scenarios with direct reference to the bridge length, which could have resulted in this uptick. Notwithstanding the above, the overall behavior of the model to reduce the overhang width remains a valid observation, as the uptick remains smaller than the starting value of 1 m. Additionally, although this increase doesn't contradict the overall image, it serves to ensure the model was setup correctly and that there is no human error in setting up the equations that would consistently lead to the same results. Finally, the overhang width constitutes a challenge mainly during the construction stage, prior to curing of the concrete deck.

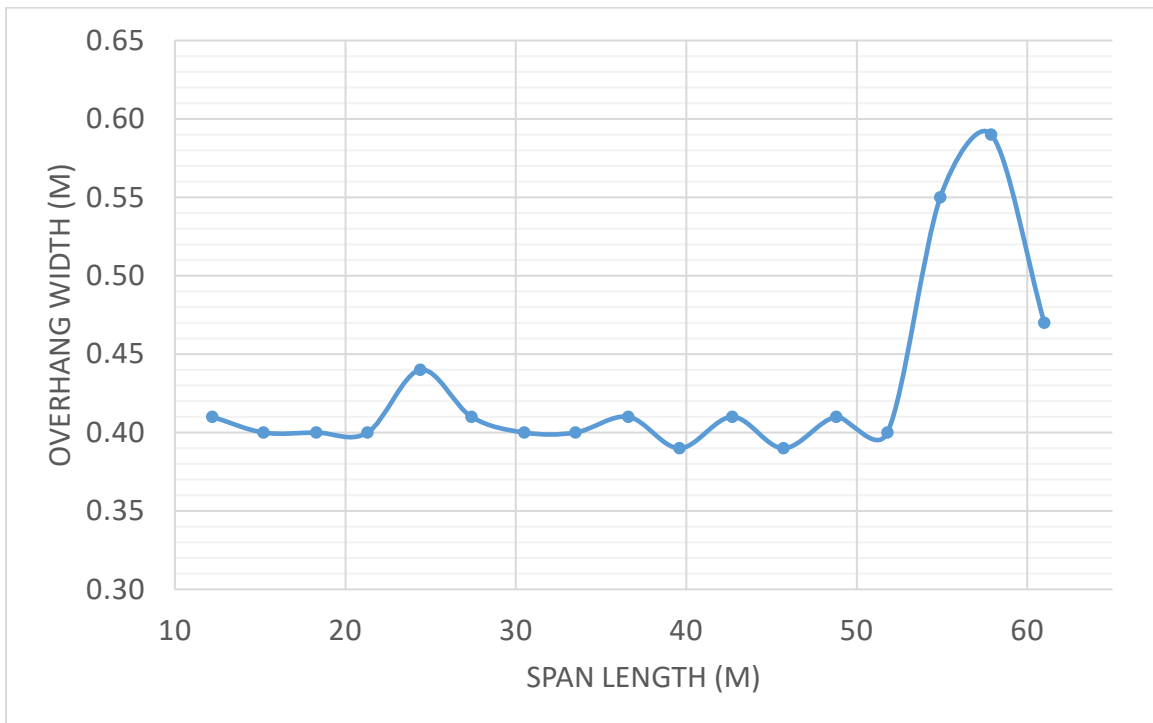


Figure 6-9 Span length (m) vs overhang width (m)

Finally, the only available resource in literature to touch on the topic of computation time is (Mona & Saka, 2019), where the runtime for each algorithm has been documented. See Table 6-5 below.

Table 6-5 Optimization summary for I-beam bridge, (Mona & Saka, 2019)

<i>Algorithm</i>	<i>Computation time (minutes)</i>
<i>Artificial bee colony algorithm (ABC)</i>	1254
<i>Biogeography-based optimization algorithm (BBO)</i>	2613
<i>Exponential big bang-big crunch algorithm (EBB-BC)</i>	1211
<i>Symbiotic organisms search algorithm (SOS),</i>	5273
<i>Enhanced artificial bee colony algorithm (EABC)</i>	Not applicable

Referring back to Model 1, the model achieved similar levels of optimization within the first 15 minutes when compared with the datum study. Whereas results from model 3 showed a linearly proportional objective function within 2 runs (1 hour total). All in all, considering 60 minutes as the bench mark for this study, it presents a substantial upgrade when it comes to processing time, Solver was able to achieve comparable design improvements in 5% of the time required with the referenced study.

Chapter 7

Conclusions

Chapter 7 Conclusions

7.1 Research Findings

The list below is a visit to the objectives of this paper, with the goal of evaluating and reviewing how much of each goal was fulfilled.

Objective 1

“To establish an optimization model for composite plate girder bridges that utilizes the maximum number of design variables that is yet to be undertaken in the literature”.

This research succeeded in tackling design of composite plate girder bridges using a mythology, not present in the literature. On one hand, existing literature mostly focused on hot-rolled profiles with matching flanges, whereas this study explored built up profiles. On the other hand, the objective function was structured in a way that accommodates the number of cross frames as an additional variable. All in all, a total of 9 design variables have been used in the optimization model:

- Top flange width.
- Top flange thickness.
- Web height.
- Web thickness.
- Bottom flange width.
- Bottom flange thickness.
- Number of girders.
- Deck overhang width.
- Number of cross frames (diaphragm).

Objective 2

“To present a bridge model that conforms to the highest number of provisions in AASHTO LRFD Bridge Design Specifications”.

The presented design example in chapter 4 gave an overview of the overwhelming procedure that was taken in order to cover all major aspects of the AASHTO LRFD provisions. The model included a total of 57 design constraint, covering both, major and miscellaneous design aspects.

Moreover, the desire to build this model meant that many unique aspects of bridge engineering had to be studied and investigated thoroughly, items that otherwise might not have received the same level of attention, had the model been done using any conventional structural design software. In other words, the more we interacted with the AASHTO provisions, the clearer the overall image of the design had become.

Objective 3

“To study the capability of Excel Solver as a readily-available tool for tackling non-linear problems using the genetic algorithm”

The viability of Solver as a readily-available tool for addressing the design of highly complex and regulated structures was confirmed. The application of Solver as non-specialized software, meant that more effort could be directed at the problem in question, rather than spending time and effort to fulfill the programming prerequisites, needed to build an optimization model. The viability of this application means that countless design routines, which are solved iteratively, could now implement a form of optimization.

Solver has been shown to excel in its ability to simulate real-life scenarios by imposing design constraints that reflect any possible limitation on the design. In the same vein, the capability of exploring unconventional design configurations while also meeting the predefined resources [or stock levels], makes it a highly sought-after tool.

Objective 4

“To compare the efficiency of this approach with existing literature”

The presented models showed results, comparable with the existing literature. Model 1 showcased a 20.5% reduction in the steel from the initial design. This improvement exceeded the literature by 2.1%. While also exploring unique design decisions, such as reducing the number of girders and reducing the width of the overhang.

This level of optimization was achieved with a total computation time of 60 minutes per bridge problem, which amounted to 5% of the total time used in the literature.

Objective 5

“To confirm the fidelity and repeatability of the genetic optimization algorithm”

Model 3 explored the same bridge at different span lengths, this approach was intended as an assurance of the repeatability of the system. The model showed consistent behavior for the objective function with no stray results that contradict the overall trend. Moreover, the logical formulation of model 2 further confirmed the fidelity of the system.

Objective 6

“To quantify any behavior that may arise between the different bridge components”

Higher fluctuations in the design variables in model 3 have been linked to the overall significance of the respective variable in the optimization algorithm. This hypothesis does align with the design philosophy of the bridge and how the sections are expected to react to imposed loads.

The model confirmed that site conditions permitting the use of deeper webs will yield the highest return on investment in terms of capturing the maximum potential of the girders for the least amount of material, as opposed to adding additional girders.

7.2 Use Cases

It should be noted that the viability of a design at a research level does not necessarily mean a viable design commercially, even when the design adheres to all code provisions and regulations.

This insight stems from my personal work experience, having completed a number of years working at an industry where steel makes up 95% of the final product's weight. It is not a rare occurrence, that manufacturers would upgrade a client's thickness specifications from 1.2mm to 1.5mm, and that is free of charge, as an example. Prolonged lead times, economic order time (EOT) and cash flow issues can dictate pushing your existing premium stock at the price of the inferior alternative. Especially if it means securing an immediate payment. The thickness example could be applied to any parameter and material specifications.

Optimization is a general-purpose tool that is not restricted to a product type. However, given the nature of bridges and how a single design requirement such as a depth limitation could force the optimum design into a completely different shape. Engineering offices/ consultants with direct insight into fab shops and steel mills, are likely to be the ones to benefit from incorporating an optimization model.

Additionally, entities taking up the construction of multiple bridges in a short period of time can benefit from nesting multiple projects into the same optimization model, coupled with existing material stock levels. This will lead to an optimization model that adapts to available resources.

Simply put, a bridge design that doesn't take the commercial aspects, logistics and the hidden costs of supply chain, even when it sits the top hills of global optima, could still mean a project operating at a loss.

The above remarks are by no means meant to gatekeep the process of optimization from smaller engineering offices. While it is a fact, these establishments are usually subjected to higher costing rates, given their smaller order quantities. However, the same optimization routine can be applied to parts of the bridge design that are within the establishment's control. Such as the distribution of the shear studs. This is mostly a design element that is dominated by the labor cost rather than material cost. Meaning that regardless of the overall design, some form of optimization can be applied and controlled.

7.3 Recommendations for Future Work

- Neural networks and deep learning are topics that weren't discussed in this paper. However, the ability of these methods to recognize patterns and act upon the accumulated knowledge is a feature that would benefit the design of bridges.
- The emergence of open-source libraries such as Brain.js for deep learning could further bridge the gap between academic writing and the commercial market when it comes to the field of product optimization.
- Solver tool is built in as a VBA model whose source code could be further inspected, edited and tweaked to incorporate custom algorithms, while still making use of the flexibility of spreadsheet models.
- Cooperate with local consultants and evaluate the resulting design configurations with emphasis on the commercial aspect.

References

- American Institute of Steel Construction . (2011). *Steel Construction Manual*. American Institute of Steel Construction . 14th edition.
- AASHTO. (2017). *AASHTO LRFD Bridge Design Specifications*. Washington: American Association of State Highway and Transportation Officials.
- Arora, J. S. (2016). *Introduction to Optimum Design*. Academic Press.
- Briones, L., Morales, V., Iglesias, J., & Morales, G. (2019). Application of the microsoft excel solver tool in the optimization of distillation sequences problems. *Computer Applications in Engineering Education*, 10.1002/cae.22193 .
- D. Goldberg, M. P. (1986). Engineering optimization via genetic algorithm. *Computer Science*, ASCE, 471-482.
- Dorigo, M. (1992). *Optimization, Learning and Natural Algorithms*. Italy: Politecnico di Milano.
- Faluyi, F., & Arum, C. (2012). Design Optimization of Plate Girder Using Generalized Reduced Gradient and Constrained Artificial Bee Colony Algorithms. *International Journal of Emerging Technology and Advanced Engineering*, ISSN 2250-2459.
- Fisher, J. W., Kulak, G. L., & Smith, I. C. (1998). *A Fatigue Primer for Structural Engineers*. National Steel Bridge Alliance.
- Garrell, P. L. (2011). *Steel Plate Availability for Highway Bridges*. Steelwise.
- Goldberg, D. E., & Holland , J. H. (1988). Genetic Algorithms and Machine Learning. 3(95-99).
- Hibbeler, R. (2014). *Mechanics of Materials*. Pearson.
- Joiner, J. H. (2011). Engineering History and Heritage. 164(2).
- Kennedy, J., & Eberhart, R. C. (1995). Particle swarm optimization. IEEE.

- Kim, J. B., Kim, R. H., & Eberle, J. (2013). *Simplified LRFD Bridge Design*. CRC Press. 1st edition.
- M. I., & Saka, M. P. (2019). Design Optimization of Bridge Structures under Code Provisions using Metaheuristic Algorithms. *Advances in Engineering Software*.
- Ministry of municipal & Rural Affairs. (2013). *Bridges, Tunnels, Culverts and Pedestrian*. Ministry of municipal & Rural Affairs.
- Narendra, T. (2014). *Highway Bridge Superstructure Engineering*. CRC Press, 1st edition.
- Poncelet, J. V. (1870). *Introduction à la mécanique industrielle*. France: Hachette Livre BNF.
- Ragsdale, C. (2007). *Spreadsheet Modeling & Decision Analysis*. South-Western College Pub; 5th edition.
- Roeder, C. W., Barth, K., & Bergman, A. (2002). *Improved Live Load Deflection Criteria for Steel Bridges*. National Cooperative Highway Research Program.
- Sparke, P. (2002). *A Century of Car Design*. B.E.S. Publishing.
- *Step by step guide for Excel's Solver*. (n.d.). Retrieved from FrontlineSolvers: <https://www.solver.com/solver-tutorial-using-solver>
- Torres, G. B., Brotchie, J. F., & Cornell, C. A. (1966). program for the optimum design of prestressed concrete highway bridges. *PCI Journal*, 11(3), 63–71.
- Vinay Agrawala, V. C. (2013). Optimum Design of Welded Steel Plate Girder using Genetic Algorithms. *International Journal of Current Engineering and Technology*, ISSN 2277 - 4106.
- Zhao, J. J., & Tonnias, D. E. (2017). *Bridge Engineering. Design, Rehabilitation, and Maintenance of Modern Highway Bridges*. McGraw Hill; 4th edition.

Appendix A

كلية الهندسة

جامعة البحرين

قسم الهندسة المدنية



التصميم الأمثل لمنشآت الجسور ذات العوارض الفولاذية

أطروحة مقدمة كجزء من متطلبات الحصول على درجة
الماجستير في الهندسة المدنية

إعداد

محمد فؤاد محمد الملاذي

الرقم الجامعي: 20126173

إشراف

د . سميح ارهان

أستاذ مساعد

جامعة البحرين

د . منى عبد اللطيف عبد الله إسماعيل

أستاذ مساعد

جامعة البحرين

مملكة البحرين

ديسمبر 2022